

UCSF

UC San Francisco Electronic Theses and Dissertations

Title

Regulation of Cytokinesis Machinery by the Anaphase-Promoting Complex

Permalink

<https://escholarship.org/uc/item/89f8b04b>

Author

Tully, Gregory Herbert

Publication Date

2007-09-13

Peer reviewed|Thesis/dissertation

Regulation of Cytokinesis Machinery by the Anaphase Promoting Complex

by

Gregory Herbert Tully

DISSERTATION

Submitted in partial satisfaction of the requirements for the degree of

DOCTOR OF PHILOSOPHY

in

Cell Biology

in the

GRADUATE DIVISION

of the

UNIVERSITY OF CALIFORNIA, SAN FRANCISCO

UMI Number: 3274663

Copyright 2007 by
Tully, Gregory Herbert

All rights reserved.

UMI[®]

UMI Microform 3274663

Copyright 2007 by ProQuest Information and Learning Company.
All rights reserved. This microform edition is protected against
unauthorized copying under Title 17, United States Code.

ProQuest Information and Learning Company
300 North Zeeb Road
P.O. Box 1346
Ann Arbor, MI 48106-1346

Copyright 2007

by

Gregory Herbert Tully

Acknowledgements

First and foremost, I wish to thank my thesis advisor Dave Morgan. He not only opened up the world of cell division to me but his patience and prodding enabled me to reach the finish line. Dave's door is always open (literally) and that reflects his readiness to talk with me about my work and my life.

Pat O'Farrell and Dave Toczyski immensely contributed to my work. Listening to Pat rant against the current dogma was refreshing and ultimately, taught me to constantly re-think my assumptions. Dave T.'s creativity was especially helpful in overcoming many roadblocks I encountered.

Sebastián Bernales, Alex Engel, and Muluye Liku are not only my closest friends in my class, they all stepped up to help me learn new techniques for my project. Whether it was studying Macro together or traveling to Oxford and Chile, we had a blast!

My best and hardest times in graduate school were spent with the members of the Morgan lab. I am truly grateful for the support, encouragement, and scientific input that I received from past and present members of the lab: Maria Enquist-Newman, Jeff Ubersax, Erika Woodbury, Liam Holt, Monica Rodrigro-Brenni, Mary Matyskiela, Jon Schaefer, Topher Carroll, Mart Loog, Susi Steggerda, Dave Randle and Maria Peraz. From teaching me how to silver stain to editing my thesis, each member of the lab contributed to my growth as a scientist.

I especially want to thank Matt Sullivan for his guidance. Daily, he challenged me to form new hypotheses and then pushed me to break them down! His mentoring catapulted my project from a series of observations into a working model.

When I failed qualifying exams, my family was there to catch me. My parents and sisters were steadfast in their love and support. They gave me the strength to get back up off my feet and succeed through the rest of graduate school.

I also want to thank Graciela's parents for their encouragement over the years. Luisa Malentacchi's constant inquiries about biology, from cancer to human development, always opened my eyes to see the big picture in my research.

Six years ago today, I started graduate school. Little did Graciela and I know what we were getting into! Graduate school has tested our marriage in many ways but ultimately, it has made our love stronger. Graciela's colossal support and confidence was my foundation. Muchas gracias Graciela.

Sebastián Bernales took the electron micrograph of the budding yeast cell in cytokinesis (Chapter 1 Fig. 2B). Nolan Ko (Stanford University) carried out the cross between *myo1Δ::kanMX6/MYO1-GFP* and *iqg1Δ42::LEU2/+* and analyzed the tetrads (Chapter 2 Fig. 5C).

With this exception, the rest of the work was performed by Gregory H. Tully, under the direction and supervision of David O. Morgan.

**Regulation of Cytokinesis Machinery by
the Anaphase-Promoting Complex**

by

Gregory Herbert Tully

Abstract

In all eukaryotes, cytokinesis depends on the contraction of the actomyosin ring, a ring of actin, myosin, and several other proteins that forms at the division site. The timing of contraction and subsequent disassembly of the actomyosin ring are poorly understood. The anaphase-promoting complex (APC) is an E3 ubiquitin ligase that controls several key steps in mitosis by targeting specific proteins for degradation. We hypothesized that the APC also controls cytokinesis by regulating the actomyosin ring.

We began by searching for novel APC substrates among proteins known to function in cytokinesis. Out of over 75 proteins tested, we found that Iqg1, an essential component of the actomyosin ring, is an APC substrate *in vitro* and is degraded in an APC-dependent manner after cytokinesis *in vivo*. To characterize the functional interaction between the APC and the actomyosin ring, we used live cell microscopy to analyze the behavior of the actomyosin ring components in *apc* mutants. In wild-type cells, fluorescent versions of actomyosin ring components visibly form a ring at the bud neck, then contract and disappear from the site of cytokinesis. In cells lacking *CDH1*, the APC activator during the time of cytokinesis, we find that these proteins behave normally during actomyosin ring contraction but then co-localize in multiple foci, rather than disappearing. From this we infer that the mutants cannot disassemble the actomyosin ring, and that APC^{Cdh1} may be essential for this process.

Actomyosin disassembly defects have been reported in septin (a structural scaffold for cytokinesis proteins) and myosin regulatory light chain (*mlc2*) mutant cells. We find that deletion of *CDH1* exacerbates these defects, which suggests that APC^{Cdh1}

functions in parallel to both septins and *MLC2*. In addition, we find that APC^{Cdh1}-mediated degradation of Iqg1 and Mlc2 activity are both required for actomyosin ring disassembly. Therefore, the APC, septins, and myosin regulatory light chain cooperate to ensure complete disassembly of the cytokinesis machinery.

The APC controls entry to and exit from mitosis. The results from these experiments demonstrate a function of the APC in cytokinesis, regulating disassembly of the actomyosin ring.

Table of Contents

Chapter 1 – Introduction	1
Chapter 2 – Identification of Iqg1 as a novel APC ^{Cdh1} substrate	17
Chapter 3 – The APC ^{Cdh1} regulates actomyosin ring disassembly	45
Appendix	95
Bibliography	120

List of Tables and Figures

Chapter 1

Figure 1. Actomyosin ring formation in the cell cycle. _____ 13

Figure 2. Contraction and septation are simultaneous. _____ 15

Chapter 2

Figure 1. APC substrate candidates identified in protein screen. _____ 35

Figure 2. Iqg1 is the only APC substrate candidate ubiquitinated by APC^{Cdh1}. _____ 37

Figure 3. Iqg1 degradation through the cell cycle depends on the APC. _____ 39

Figure 4. Characterization of the APC destruction signal on Iqg1. _____ 41

Figure 5. Non-degradable $\Delta 42$ -iqg1 is stable throughout the cell cycle, suppresses *myo1* Δ lethality, and is lethal when over-expressed. _____ 43

Chapter 3

Figure 1. Cdh1 is required for normal disassembly of the actomyosin ring. _____ 70

Figure 2. Myo1, Mlc2, Mlc1, and Iqg1 exhibit similar disassembly defects in APC mutant cells. _____ 72

Figure 3. APC activity is required for myosin ring disassembly. _____ 74

Figure 4. APC^{Cdh1} is required to disassemble the myosin light chains Mlc2 and Mlc1 and the IQGAP, Iqg1. _____ 76

Figure 5. Myo1 co-localizes with Mlc2, Mlc1, and Iqg1 in *cdh1* Δ cells. _____ 80

Figure 6. Deletion or stabilization of several APC^{Cdh1} substrates does not affect myosin disassembly. _____ 82

Figure 7. Deletion of <i>IQG1</i> or <i>MYO1</i> partially rescues the disassembly defect in <i>cdh1Δ</i> cells.	85
Figure 8. Mlc2 and APC ^{Cdh1} function together to disassemble the actomyosin ring.	88
Figure 9. Deleting <i>CDH1</i> lowers the restrictive temperature of a septin mutant.	92

Appendix

Figure 1. <i>cdh1Δ</i> and <i>mlc2Δ</i> cell clustering is enhanced in a <i>mlc2Δ cdh1Δ</i> double mutant.	96
Figure 2. Myo1 and Mlc2 co-localize after ring contraction in <i>cdh1Δ</i> cells.	98
Figure 3. Myo1 and Iqg1 co-localize after ring contraction in <i>cdh1Δ</i> cells.	100
Figure 4. Myo1 and Mlc1 co-localize after ring contraction in <i>cdh1Δ</i> cells.	102
Figure 5. Myo1 and Sec2 do not co-localize after ring contraction in <i>cdh1Δ</i> cells.	104
Table 1. Cell cycle abundance of cytokinesis proteins.	106
Table 2. Microscopy data of ring contraction, disassembly, and dot mobility for all strains observed.	114
Table 3. Colocalization of Myo1-GFP with mCherry-tag proteins.	116
Table 4. Myo1 dots outside bud neck in <i>mlc2Δ cdh1Δ</i> strains.	118

CHAPTER 1

Introduction

Cytokinesis

Cytokinesis is the complex process by which the cell divides after completing nuclear division (mitosis). In all eukaryotes, this process depends on the contraction of a ring of actin and non-muscle myosin (myosin II) that forms at the division site. The mechanisms that control the assembly, contraction, and disassembly of this ring are poorly understood (Robinson and Spudich, 2000; Glotzer, 2005; Eggert *et al.*, 2006).

Cytokinesis regulation has been extensively studied in fungal and animal cells. Research in the budding yeast *S. cerevisiae* and the fission yeast *S. pombe* has revealed in much detail the mechanisms of actomyosin ring assembly, composition, and contraction (Wolfe and Gould, 2005). In budding yeast, actomyosin ring contraction takes 5-7 minutes and is followed by septum formation and cell abscission (Kitayama *et al.*, 1997; Bi *et al.*, 1998; Lippincott and Li, 1998). The proteins responsible for cytokinesis in budding yeast have homologs in higher eukaryotes (including humans), suggesting that budding yeast is a valid model organism to study the fundamental molecular basis of cytokinesis (Tolliday *et al.*, 2001).

Cytokinesis Machinery

The cytokinesis machine is composed of proteins that power the three major steps of yeast cytokinesis: actomyosin ring contraction, septation, and abscission (Fig. 1). Upstream of these three processes are the septins. Preparations for cytokinesis begin in late G1 with the formation of a septin ring at the presumptive bud site (Versele and Thorner, 2005). The septin ring is composed of five septin subunits, all of which are GTP-binding proteins: Cdc3, Cdc10, Cdc11, Cdc12, and Sep7/Shs1. Septins have 2

functions in cytokinesis: (1) to recruit the cytokinesis proteins to the bud neck in late G1 (primarily Myo1 and Hof1, as discussed below); and (2) to act as a diffusion barrier to compartmentalize factors required for cytokinesis (Dobbelaere and Barral, 2004). As expected, temperature-sensitive septin mutants arrest as chains of cells at the restrictive temperature, characteristic of failure to cytokinesis. Further studies have revealed that at restrictive temperature, myosin ring contraction and disassembly are slower (Dobbelaere and Barral, 2004). In addition, components of the actomyosin ring are mislocalized as dots around the cell (Roh *et al.*, 2002; Iwase *et al.*, 2007).

Septins are recruited to the presumptive bud site in late G1 by the activity of the Cdc42 GTPase (Iwase *et al.*, 2006). Septins are GTP-binding proteins that form filaments *in vitro*. *In vivo*, septin filaments have also been seen by electron microscopy (Haarer and Pringle, 1987). Improvements in microscopy have greatly enhanced our model of septin ring dynamics during cell division. From its formation until anaphase, the septin ring appears as an hourglass. Polarized fluorescence microscopy of this hourglass structure showed that it consists of filaments aligned along the mother-daughter axis of the bud neck. In anaphase, the hourglass structure transitions into two circumferential separate rings after rotating 90 degrees along the plane of the membrane (Vrabioiu and Mitchison, 2006). After ring splitting, the 2 septin rings maintain a diffusion barrier that locks in the cytokinesis machinery around the bud neck during cytokinesis (Dobbelaere and Barral, 2004).

Shortly after the appearance of the septin ring, myosin II (called Myo1 in yeast) forms a ring at the bud neck in a septin-dependent manner (Fig. 1) (Bi *et al.*, 1998; Lippincott and Li, 1998; Luo *et al.*, 2004). Myo1, like myosin II, contains a heavy chain

that consists of an N-terminal motor domain and a C-terminal coiled-coil tail. The motor domain is required for motility along actin filaments, whereas the tail promotes bipolar filament formation. Sedimentation experiments suggest that Myo1 is a trimer (Lister *et al.*, 2006). Between the motor and coiled-coil tail lie the IQ1 and IQ2 domains, which are required for association with the myosin light chains. Regulatory light chain Mlc2 and essential light chain Mlc1 form rings that co-localize with the Myo1 ring early in the cell cycle. Mlc1 and Mlc2 bind directly to Myo1 via its IQ1 and IQ2 motifs, respectively (Luo *et al.*, 2004). As expected, Mlc2 ring formation requires the presence of Myo1; however, Mlc1 localization does not. Mlc1 associates with multiple proteins such as the type V myosin, Myo2, secretory vesicles, and IQGAP (Shannon and Li, 2000; Wagner *et al.*, 2002; Luo *et al.*, 2004). Its association with proteins other than Myo1 may provide alternate methods for the localization of Mlc1 to the bud neck.

In higher eukaryotes, phosphorylation of the regulatory light chain promotes myosin filament assembly and activation (Scholey *et al.*, 1980; Moussavi *et al.*, 1993); however, in budding yeast, Mlc2 does not appear to be controlled by phosphorylation. Mlc2 activity seems to disassociate myosin, as disassembly is delayed in cells lacking Mlc2 (Luo *et al.*, 2004).

Although myosin II is an actin motor, its localization is independent of filamentous (F)-actin. In fact, the minimum domain required for its localization is a 500 amino acid portion of its tail (Lister *et al.*, 2006). It is also interesting to note that the motor domain of Myo1 is not required for its cellular function (Lord *et al.*, 2005). Constructs lacking the motor domain were able to fully rescue a *myo1Δ* defect just as well as full-length Myo1. Myo1 needs to be localized to the bud neck for efficient

cytokinesis but its main function does not seem to require motor activity (Lord *et al.*, 2005).

Genetic evidence argues that there are two major cytokinesis mechanisms in budding yeast. In the S288C genetic backgrounds, Myo1 is not required for growth but *myo1Δ* cells are very sick (Watts *et al.*, 1987; Rodriguez and Paterson, 1990). A high percentage of *myo1Δ* cells form clusters of cells that have not completed cytokinesis. Over time, the *myo1Δ* colonies develop suppressors that over-activate the septation pathway (Schmidt *et al.*, 2002; Tolliday *et al.*, 2003). The ability of *myo1Δ* cells to grow demonstrates that there is an alternate pathway that leads to cytokinesis. This alternate pathway requires the activity of Cyk2/Hof1, an upstream activator of septation, as *hof1Δ* is synthetic lethal with *myo1Δ* (Vallen *et al.*, 2000). Although septation is highly irregular in *myo1Δ* cells, cell wall formation ultimately pinches apart the mother and daughter cells (Vallen *et al.*, 2000). The synthetic lethality of *myo1Δ* and *hof1Δ* demonstrates that there are 2 main pathways of cytokinesis in yeast: the actomyosin and the septation pathway.

Hof1, a member of the Pombe Cdc15 homology (PCH) family, is the most upstream activator of the septation pathway. The recruitment of Hof1 to the bud neck in G1/S requires the septin ring (Kamei *et al.*, 1998; Lippincott and Li, 1998). Similar to Myo1, Hof1 co-localizes with the septin ring until ring splitting, after which it co-localizes with the actomyosin ring (Vallen *et al.*, 2000). Genetic analysis showed that Hof1 is an upstream activator of the septation pathway. Concurrent with contraction, chitin synthase (Chs2) builds a primary septum immediately behind the invaginating plasma membrane (Fig. 2) (Cabib *et al.*, 2001; Schmidt *et al.*, 2002). After ring contraction, the primary septum reaches across the bud neck and secondary septa are then

deposited on both sides of the primary septum. Cell splitting occurs when Chs3, a chitinase, hydrolyzes the primary septum (Kuranda and Robbins, 1991; Colman-Lerner *et al.*, 2001) (Fig. 2).

Coinciding with septation, secretory proteins and vesicles concentrate at the bud neck (Fig. 2) (Finger and Novick, 1998). Their localization is dependent on type V myosin Myo2 activity. Precisely what the role of secretory vesicle recruitment to the bud neck after actomyosin ring contraction is unclear. One idea is that as the bud neck constricts, new plasma membrane must be deposited by fusion of the exocytosis machinery. However, how much new membrane deposition is needed at the cleavage furrow is questionable. Another model is that secretory vesicles act as carriers to transport proteins to the site of cytokinesis. It has been shown that the essential role for Mlc1 does not depend on its association with Myo1 or Iqg1 (discussed below) but rather its association with secretory vesicles (Wagner *et al.*, 2002).

The final preparations for cytokinesis occur as chromosomes separate in anaphase, when the protein Iqg1, a member of IQGAP family, coordinates actin recruitment and actomyosin ring contraction (Fig. 1) (Epp and Chant, 1997; Lippincott and Li, 1998; Osman and Cerione, 1998). Iqg1, like all IQGAPs, has multiple domains. The IQ repeat domain, which binds calmodulin-like proteins, is required for its recruitment to the bud neck via its interaction with Mlc1 (Boyne *et al.*, 2000; Shannon and Li, 2000). The Calponin Homology (CH) domain is required for actin localization, and this domain binds to actin filaments *in vitro* (Shannon and Li, 1999). Although Iqg1 lacks an identifiable GAP motif, it does have a GTPase Related Domain (GRD). In yeast, this domain has been shown to bind Tem1, a Ras superfamily small GTPase that is

involved in mitotic exit and cytokinesis (discussed below) (Shirayama *et al.*, 1994; Shannon and Li, 1999). In higher eukaryotes IQGAP associates with Cdc42 and Rac1, two Rho family small GTP-binding proteins (Brill *et al.*, 1996; Hart *et al.*, 1996; McCallum *et al.*, 1996). Iqg1 has also been shown to associate with other GTP-binding proteins such as the axial budding marker, Bud4, and the septin, Cdc12 (Osman *et al.*, 2002).

Actin filament formation at the bud neck is the last step towards building the cytokinesis machinery (Fig. 1). Actin recruitment is required for cytokinesis (even though the myosin II motor protein is not) and depends on two mechanisms: (1) Rho1 (Rho-type GTPase) activation of the formin-like proteins Bni1 and Bnr1 (Tolliday *et al.*, 2002); in many organisms, formins nucleate the formation of linear actin filaments; and (2) Iqg1/Cyk1, a member of the IQGAP family, which is recruited to bud neck by Mlc1 and binds actin filaments via its CH domain. It is unclear whether actin filament formation happens *de novo* at the bud neck or if pre-polymerized actin is recruited there (Epp and Chant, 1997; Lippincott and Li, 1998; Shannon and Li, 1999; Osman *et al.*, 2002).

Regulation of Cytokinesis Machinery

Cytokinesis must take place at the right place and at the right time. If the timing of cytokinesis is either too early or too late, chromosome segregation might be unequal and cells may become aneuploid. Proper cytokinesis requires precise orchestration of the cytokinesis machinery. In metazoans, this regulation seems to primarily center on myosin II activity by controlling the phosphorylation state of the regulatory light chain (MLC). Phosphorylation of MLC at Ser19/Thr18 promotes myosin II filament formation,

localization to the cleavage furrow, and association with actin, which allows for initiation of contraction (Scholey *et al.*, 1980; Moussavi *et al.*, 1993). Multiple proteins have been shown to regulate MLC phosphorylation, such as myosin light chain kinase (MLCK), Rho-associated protein kinase (ROCK), Citron Kinase, and myosin phosphatase (multiple kinases regulate myosin phosphatase activity as well) (Matsumura, 2005). In yeast, phosphorylation of the regulatory light chain does not appear to play a role in cytokinesis. Therefore, studies have been able to identify alternate pathways that regulate cytokinesis.

The NoCut pathway was recently identified as a regulatory mechanism that blocks the completion of cytokinesis, abscission, in response to spindle or midzone defects. The negative regulator in the NoCut pathway is Aurora Kinase (Ipl1) (Norden *et al.*, 2006). This is the first time that a checkpoint-like mechanism (abscission is delayed rather than permanently blocked) has been shown to regulate cytokinesis. Now that small-molecule inhibitors of Aurora kinases are available, the presence and significance of this pathway in higher eukaryotes can be investigated (Ditchfield *et al.*, 2003; Hauf *et al.*, 2003; Harrington *et al.*, 2004).

Cyclin dependent kinase (Cdk1) is a major cell cycle regulator that is required for progression through the cell cycle (Morgan, 1997). Similar to Aurora Kinase, Cdk1 is a negative regulator of cytokinesis. Cdk1 inactivation is required for cytokinesis, as expression of a non-degradable cyclin blocks cytokinesis (Wheatley *et al.*, 1997; Wäsch and Cross, 2002). Many Cdk1 substrates have been identified in budding yeast but the exact substrates whose phosphorylation block cytokinesis remain unknown (Ubersax *et al.*, 2003).

One group of candidate substrates are members of the mitotic exit network (MEN). Multiple MEN proteins are required for actomyosin contraction, but their activation and localization to the bud neck occurs only when Cdk1 activity is fully turned off (Jaspersen and Morgan, 2000; Menssen *et al.*, 2001). The MEN proteins that have been shown to function in cytokinesis are: Tem1, Mob1, Dbf2, Cdc15, and Cdc5 (Bardin and Amon, 2001; Wolfe and Gould, 2005). Members of the MEN group of proteins were originally identified in their role in activating the protein phosphatase Cdc14, which specifically reverses Cdk1-dependent phosphorylation. The dephosphorylation of MEN proteins by Cdc14 release serves as a positive feedback loop to further activate the MEN pathway (Jaspersen and Morgan, 2000). In addition, Cdc14-mediated dephosphorylation of the Cdk1 inhibitors Sic1 and Cdh1 promotes their activation and further attenuates Cdk1 function.

Originally, it was thought that MEN proteins activate cytokinesis by mediating the release of Cdc14 to lower Cdk1 activity; however, it is now understood that MEN proteins have a role in promoting cytokinesis independent of Cdc14 activation. Using mutants that bypass Cdc14 activation, it was shown that the Tem1 GTPase is required for septin ring splitting and actomyosin ring contraction. The association of Tem1 and Iqg1 may play a role in this regulation (Shannon and Li, 1999). Mutants of the kinase Cdc15 and Mob1 (a Dbf2-kinase associating protein) in the Cdc14 bypass background also fail to contract actomyosin rings (Luca *et al.*, 2001). In general, therefore, MEN proteins have two distinct roles in cytokinesis regulation: (1) Activate Cdc14 to reverse Cdk1 phosphorylation and attenuate Cdk1 activity; and (2) Promote actomyosin ring contraction.

The Polo-like kinase Cdc5, another MEN component, is required for assembly of the actomyosin ring through its phosphorylation of the Rho1 GEFs Tus1 and Rom2 (Yoshida *et al.*, 2006). Cdc5 kinase activity targeted toward these substrates promotes Rho1-GTP localization at the bud neck, which allows for proper actin recruitment.

The APC, a Possible Cytokinesis Regulator

Except for Aurora Kinase, most of the cytokinesis regulation described in the literature to date relates to the initiation of cytokinesis. Regulating the completion of cytokinesis is just as important because premature completion or incomplete cytokinesis may lead to aneuploidy in the progeny cells (Eggert *et al.*, 2006). One cell cycle regulator that could help control the completion of cytokinesis is the Anaphase-Promoting Complex (APC). The APC is an E3 ubiquitin ligase that together with E1 (ubiquitin-activating enzyme), E2 (ubiquitin-conjugating enzyme), and activators Cdc20 and Cdh1, covalently attaches polyubiquitinated chains to its substrates for subsequent degradation by the 26S proteasome (Peters, 2006; Thornton and Toczyski, 2006).

The APC is stable throughout the cell cycle but its activity oscillates, with low activity from Start to early mitosis and high activity in late mitosis and G1 (Amon *et al.*, 1994; King *et al.*, 1995; Lahav-Baratz *et al.*, 1995; Sudakin *et al.*, 1995; Brandeis and Hunt, 1996; Zachariae *et al.*, 1996). Activity requires the association of WD40 proteins Cdc20 and Cdh1 (Dawson *et al.*, 1995; Schwab *et al.*, 1997; Visintin *et al.*, 1997; Fang *et al.*, 1998; Lim *et al.*, 1998; Zachariae *et al.*, 1998). Cdc20 activates the APC from metaphase to late mitosis. Cdh1 takes over to complete mitotic exit and maintains APC activity during G1. In contrast to Cdc20, Cdh1 cannot activate the APC in the presence of

high Cdk1 activity (Amon, 1997; Zachariae *et al.*, 1998; Jaspersen *et al.*, 1999). Thus, APC^{Cdh1} is not active until mitotic exit when Cdk1 activity is low.

There is some evidence to support the hypothesis that the APC directly regulates cytokinesis: (1) APC mutants fail to complete cytokinesis; (2) The APC is active during cytokinesis; (3) (Straight *et al.*, 2003), demonstrated that proteasome inhibition in HeLa cells lengthened the window of time in which cytokinesis can occur, and this was independent of Cdk1 inactivity; (4) (Shuster and Burgess, 2002), demonstrated that APC activity, not Cdk1 inactivation, is required for cleavage furrow formation in sea urchin embryos; and (5) Many of the yeast cytokinesis proteins contain APC substrate recognition signals and their levels oscillate during the cell cycle, characteristic of an APC substrate.

APC substrates contain either a destruction box (D-box) motif with the amino acid sequence RxxLxxxxN (Glotzer *et al.*, 1991) or a KEN-box motif with the amino acid sequence KENxxxN/D/S (Pfleger and Kirschner, 2000). New APC recognition sequences have been identified as more and more substrates are discovered, but they have not been shown to be as prevalent as the D- or KEN-box (Sullivan and Morgan, 2007). Scanning the sequences of cytokinesis proteins reveals that Hof1 contains a D-box and is absent in G1 when APC^{Cdh1} is active. Iqg1 contains 2 D-boxes and is also absent in G1 arrested cells (Lippincott and Li, 1998). Myo1 also contains 2 D-boxes and 2 KEN boxes (see Appendix Table1 for a list of all cytokinesis proteins).

The APC was first discovered over 10 years ago and has two essential functions in cell division: (1) To mediate the destruction of Securin (Pds1) so that sister chromatids can separate and initiate anaphase; and (2) To mediate the destruction of mitotic cyclins,

which causes Cdk1 activity to drop, allowing the cell to exit mitosis, complete cytokinesis, and reset origins for the next round of cell division (Thornton and Toczyski, 2003). Several other proteins have been identified as APC substrates, which suggests that the APC helps control other cell cycle processes as well. These substrates include proteins involved in spindle stability (Ase1, Fin1) (Juang *et al.*, 1997; Woodbury and Morgan, 2007) and elongation (Cin8, Kip1) (Gordon and Roof, 2001; Hildebrandt and Hoyt, 2001), mitotic exit (Cdc5, Spo12) (Charles *et al.*, 1998; Shirayama *et al.*, 1998; Shah *et al.*, 2001), DNA replication (Dbf4) (Cheng *et al.*, 1999; Oshiro *et al.*, 1999; Ferreira *et al.*, 2000), mitotic entry (Hsl1) (Burton and Solomon, 2001), and its own activity (Cdc20) (King *et al.*, 1995; Shirayama *et al.*, 1998). Although Pds1 and the mitotic cyclins are the only substrates whose destruction by the APC is required for the cell cycle (Thornton and Toczyski, 2003), the timely destruction of the other known substrates is thought to increase the efficiency and robustness of cell cycle progression (Rape *et al.*, 2006). Thus, APC regulation of cytokinesis may promote efficient cytokinesis by cooperating with additional regulatory pathways to turn off the cytokinesis machine before the start of the next cell cycle.

FIGURES

Figure 1. Actomyosin ring formation in the cell cycle. The septin ring, followed by the myosin II ring, is formed in late G1. Upon Cdk1 inactivation and Cdc14 activation, Iqg1 forms a ring at the bud neck, which promotes the concentration of F-actin. Once the cytokinesis machine is successfully assembled, the cell undergoes cytokinesis. Diagram courtesy of David Morgan from “The Cell Cycle: Principles of Control.”

Figure 1.

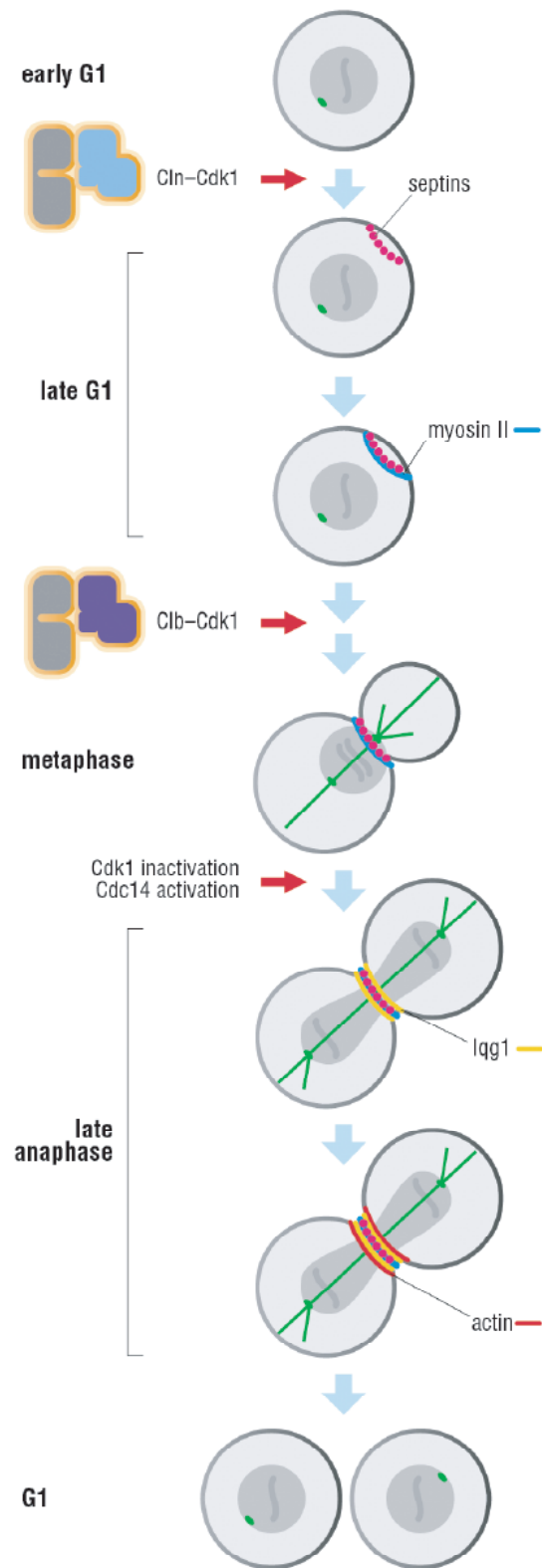


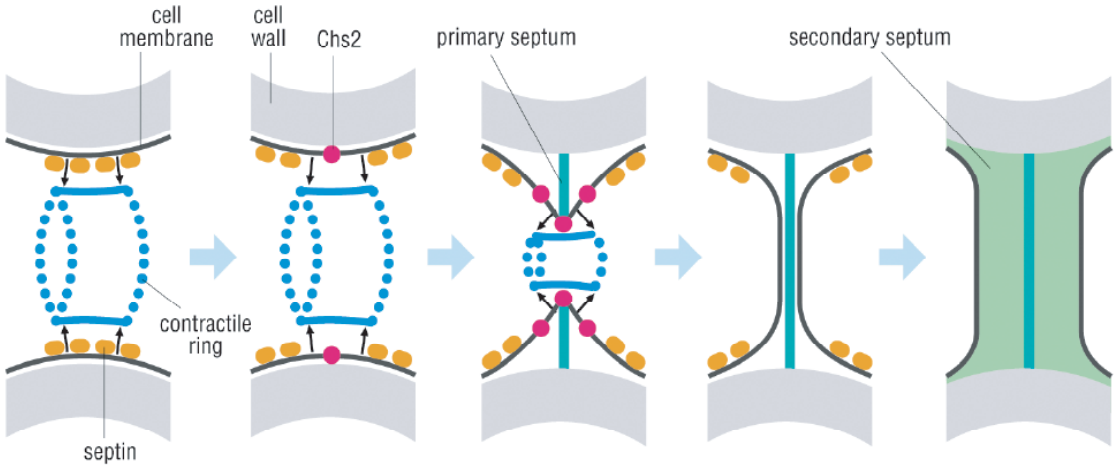
Figure 2. Contraction and septation are simultaneous. (A) The diagram models the formation of the primary and secondary septa concurrent with bud neck contraction.

Diagram courtesy of David Morgan from “The Cell Cycle: Principles of Control.”

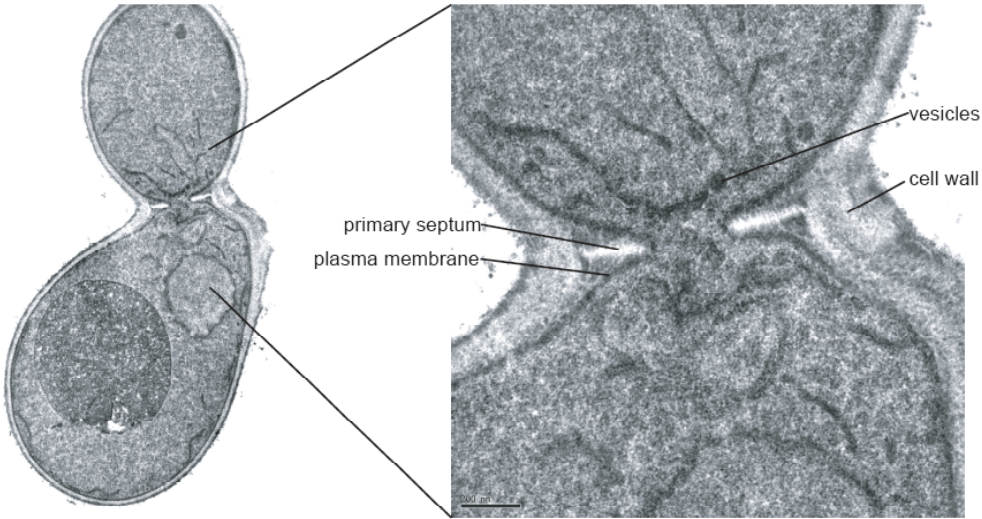
(B) Electron micrographs of a budding yeast cell taken during cytokinesis. The primary septum is visible behind the contracting plasma membrane. Vesicles are visible adjacent to the invaginating plasma membrane. The cell wall is also shown. Images courtesy of S. Bernales.

Figure 2.

A.



B.



CHAPTER 2

Identification of Iqg1 as a novel APC^{Cdh1} substrate

RESULTS

APC substrate screen of cytokinesis proteins

To identify novel APC substrates involved in cytokinesis, we set up a screen to select cytokinesis proteins whose levels fluctuated in a manner characteristic of an APC substrate—abundant in G2/M when the APC is inactive and absent in G1, when the APC is active. We screened 110 proteins that were known to function in cytokinesis based on their description in the *Saccharomyces* Genome Database. We were able to locate 103 of the 110 proteins in the tandem affinity purification (TAP) tag library, a library of strains in which most open reading frames are fused to a TAP tag consisting of two immunoglobulin-binding domains of protein A from *Staphylococcus aureus* (zz-tag), a cleavage site for the tobacco etch virus (TEV) protease, and the calmodulin-binding peptide (CBP) (Rigaut *et al.*, 1999; Ghaemmaghami *et al.*, 2003). We grew up the 103 TAP tag strains to log phase and then arrested them in G1 or G2/M by addition of alpha-factor or nocodazole, respectively. The arrested cultures and a culture of log-phase cells were harvested and lysed in urea buffer to extract as much protein as possible. Protein abundance of the TAP tag protein for each condition was analyzed by polyacrylamide gel electrophoresis (PAGE) and Western blotting against the zz-tag. We analyzed the cell cycle abundance for each protein at least twice. Of the 103 proteins tested, 78 had a visible band on a Western blot. Of these 78 proteins, 7 were repeatedly abundant in G2/M and absent in G1. Western blots for these candidates are shown in Fig. 1 (see Appendix Table 1 for data of all 103 proteins). The 7 APC candidates are: Iqg1, Hof1, Mob1, Bud4, Tem1, Elm1, and Bud2. Iqg1 and Hof1 are regulators of the actomyosin ring and

separation pathway. Mob1 and Tem1 are components of the Mitotic Exit Network (MEN), which is required for full activation of Cdc14, a phosphatase that targets Cdk1 substrates. (3) Bud4, Bud2, and Elm1 are involved in budding and bud morphogenesis. Interestingly, Bud4 is a distant homolog of Anillin, a contractile ring protein in higher eukaryotes and a known APC substrate (Zhao and Fang, 2005).

All candidates except Bud2 have a cell cycle transcription profile. This is characteristic of APC substrates because they need to be re-synthesized at some point during the cell cycle after their degradation. In addition, Iqg1, Hof1, and Elm1 all have either a D- or KEN-box. The fact that Mob1, Bud4, Tem1, and Bud2 do not contain these APC recognition motifs is intriguing as new substrates have recently been identified with novel recognition sequences (Sullivan and Morgan, 2007). At the bottom of Fig. 1 we included Skt5 to illustrate a protein that is not considered an APC candidate. Skt5 is transcribed in a cell cycle dependent manner and contains both a D-box and KEN sequence but its protein levels are not cell cycle regulated, as it is abundant in both G1 and G2/M.

These 7 proteins fit the profile of an APC candidate but their cell cycle instability could be due to a number of factors independent of APC activity, such as inherent protein instability, degradation mediated by other E3 ubiquitin ligases, or lysosomal degradation. Thus, further analysis was necessary to determine whether any of the 7 proteins are APC substrates.

***In vitro* APC ubiquitination assays of the candidate proteins**

To further test whether these candidates are APC substrates, we carried out *in vitro* ubiquitination reactions of these 7 proteins using ^{35}S -labeled *in vitro* transcribed and translated substrate. The results of the reactions are shown in Fig 2. We used Pds1 (securin) as a positive control in all reactions. Upon addition of APC^{Cdh1}, Pds1 is ubiquitinated and the ubiquitinated products form a ladder of slower migrating bands when analyzed by PAGE (second lane from left Fig. 2A, B). Of all the candidates tested, only Iqg1 showed slower migrating bands upon addition of APC^{Cdh1} (Fig. 2A, B). Neither Hof1 nor Elm1 were ubiquitinated despite containing a D-box and/or KEN sequence. In fact, Hof1 was recently identified as a substrate of the SCF^{Grr1} (Blondel *et al.*, 2005). This explains its cell cycle abundance profile and also highlights the specificity of the *in vitro* APC ubiquitination reaction: A protein with a D-box and KEN sequence, which contains lysines available for ubiquitination, was not recognized by APC^{Cdh1}.

As Iqg1 was ubiquitinated *in vitro* by the APC, abundant in G2/M, and absent in G1-arrested cells, we next wanted to determine whether it is a bona fide APC substrate *in vivo*. We first compared its turnover in cells arrested in G1 and G2/M by doing a pulse chase of *GAL-IQGI-TAP* (*IQGI* transcription was induced by addition of galactose, then halted by addition of dextrose, and protein samples were taken at the designated time thereafter). As expected, Iqg1 was unstable in G1-arrested cells and stable in G2/M cells (Fig. 3A). The half-life of Iqg1 was about 20 minutes in G1 cells. We next tested whether this instability requires APC activity. We compared the turnover of Iqg1-TAP in 2 strain backgrounds: (1) wild-type and (2) a temperature sensitive *cdc23-1* mutant (Cdc23 is a key subunit of the APC). We grew both strains to log phase at the permissive temperature (room temperature), arrested the cells in G1 with alpha-factor and then shifted to the

restrictive temperature (37°C) for 30 minutes to inactivate the APC before adding dextrose. Iqg1 was degraded in the wild-type strain but stable in the *cdc23-1* background (Fig. 3B). Therefore, the G1 instability of Iqg1 depended on APC activity. We then monitored Iqg1 abundance when expressed from its endogenous promoter in synchronized cells. Cells were arrested in G1 with alpha-factor and then released into the next cycle by washing out the pheromone. As expected, no Iqg1 was present in G1-arrested cells (Fig. 3C). 30 minutes after release, its levels rose with those of the cyclin Clb2, a well-characterized APC substrate. At 60 minutes, Iqg1 abundance peaked and then abruptly fell off, disappearing by the 90 minute point. Iqg1's cell cycle instability mirrored that of Clb2, except that Iqg1 levels dropped one time point (15 minutes) later. Clb2 is degraded upon exit from mitosis but Iqg1 was degraded later, indicating that it may be a worse APC substrate. This one possible explanation of how Iqg1 avoids premature degradation by the APC until its function in cytokinesis is complete.

The observation that Iqg1 was degraded after Clb2 suggests that its ubiquitination is activated by Cdh1 and not Cdc20. All of the known Cdc20-specific substrates (Pds1, Clb5, and Dbf4) are degraded upon entry into mitosis, but Iqg1 was not degraded until exit from mitosis or even after cytokinesis. Cdc20 is targeted for ubiquitination and hence degradation by APC^{Cdh1} concurrent with Clb2. As Iqg1 was degraded after Clb2, when Cdc20 is fully destroyed, then Cdh1 must be the activator that targets it for ubiquitination.

After identifying Iqg1 as a bona fide APC^{Cdh1} substrate, we next set out to identify the region on Iqg1 that is required for its recognition by APC^{Cdh1}. Fig 4A shows a diagram of the characterized domains of Iqg1. As mentioned above, it contains 2 D-boxes

and 2 KEN sequences in the N-terminal half (indicated by (*) in Fig. 4A). By taking advantage of the *in vitro* transcription and translation system, we divided Iqg1 into 3 overlapping fragments to identify the regions required for ubiquitination. Fig. 4B shows the APC^{Cdh1} ubiquitination reactions of these fragments. A fragment containing the first 750 amino acids was ubiquitinated by the APC. As shown in the diagram in Fig. 4A, this fragment contained the 2 D-boxes and 2 KEN sequences. However, when we deleted the first 42 amino acids, no ubiquitinated products were visible even though this construct (43-750) contained all the known destruction sequences. In addition, we tested the 1-750 fragment of Iqg1 but with the key amino acids of the D-boxes and KEN sequences mutated to alanine, and it was still ubiquitinated by the APC (data not shown). Therefore, the D-boxes and KEN sequences in Iqg1 are not required for ubiquitination by the APC and the true destruction sequence must lie in the first 42 amino acids.

We studied the amino acid sequence of this region and identified residues that resembled a D-box between amino acids 33 and 43. The D-box sequence is RxxLxxxxN whereas the sequence on Iqg1 is RxxSxxxxN. Although leucine and serine are chemically different, the presence of the exact spacing between the arginine and asparagine suggested it may be recognized by the APC. To specifically test these amino acids, we *in vitro* transcribed and translated a fragment of Iqg1 that contained alanine substitutions of each candidate residue and combinations thereof (Fig 4C). Mutation of either R34, S37, or K40 to alanine significantly decreased ubiquitination, and mutation of all three residues together (plus the final N) brought substrate ubiquitination down to background levels (Fig. 4C). We also tested whether substituting the S for an L would increase substrate ubiquitination as it more closely resembled a classic D-box. Substituting S for L

proved to be inhibitory to ubiquitination (Fig 4C). In addition, K39 was also important for ubiquitination (data not shown). As we did not test more surrounding residues, we do not know if mutating any other residues in this region would also have affected ubiquitination.

Thus far, we have demonstrated that a D-box like sequence in the N-terminus of Iqg1 is required for ubiquitination by APC^{Cdh1}. To test if this same region is also required for ubiquitination and degradation *in vivo*, we performed pulse-chase experiments comparing wild type *GAL-IQG1-TAP* to *GAL-Δ42-iqg1-TAP* in G1-arrested cells (Fig 5A). Wild-type Iqg1 was unstable but Δ42-iqg1 was stable. This suggests that the first 42 amino acids of Iqg1 are in fact required for recognition by the APC. We further analyzed the cell cycle abundance of Δ42-iqg1-TAP, expressed from its endogenous promoter. As expected, Δ42-iqg1-TAP levels rose with Clb2 but did not drop off (Fig. 5B). The mutant was stable throughout the cell cycle and even while cells were re-arrested in G1. We did notice that the initial levels of Δ42-iqg1-TAP were low in G1 arrested cells (Fig. 5B 0 min). We believe this is due to inherent protein instability, independent of APC activity. At 75 and 90 min, Clb2 levels dropped off yet Δ42-iqg1-TAP levels did not change. Instead, Δ42-iqg1-TAP levels seemed to gradually decrease over time.

To summarize, the APC^{Cdh1} destruction sequence is located within the first 42 N-terminal residues of Iqg1. Based on *in vitro* studies, R34, S37, K40, and N42 are important for recognition by the APC. When we tested the stability of Iqg1 with only the R, S, and N mutated to A in G1-arrested cells, it was still turned over (data not shown). This has also been seen for other well-characterized APC substrates such as Cdc5 and Clb5 (data not shown). Simply mutating the important residues of the D-box to alanine

did not block its degradation *in vivo*. Instead, deletion of the D-box was the only way to fully stabilize the substrate *in vivo*.

The non-degradable $\Delta 42$ -*iqg1* strain was viable and showed no obvious morphological defects. As Iqg1 is an APC^{Cdh1} substrate and a *cdh1* Δ is viable (even though it has gross morphologic abnormalities such as large cells, chains of cells, and slower doubling time), then it is not surprising that cells could survive with stable Iqg1. In collaboration with the Pringle laboratory at Stanford University, we discovered that a strain lacking *MYO1* (which is essential in the S288C yeast background) could survive only in the presence of non-degradable Iqg1 (Fig. 5C) (Ko *et al.*, in press). In the W303 background, *MYO1* is not essential but very sick—a large percentage of cells cluster, characteristic of a cytokinesis phenotype. Consistent with the S288C result, the presence of non-degradable $\Delta 42$ -*iqg1* in a *myo1* Δ (W303) significantly improved viability and reduced cell clustering (Ko *et al.*, in press).

Although non-degradable Iqg1 did not cause any cell cycle defects when expressed at endogenous levels, it caused severe growth defects when overexpressed (whereas overexpressed wild-type Iqg1 was viable) (Fig. 5D). Iqg1 binds to multiple proteins whose activities are essential in the cell cycle. It is possible that overexpressing nondegradable Iqg1 produces so much protein that it sequesters these essential proteins. One candidate is Mlc1, an essential protein that binds the IQ motifs on Iqg1 and is thought to be limiting in the cell (Tolliday *et al.*, 2003). Interpreting data from overexpression of proteins is problematic, but the fact that high levels of Iqg1 was lethal to the cell highlights how important it is for the APC to keep Iqg1 levels in check.

DISCUSSION

The goal of the work described in this section was to discover APC substrates that function in cytokinesis. We began with a simple *in vivo* approach, followed by a sensitive *in vitro* assay, which enabled us to screen through numerous cytokinesis proteins and led to the identification of Iqg1 as a novel APC^{Cdh1} substrate. Iqg1 was absent in G1-arrested cells, when the APC^{Cdh1} is active, and present in G2/M-arrested cells when the APC is inactive. Iqg1 degradation in G1 depended on APC activity, and furthermore, its protein levels rose and fell like those of the Cdk1 cyclin, Clb2, a well-described APC^{Cdh1} substrate. We also observed that Iqg1 was directly ubiquitinated by APC^{Cdh1} *in vitro*. Its ubiquitination did not require classic D-boxes and KEN sequences; in fact, a D-box-like sequence located in the first 42 amino acids was required for ubiquitination *in vitro*. This region was also required for its degradation *in vivo*, as deletion of this domain stabilized Iqg1 throughout the cell cycle.

Iqg1 is related to the IQGAP family of proteins (Brown and Sacks, 2006). In budding yeast, Iqg1 contributes to cytokinesis by promoting both actomyosin ring contraction and septation (Epp and Chant, 1997; Shannon and Li, 1999). As Iqg1 is an essential activator of both pathways that lead to mother-daughter cell separation, then its degradation in G1 would irreversibly shut off the cytokinesis machine and ensure that the cell does not attempt a premature cytokinesis in the following cell cycle. When Iqg1 was stabilized by deletion of the first 42 amino acids, it was able to promote cytokinesis even in the absence of *MYO1*.

Our characterization of the APC recognition sequence on Iqg1 was incomplete for 2 reasons: (1) Every amino acid we mutated to alanine negatively affected its ubiquitination. As we did not identify an amino acid in that region whose substitution to alanine did not affect ubiquitination, we do not know whether there is a hierarchy of important residues. (2) We did not determine whether this region is sufficient for ubiquitination by the APC. Although the smallest construct we used in *in vitro* reactions was 250 amino acids, further experiments that minimize this region would allow for a better description of the recognition sequence. Although our analysis of the APC recognition sequence is incomplete, our experiments revealed a novel APC recognition sequence (RxxSxxKxN).

The presence of a serine instead of the typical leucine at position 4 in the sequence may in fact confer lower substrate affinity to APC^{Cdh1}. [this is pretty speculative stuff] This is supported by the observations that Iqg1 was degraded after Clb2, which contains one D-box and multiple KEN boxes (Hendrickson *et al.*, 2001; Schwab *et al.*, 2001). *In vitro*, Iqg1 appeared to be a poorer substrate than Pds1. The *in vitro* ubiquitination reactions in Fig. 4 used methylated ubiquitin, which prevents the formation of ubiquitin chains. This enhanced the production of multi-ubiquitin products and increased the signal of the mono, di, and tri-ubiquitinated products. When we used wild-type ubiquitin in the reactions, Iqg1 appeared to be a significantly poorer substrate than Pds1 (data not shown). APC substrate preference is an interesting problem that has recently begun to be explored (Rape *et al.*, 2006). Budding yeast is an ideal organism to compare substrate preference *in vivo* because many APC substrates can be simultaneously tagged and cells can be synchronized with high temporal resolution.

Future experiments that clearly define the order of degradation of APC^{Cdh1} substrates (Clb2, Cdc20, Cdc5, Ase1, Fin1, Kip1, Spo12, Hsl1, and Iqg1), in combination with *in vitro* data, may provide clues to the ordering of APC substrate ubiquitination and how it is achieved.

The cell cycle abundance screen identified 7 proteins that were low in abundance in G1 and abundant in G2/M. Of these 7 proteins, only Iqg1 was identified as an APC substrate (based on *in vitro* APC reactions). Hof1 was later identified as a SCF substrate. This leads us to ask how the abundance of other 5 proteins is regulated. Although the *in vitro* APC reactions of these 5 proteins did not show any ubiquitinated products, it is still possible that degradation *in vivo* may require APC activity. We believe this explanation unlikely as all of the known APC^{Cdh1} substrates tested by the *in vitro* assay have been successfully ubiquitinated (data not shown). However, to definitely demonstrate whether the absence of protein in G1 requires APC^{Cdh1} activity, cells deleted for both *CDH1* and *CLB2* could be arrested in G1 with alpha-factor (*CLB2* must be deleted so that cells lacking *CDH1* can arrest in G1; (Schwab *et al.*, 1997) and the TAP tag protein levels analyzed by Western blotting. Independent of the outcome, determining the exact timing of degradation in the cell cycle for these 5 proteins may provide clues about how they are turned over.

The SCF is another ideal E3 candidate that may mediate the turnover of these 5 proteins in the cell cycle. Recently, a proteomic screen was carried out in search of novel SCF^{Grr1} substrates (Benanti *et al.*, in press). Among our 5 candidate proteins, only Bud4 showed faint signs of substrate activity *in vivo* (personal communication, Dr. Jennifer Benanti).

Although our screen led to the discovery of a novel APC substrate, it was far from complete. A more comprehensive approach could have included all of the bud neck localized proteins (58 more proteins). On the other hand, only testing proteins that were known to function in cytokinesis assured us that the degradation of candidate proteins might actually contribute to cytokinesis control. In addition, our candidates were biased in that they were mostly activators of cytokinesis. If the APC^{Cdh1} mediates the destruction of an inhibitor, then it was most likely not chosen for the screen.

Some of the lessons we learned from taking this approach to identify novel APC substrates are: (1) Rather than focus on proteins involved in a process, it seems more fruitful to focus on all proteins whose transcription is cell cycle regulated (about 1000 genes, (Spellman *et al.*, 1998). To date, the transcription of all known APC substrates is cell cycle regulated. If the cell destroys a protein then it must re-synthesize it at some point during the cell cycle. (2) Recently a screen comparing the fluorescence of GFP tagged proteins (from the GFP library) between wild-type and *grr1Δ* cells was used to identify SCF^{Grr1} substrates in budding yeast (Benanti *et al.*, in press). This screen did not require Western blotting to analyze protein levels, which can be influenced by lysis conditions and antibody disparities, and it was automated to screen the yeast proteome. This approach could be used to comprehensively search for novel APC substrates. The E3 mutant strain could be a *cdh1Δ* or deletion of non-essential subunits of the holoenzyme. (3) Any substrate identified in these screens must be tested for direct APC ubiquitination, so another approach would be to test all the cell cycle regulated proteins in batch APC reactions. Lysates of TAP tag strains could be pooled together, bound to

IgG beads, and then subjected to APC *in vitro* reactions using radiolabeled ubiquitin assays. Any APC target that receives a radioactive ubiquitin can then be quickly detected using a scintillation counter. Another advantage to performing APC reactions while candidate substrates are bound to beads is that the APC components (E1, E2, APC, Cdh1, ATP, ubiquitin) are removed after the reaction and can immediately be used on another batch of TAP tag proteins bound to beads. This method would need to be optimized using known APC substrates as positive controls but it may provide a quick approach to screen for direct substrates.

There is an inherent problem with identifying novel APC^{Cdh1} substrates. As *CDH1* is not essential, the destruction of any APC^{Cdh1} substrate will not greatly affect the cell cycle. Rendering the substrates non-degradable will not halt the cell cycle, so understanding how its degradation contributes to the cell cycle is difficult. Sensitive bioassays such as monitoring the dynamics of cell cycle markers by fluorescence microscopy (as done in the following chapter) is a powerful way to describe any defects associated with stabilizing an APC^{Cdh1} substrate. Alternatively, manipulating the genetic background to sensitize cells to the presence or absence of the APC^{Cdh1} substrate (as done with the non-degradable Iqg1 in a *myo1Δ* background) is another approach that can shed light on how APC regulation of these proteins contributes to cell division.

One reason to pursue the identification of substrates whose degradation is not essential for a normal cell cycle is that cancer cells routinely stimulate or inhibit parallel pathways to promote their uncontrolled proliferation (Morgan, 2007). As the degradation of these substrates in wild type cells is not essential, therapies that target their stabilization or degradation may specifically block proliferation of cancer cells.

MATERIALS AND METHODS

Strains, Plasmids, Growth Conditions, and Genetic Methods

All strains were based on the W303 or S288C genetic background as indicated and were grown at 30 °C unless otherwise indicated. 2% glucose was used as carbon source except for experiments involving induction of gene expression under control of the *GAL* promoter, for which 2% raffinose plus 2% galactose were used. Standard procedures were used for growth of *Escherichia coli*, genetic manipulations, polymerase chain reaction (PCR), and other molecular biological procedures (Guthrie and Fink, 1991).

To construct $\Delta 42$ -*iqg1*-TAP strain, the *Iqg1*-TAP strain from the TAP-tag library (Ghaemmaghami *et al.*, 2003) was transformed with plasmid pGT04. Plasmid pGT04 was constructed using two steps of PCR. In the first step, a fragment of *IQG1* (nucleotides -262 to +3 relative to the A of the start codon) was amplified from genomic DNA with a *Bam*HI site incorporated into the 5' primer and a 3' primer that included nucleotides corresponding to positions +127 to +141 of *IQG1*. A second fragment (nucleotides +127 to +277) was also amplified from genomic DNA using a 5' primer that included nucleotides corresponding to positions -15 to +3 of *IQG1* and a 3' primer that included an *Xba*I site. In the second step, the PCR products from the first step were purified and used as template with the *Bam*HI-site-containing 5' primer and the *Xba*I-site-containing 3' primer. The resulting product, which contained 262 nucleotides of the *IQG1* promoter, a start codon, and 151 nucleotides (from +127 to +277) of open-reading-frame sequence, was cut with *Bam*HI and *Xba*I, gel-purified, and inserted into *Bam*HI/*Xba*I-cut pRS305 (Sikorski and Hieter, 1989).

Plasmids p*GAL-IQG1-TAP* and p*GAL-Δ42-iqg1-TAP* were constructed by transforming W303 *MAT a* yeast cells with *Bam*HI/*Hind*III-cut pRSAB1234 with PCR-amplified full-length or truncated (lacking codons 2-42) *IQG1*; the amplified fragment contained 22 (5') and 21 (3') base pairs of flanking vector sequences to allow the *in vivo* recombination.

APC Substrate Screen

All strains used were from the TAP tag library (Ghaemmaghami *et al.*, 2003). Strains were grown to Log phase (O.D. 0.2) then arrested in G1 with 10mg/ml α -factor (Sigma-Aldrich, St. Louis, MO) or arrested in G2/M with 10mg/ml of nocodazole (Sigma-Aldrich, St. Louis, MO). When >90% of cells were arrested (3-4 hours later) 5ml of culture was collected by centrifugation, washed in water, and cell pellets were snap-frozen in liquid nitrogen.

To extract proteins (as described in (Ubersax *et al.*, 2003)), cell pellets were re-suspended in 200ml of Urea buffer (20mM Tris pH 7.4, 8M Urea, 2M Thiourea, 4% CHAPS, 1% DTT, 50mM NaF, 80mM beta-Glycerophosphate, 1mM Na₃VO₄, 1mM PMSF) and 0.5mm glass beads (to just below meniscus) were added. The cells were vigorously shaken in a bead beater 3 times for 1 min with 1 min rest in between. Cell lysates were spun out of tubes by poking a hole in the bottom with a 21.5 gauge needle and centrifuged in a microfuge at 7,000 rpm for 30 seconds. Cell lysates were then spun in a microfuge at 14,000 rpm for 10 min to spin down cell debris. Supernatants were collected and protein assays were calculated using Bradford method. 10ug of protein were loaded (4-10% polyacrylamide gels depending on average size of TAP-tag proteins)

with SDS sample buffer in each lane. TAP-tag levels were determined by Western blotting using a rabbit polyclonal anti-c-MYC primary antibody (Santa Cruz Biotechnology, Santa Cruz, Cat. No. SC-764), an HRP-conjugated donkey anti-rabbit-IgG secondary antibody (Amersham, Arlington Heights, Cat. No. NA934V). Western blotting was also done using peroxidase anti-peroxidase soluble complex produced in rabbit (Sigma-Aldrich, Cat. No. P1291). All blots were further analyzed with SuperSignal West Pico chemiluminescence system (Pierce Biotechnology, Rockford, IL).

APC Ubiquitination Assays

To perform ubiquitination assays, reaction components were expressed and purified as described previously (Carroll and Morgan, 2005). Substrates were produced in rabbit-reticulocyte lysates by coupled transcription and translation in the presence of ³⁵S-methionine, following the manufacturer's instructions (Promega) (see (Sullivan and Morgan, 2007)). For all candidates tested, a T7 promoter sequence and Kozak site added upstream were made using two steps of PCR. In the first step, the desired fragment was PCR-amplified using a 5' primer containing a sequence of 23 nucleotides that overlapped the 5' primer used in the second step plus 30-40 nucleotides of coding sequence beginning with a start codon. The 3' primer contained ~50 nucleotides of coding sequence ending with a stop codon. In the second step, the product from the first step was used as template with the same 3' primer and a 5' primer of 119 nucleotides that included a T7 promoter and a Kozak site. Point mutations in the *IQG1* sequence (Fig. 4) were introduced by incorporation into the 5' primer used in the first step. Ubiquitination reactions were performed and monitored using a Molecular Dynamics PhosphorImager

(GE Healthcare) as described previously (Carroll and Morgan, 2002, 2005).

GAL-Iqg1-TAP Pulse Chase Assays

Strains containing *pGAL-IQG1-TAP* or *pGAL-Δ42-iqg1-TAP* were grown to Log phase in YP medium containing 2% raffinose (30°C) as sole carbon source (Fig. 3B at 23°C), arrested in G1 or G2/M by treatment with 1 mg/ml α -factor or 10mg/ml nocodazole respectively for 4 h. Galactose (2%) was then added to induce protein expression for 1hr at room temperature (23°C), after which dextrose (2%) and cycloheximide (100 mg/ml) were added to block both transcription and translation of the *IQG1* constructs. 5ml samples were taken at the time of glucose and cycloheximide addition and at intervals thereafter. Cells were lysed in urea buffer as described above. Protein was extracted and analyzed by Western blotting. Iqg1-TAP and Δ 42-Iqg1-TAP were detected using the peroxidase anti-peroxidase soluble complex produced in rabbit (Sigma-Aldrich, Cat. No. P1291) and the SuperSignal West Pico chemiluminescence system (Pierce Biotechnology, Rockford, IL).

Iqg1-TAP Cell Cycle abundance

Strains *IQG1-TAP* and *Δ42-iqg1-TAP* were grown to Log phase in YP medium at 30°C, arrested in G1 phase by treatment with 10 μ g/ml α -factor for 4 h, and released from the arrest by washing once and resuspending in fresh YP medium. When 90% of the cells had budded, 10 μ g/ml α -factor was added again to prevent the initiation of new cell cycles. 5 ml samples were taken at the time of release from α -factor arrest and at intervals thereafter. Cells were lysed in urea buffer as described above. Proteins

(including Clb2 as a control) were analyzed by Western blotting. Iqg1-TAP and $\Delta 42$ -*iqg1*-TAP were detected using the peroxidase anti-peroxidase soluble complex produced in rabbit (Sigma-Aldrich, Cat. No. P1291). Clb2 was detected using a rabbit polyclonal anti-Clb2 primary antibody (Kellogg and Murray, 1995), an HRP-conjugated donkey anti-rabbit-IgG secondary antibody (GE Healthcare), and the SuperSignal West Pico system.

FIGURES

Figure 1. APC substrate candidates identified in protein screen. The 7 out of 103 proteins that were identified in the cell cycle arrest screen (described in Materials and Methods) are shown with their corresponding transcription peak; number of potential Cdk1 sites; D-box and KEN sequences; and duplicate Western blots illustrating their absence in G1 and presence in G2/M arrested cells. Skt5 is shown as a negative result even though it contains D-box and KEN sequences.

Figure 1.

A. APC candidates




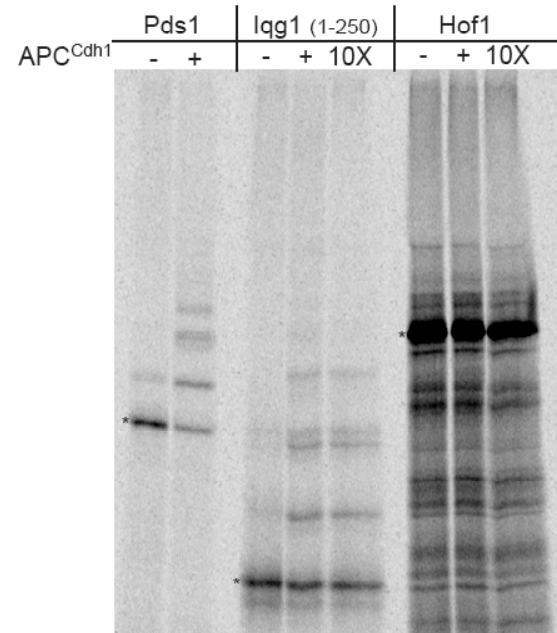
protein	peak	Cdk sites	D-box	KEN	G1-G2/M-G1-G2/M
IQG1	G2/M	4	2	2	
HOF1	G2/M	0	1	1	
MOB1	G2/M	2	0	0	
BUD4	G2/M	6	0	0	
TEM1	G2/M	0	0	0	
ELM1	S/G2	1	0	1	
BUD2		1	0	0	
SKT5	M/G1	0	1	1	

Figure 2. Iqg1 is the only APC substrate candidate ubiquitinated by APC^{Cdh1}. (A) Full length Pds1, the first 250 amino acids of Iqg1, and full length Hof1 were transcribed and translated *in vitro* and subjected to APC^{Cdh1} ubiquitination reactions as described in Materials and Methods. The unmodified substrate is identified with an (*). The -/+ columns indicate absence or presence of APC^{Cdh1} in the reaction. Ubiquitinated products are characterized by the presence of slower migrating bands corresponding to mono, di, tri, etc. ubiquitinated substrate. See Pds1 (+) and Iqg1 (+). (B) Same as above but for the remaining 5 APC substrate candidates shown in Fig. 1. Due to the 100 kDa size limit of the *in vitro* transcription and translation system, Bud2 (127 kDa) and Bud4 (165 kDa) were split into two overlapping constructs Bud2a: 1-829, Bud2b: 445-1104, Bud4a: 1-766, and Bud4b: 748-1449.

Figure 2.

A.



B.

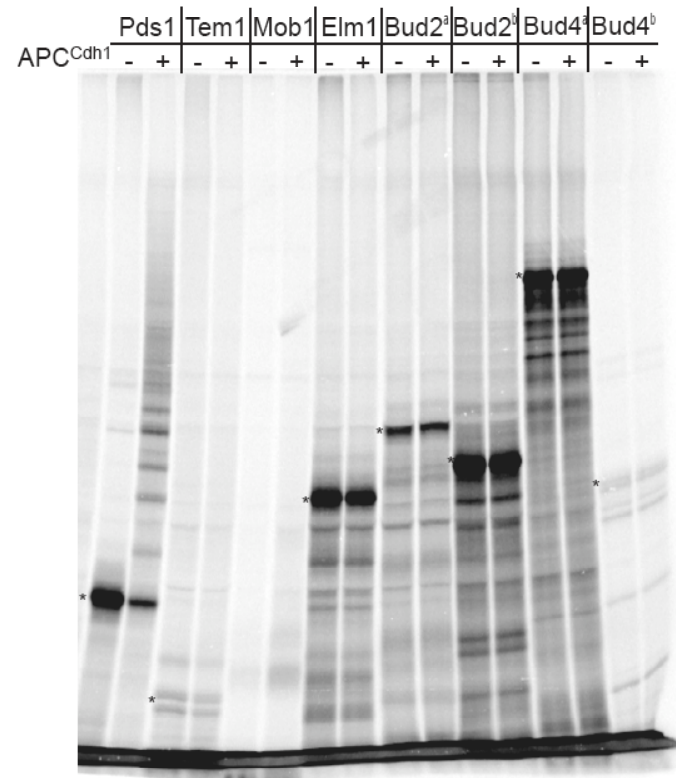


Figure 3. Iqg1 degradation through the cell cycle depends on the APC. (A) Pulse chase of *GAL-IQG1-TAP* of cells arrested in either G1 with alpha-factor and G2/M with nocodazole as described in Materials and Methods. The TAP tag proteins in all gels (A-C) were analyzed by Western blotting as described in Materials and Methods. (B) Pulse chase at 37°C of *GAL-IQG1-TAP* cells arrested in G1 with wild-type APC or in a *cdc23-1* mutant background. (C) Cell cycle expression profile of Clb2 and Iqg1-TAP tagged at its endogenous locus. Cells were arrested in G1 with alpha-factor, released and then re-arrested in G1 by addition of alpha-factor during mitosis as described in Materials and Methods.

Figure 3.

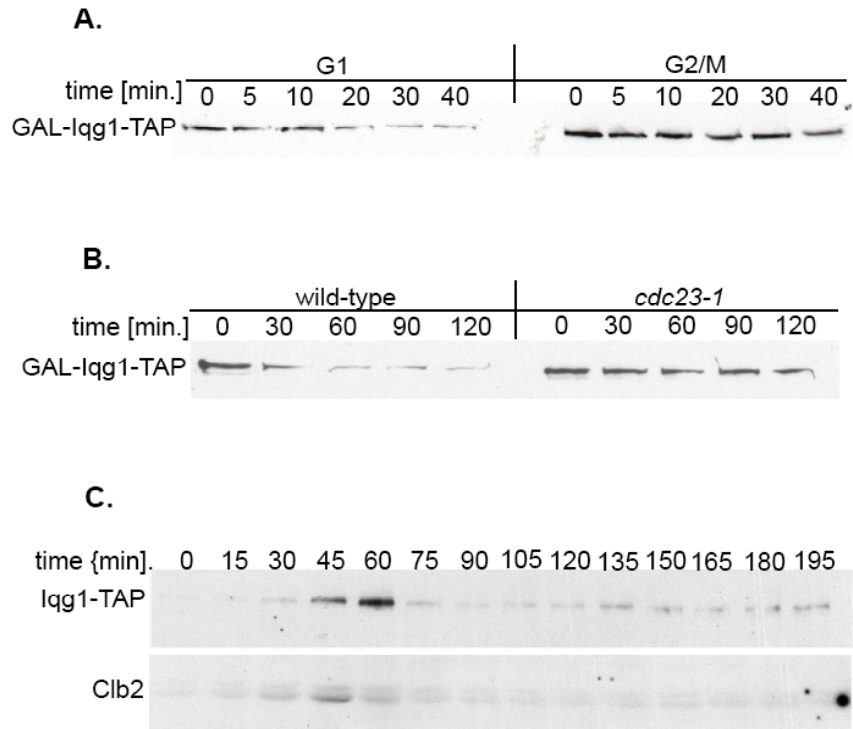


Figure 4. Characterization of the APC destruction signal on Iqg1. (A) Diagram of Iqg1 protein showing the 3 characterized domains: Calponin Homology Domain (CHD), IQ repeats (IQ), and the GTPase Related Domain (GRD). Predicted D-boxes and KEN sequences are indicated by (*) along with the actual APC destruction signal between residues 33-43. (B) APC^{Cdh1} ubiquitination reaction of *in vitro* transcribed and translated Iqg1 fragments. Unmodified substrates are indicated by (*). The residue numbers correspond to the location of the fragment on full length Iqg1. +/- above each well indicates absence or presence of APC^{Cdh1} in the reaction. Ubiquitinated products are characterized by the presence of slower migrating bands. (C) APC^{Cdh1} ubiquitination of Iqg1 (33-250aa) testing the importance of residues between amino acid 33 and 43. 3A is the combination of R34A, S37A, N42A and 4A is the same as 3A but with K40A. A nonspecific background band is also indicated.

Figure 4.

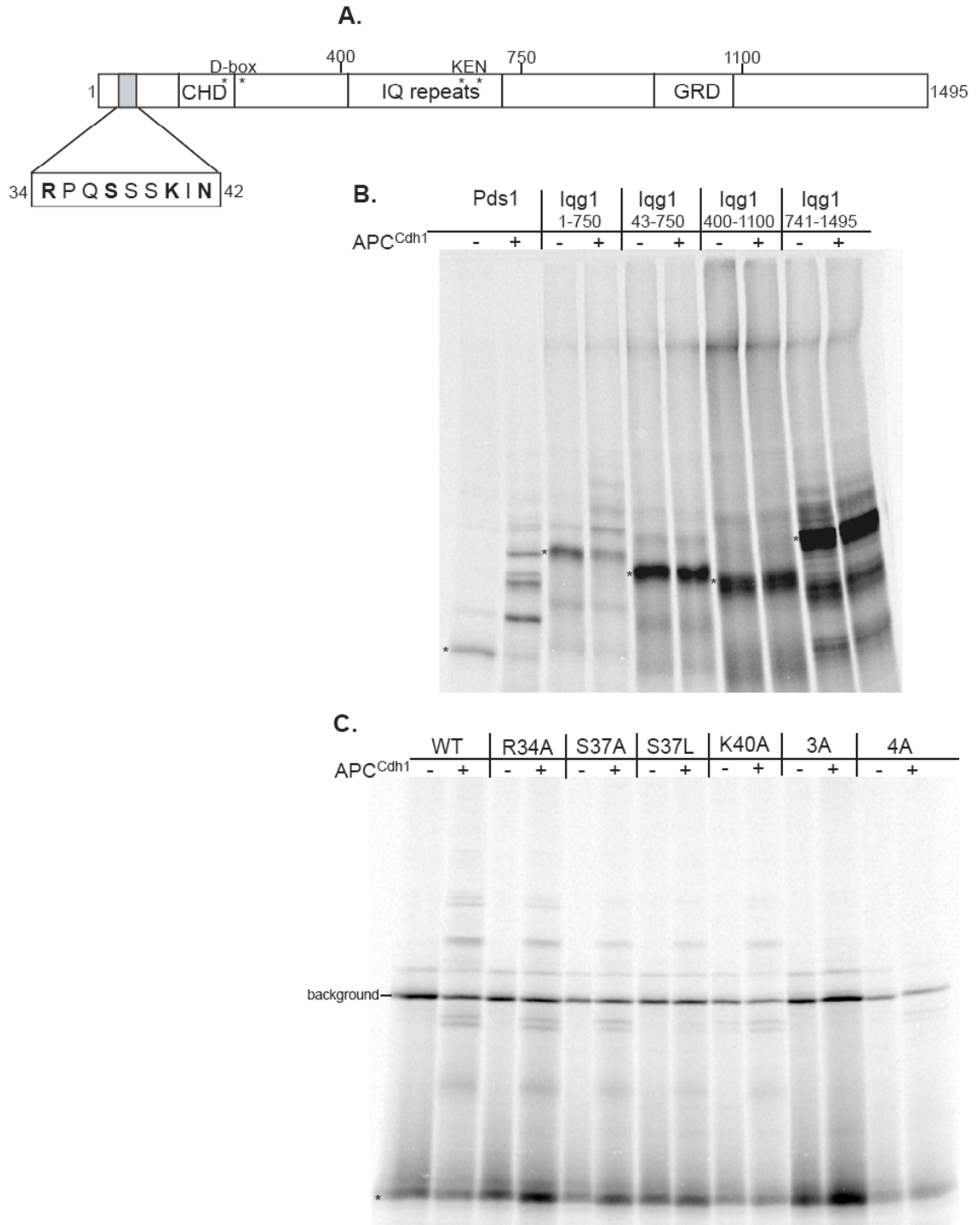
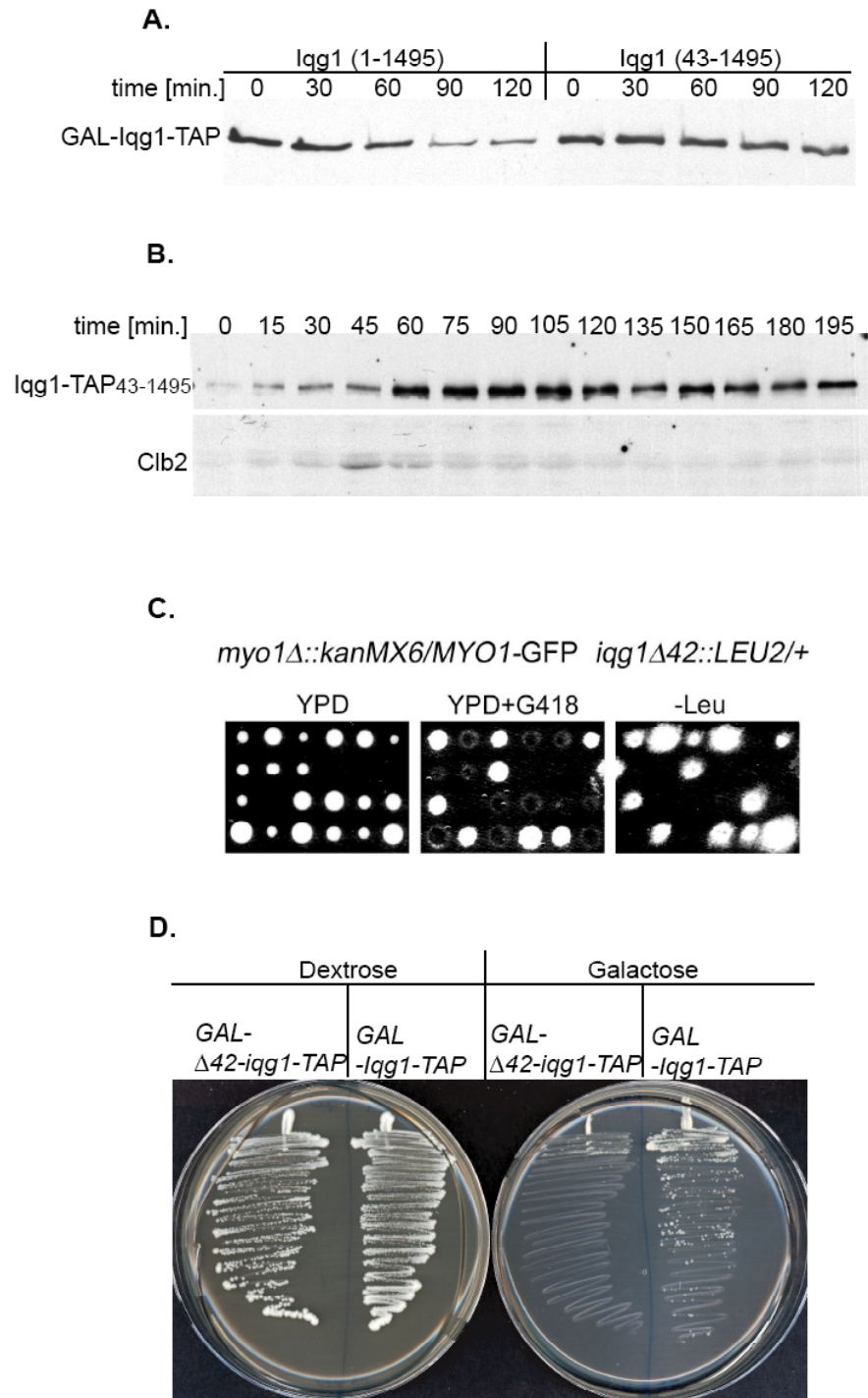


Figure 5. Non-degradable $\Delta 42$ -iqg1 is stable throughout the cell cycle, suppresses *myo1* Δ lethality, and is lethal when over-expressed. (A) Pulse chase of TAP tagged full length Iqg1 and $\Delta 42$ -iqg1 in G1 arrested cells. Proteins in all gels (A-B) were analyzed by Western blotting as described in Materials and Methods. (B) Cell cycle expression of $\Delta 42$ -iqg1-TAP in cells arrested in G1 with alpha-factor, released and re-arrested in G1 by addition of alpha-factor in mitosis as described in Materials and Methods. (C) Tetrad analysis of heterozygous *myo1* Δ ::*KANMX6* crossed to heterozygous *\Delta 42*-*iqg1*::*LEU2*. *myo1* Δ haploids only survive when non-degradable *\Delta 42*-*iqg1* is present. (D) Non-degradable Iqg1 is lethal when overexpressed. *GAL*- $\Delta 42$ -*iqg1*-TAP and *GAL*-*IQG1*-TAP cells were streaked on either dextrose or raffinose/galactose plates to test growth.

Figure 5.



CHAPTER 3

The APC^{Cdh1} regulates actomyosin ring disassembly

RESULTS

APC mutant cells display a cytokinesis defect

To determine if APC activity helps control cytokinesis, we analyzed cytokinesis in cells defective in APC function. In exponentially growing wild-type cells, about 3% were visible as clusters of triplets and quadruplets. In cells lacking *CDH1*, the number of clustered cells rose 3-fold to 9% (Appendix Fig. 1), suggesting that APC^{Cdh1} activity is required for efficient cytokinesis.

We next analyzed the effects of APC defects on the localization of proteins known to regulate yeast cytokinesis. We found that the localization of many GFP-tagged cytokinesis proteins (Cdc12, Hof1, Bni1, Bnr1, Cyk3, Mob1, Myo2, and Tus1; data not shown) was not affected by deletion of *CDH1*, when analyzed in ethanol-fixed cells. However, we did notice a difference in the localization of Myo1. Multiple Myo1-GFP foci (Fig. 1A) were seen in *cdh1Δ* cells that had completed cytokinesis—characterized by the presence of large actin patches and absence of a Myo1 ring at the bud neck. In contrast, no Myo1-GFP was visible in wild-type cells that did not have a ring at the bud neck.

We next analyzed the localization dynamics of Myo1-GFP in an asynchronous population of live cells, acquiring images every minute for 30 minutes. In wild-type cells, the myosin ring appeared at the time of bud emergence and remained at the bud neck until cytokinesis. During cytokinesis, the myosin ring contracted to a single dot in an average time of 5.7 min (+/- 1.1 min; n=39 cells) (Fig. 1B; see Appendix Table 2 for contraction times in all strains). The myosin dot disappeared an average of 5-7 minutes

later, suggesting that the myosin ring had fully disassembled. In *cdh1Δ* cells, as in wild-type cells, the Myo1 ring appeared with the formation of the new bud. During cytokinesis, the ring contracted to a single dot in 6.5 min (+/- 1.3 min; n=27 cells) (Fig. 1C). However, the Myo1 dot did not disappear after the completion of ring contraction. Instead, myosin remained at the site of cytokinesis and punctate foci were visible away from the site of cytokinesis.

Consistent with our initial observations in fixed cells, myosin foci were only visible in G1 cells when a Myo1 ring was not present. To determine how long the myosin foci remained in G1 cells, we lengthened the time between image acquisition from one to 10 min and analyzed Myo1 foci in *cdh1Δ* cells from contraction until formation of the new ring in the next cell cycle. Multiple myosin foci were visible until the formation of a new myosin ring (Fig. 1D). The presence of multiple myosin dots after ring contraction, and their persistence throughout G1, suggests that Cdh1-dependent APC activity normally promotes myosin ring disassembly immediately after ring contraction.

To better quantitate the *cdh1Δ* phenotype, we counted the number of cells with at least one visible Myo1 dot more than 10 min after the completion of ring contraction. 35% of wild-type cells (16/46 cells) had a Myo1 signal after this time, whereas multiple Myo1 dots were found in all *cdh1Δ* cells (33 cells) (Fig. 2A, Appendix Table 2). The Myo1-GFP signal disappeared in only one of the 33 *cdh1Δ* cells, 25 min after ring contraction. In a more detailed approach to quantitation of Myo1 foci, we also counted the maximum number of Myo1 dots per cell at least 10 min after ring contraction. 9% of wild-type cells and 93% of *cdh1Δ* cells contained multiple dots (Fig. 2B). In summary, Myo1 was not visible in the majority of wild-type cells 10 min after ring contraction, and

in those rare cases where dots were visible, the signal was very faint and was found only at the site of ring contraction. In contrast, all *cdh1Δ* cells contained Myo1 dots 10 minutes after ring contraction, and multiple dots were apparent in most cells. One of these dots was always present at the site of cytokinesis, whereas the others were located throughout the cell.

Many (but not all) of the myosin dots that persist in *cdh1Δ* cells are highly mobile. We tracked their movement and saw that in 64% of *cdh1Δ* cells (21/33 cells) the myosin dots traveled towards and merged with the dot at the bud neck at a rate of approx. 1 μm/min (see asterisks in Fig. 1C). In 86% of these cells, myosin dot movement toward the bud neck occurred exclusively in the daughter cell.

To confirm that holoenzyme APC activity, and not just Cdh1, is required for myosin ring disassembly, we analyzed cells lacking all APC activity. As the APC is essential for viability, we used a strain background (*pds1Δ, clb5Δ, 10XSIC1*) in which the APC is not required for viability (Thornton and Toczyski, 2003). In this strain background, with wild-type APC present, the myosin signal disappeared within 10 min after ring contraction in 3 of 4 cells where ring contraction could be observed (Fig. 2A, 3A). We then monitored Myo1-GFP dynamics in cells lacking *APC2*, an essential subunit of the APC holoenzyme. As in *cdh1Δ* cells, myosin dots were present in most *apc2Δ* cells (5/7 cells; 71%) at least 10 min after ring contraction (Fig. 2A, 3B). These results further suggest that the APC, in combination with its activator Cdh1, is required for proper disassembly of myosin after ring contraction.

APC^{Cdh1} is required for Myosin Regulatory Light Chain and IQGAP ring disassembly

Multiple proteins associate with myosin in the actomyosin ring, and we investigated whether the APC might also regulate the disassembly of these proteins. We first examined the disassembly of the regulatory myosin light chain, Mlc2, which binds to the IQ2 motif of myosin. In wild-type cells, the behavior of Mlc2-GFP was similar to that of Myo1. It contracted in an average time of 5.1 min (+/- 1.2 min, n=14 cells) (Fig. 4A, Appendix Table 2). The Mlc2 signal disappeared in 15 of 17 cells (88%) within 10 min of ring contraction (Fig. 2A). In *cdh1*Δ cells, Mlc2 contracted in about 6.9 min (+/- 1.7 min, n=15 cells) but then persisted as punctuate foci (Fig. 4B). Multiple Mlc2 foci were visible in 100% of cells (11) for at least 10 minutes after ring contraction (Fig. 2A). 73% of these cells contained 3 or more Mlc2 dots whereas the remaining 27% had 2 dots (Fig. 2B). The presence of Mlc2 foci after ring contraction in a *cdh1*Δ cell suggests that APC activity is required to disassemble Mlc2 complexes.

Mlc1, the essential myosin light chain, co-localizes with Myo1 during contraction and then shuttles around the cell on secretory vesicles (Wagner *et al.*, 2002). We analyzed the behavior of GFP-Mlc1 expressed under the control of the *MET* promoter in live cells. Mlc1 in wild-type cells contracted to a dot in an average time of 5.7 min (+/- 1.1 min, n=24 cells, Fig. 4C, Appendix Table 2). As previously described, Mlc1 did not disappear after ring contraction but was visible in all 22 cells 10 min after ring contraction. In *cdh1*Δ cells, Mlc1 contracted with similar kinetics (6.2 +/- 1.6 min, n=14 cells) and in all cells Mlc1 dots were visible 10 min after ring contraction (Fig. 2A, 4D). The number of cells with 3 or more Mlc1 dots increased from 57% of wild-type cells to

93% of *cdh1Δ* cells (Fig. 2B). In addition, the number of cells where Mlc1 foci were observed moving toward the bud neck increased from 14% of wild-type cells to 63% of *cdh1Δ* cells. Thus, in the absence of Cdh1, there are more Mlc1 foci and more cells in which Mlc1 moves toward the bud neck, suggesting that APC^{Cdh1} activity may aid in disassembling a subpopulation of Mlc1 complexes after ring contraction.

We also analyzed a GFP-tagged version of the IQGAP protein, Iqg1, which is known to interact with the actomyosin ring through an association with Mlc1. In wild-type cells, Iqg1 contracted in an average time of 4.6 min (+/- 1.0 min, n=7 cells) (Fig. 4E). In only 1 out of 11 cells (9%) Iqg1 was visible 10 minutes after ring contraction (Fig. 2A). In *cdh1Δ* cells, Iqg1 contracted in 5.3 min (+/- 1.5 min, n=8 cells), and was visible in all cells 10 min after ring contraction (Fig. 4F, Fig. 2A). 60% of *cdh1Δ* cells contained 3 or more Iqg1 dots and the remaining 40% contained 2 dots (Fig. 2B). We conclude that Iqg1 disassembly, like that of Myo1 and Mlc2, is regulated by APC^{Cdh1}.

Myo1 co-localizes with Mlc2, Iqg1, and Mlc1 in *cdh1Δ* cells.

As the disassembly of Myo1, Mlc2, and Iqg1 are all defective in APC mutant cells, we next determined whether these proteins remain associated in an APC mutant after ring contraction, or whether they form separate macromolecular foci. We first analyzed the co-localization of Mlc2 and Myo1 by constructing a *cdh1Δ* strain carrying Mlc2-GFP and Myo1 tagged at its C terminus with mCherry (Myo1-Cherry). We acquired images of both proteins every 5 min in asynchronous cells. In 8 out of 8 cells in which Myo1-Cherry dots were visible after ring contraction, we observed co-localization of Mlc2-GFP at all time intervals and for every dot visible (Fig. 5A, Appendix Table 2;

see Appendix Fig. 2 for entire time course). The complete co-localization of Myo1 and Mlc2 suggests that after actomyosin ring contraction in a *cdh1Δ* cell, Myo1 and Mlc2 move around the cell together in large macromolecular complexes.

We also tested whether Myo1 and Iqg1 co-localize in a *cdh1Δ* cell. We acquired images every 5 min of Myo1-Cherry and Iqg1-GFP in *cdh1Δ* cells. In 100% of cells (14/14), Iqg1-GFP dots co-localized with all Myo1-Cherry dots at all time points after actomyosin ring contraction (Fig. 5B, Appendix Table 3, Appendix Fig. 3). Therefore, Myo1 remains associated with both Mlc2 and Iqg1 after ring contraction in *cdh1Δ* cells.

We next tested whether the Mlc1 dots present after ring contraction in *cdh1Δ* cells co-localize with Myo1 foci. We analyzed the co-localization of Myo1-Cherry and GFP-Mlc1 in asynchronous *cdh1Δ* cells. In 8 of the 11 cells that contained visible Myo1-Cherry dots after ring contraction, GFP-Mlc1 dots co-localized with all Myo1-Cherry dots at every time interval (Fig. 5C, Appendix Table 3, Appendix Fig. 4). No GFP-Mlc1 signal was visible in 3 cells, probably due to the variable expression of GFP-Mlc1 from the *MET* promoter. Some GFP-Mlc1 dots did not co-localize with Myo1-Cherry, indicating that all Myo1 foci co-localized with Mlc1 but the reverse was not true (asterisks in Fig. 5C).

As Mlc1 is known to bind to secretory vesicles after actomyosin ring contraction, we investigated whether Myo1-Cherry co-localized with Sec2-GFP. We observed partial co-localization of Sec2 and Myo1 dots in only 1 of 8 cells that underwent cytokinesis (Fig. 5D, Appendix Table 3, Appendix Fig. 5). These results suggest that in a *cdh1Δ* cell there are at least two pools of Mlc1: one that is associated with a large complex of Myo1, Mlc2, and Iqg1, and a distinct pool that is associated with secretory vesicles. In a wild-

type cell, APC^{Cdh1} activity promotes the disassembly of the large complex consisting of Myo1, Mlc2, Mlc1, and Iqg1 immediately after cytokinesis.

Degradation of Cyclins does not promote disassembly of the myosin complex

As the APC is an E3 ubiquitin-protein ligase that mediates the destruction of its substrates by the 26S proteasome, our evidence suggests that the destruction of one or more APC substrates is required for disassembly of the Myo1 complex. One candidate substrate is the mitotic cyclin Clb2, whose degradation in late mitosis is required for exit from mitosis and the completion of cytokinesis. In a *cdh1Δ* cell, Clb2 is not completely degraded (Schwab *et al.*, 1997), and this partial stabilization of Clb2 might be expected to lead to abnormally high Cdk1 activity that inhibits myosin complex disassembly after ring contraction. This possibility seemed unlikely, however, because it is known that the Clb-Cdk1 inhibitor Sic1 accumulates in late mitosis and suppresses Clb2-Cdk1 activity, even in *cdh1Δ* cells. Nevertheless, to test whether Cdk1 activity helps govern myosin disassembly, we overexpressed Sic1 in *cdh1Δ* cells and analyzed Myo1-GFP ring disassembly. Sic1 overproduction did not rescue the myosin disassembly defect in *cdh1Δ* cells, as 95% of the cells contained Myo1 dots at least 10 min after ring contraction (Fig. 6A, B). Therefore, altering Cdk1 activity did not affect myosin complex disassembly.

If Clb2 degradation is required to inhibit myosin disassembly, then removing Clb2 should allow myosin to disassemble in a *cdh1Δ* cell. To directly test whether Clb2 degradation plays a role in myosin disassembly, we constructed a strain lacking both *CDH1* and *CLB2*. In all of the 12 cells for which we followed Myo1-GFP ring contraction, myosin dots were visible 10 min after ring contraction (Fig. 6A). Thus, Clb2

destruction is not sufficient to drive myosin disassembly. Although Cdk1 inactivation may help promote myosin disassembly, our results suggest that Cdk1 is not a major inhibitor of myosin disassembly in a *cdh1Δ* cell. It is therefore likely that the destruction of APC targets other than cyclins is critical.

Degradation of several known APC targets does not promote disassembly of the myosin complex

Ase1, Fin1, Spo12, and Hsl1 are all substrates of APC^{Cdh1}. If the degradation of any one of these substrates is required to allow myosin complex disassembly, then deleting that substrate should reverse the myosin disassembly defect in a *cdh1Δ* cell. We constructed strains lacking both *CDH1* and each candidate substrate and monitored Myo1-GFP disassembly using live cell microscopy. Deletion of *ASE1*, *FIN1*, *SPO12*, or *HSL1* did not reverse the myosin complex disassembly defect in *cdh1Δ* cells. In all double delete strains, Myo1 dots persisted for more than 10 minutes in 100% of cells for which Myo1 contracted (Fig. 6A).

The Polo-like protein kinase Cdc5 is another APC^{Cdh1} substrate whose activity is required for cytokinesis. To test whether degradation of Cdc5 is required for myosin complex disassembly, we analyzed Myo1 behavior in cells carrying a non-degradable form of Cdc5 lacking amino acid residues 5-70, which contain its D-box (Charles *et al.*, 1998; Shirayama *et al.*, 1998). In cells carrying $\Delta 5-70\text{-cdc5}$, Myo1 contracted with normal kinetics (6.1 +/- 1.3 min, n=15 cells) and in 16 out of 17 cells, Myo1 dots were not present 10 min after ring contraction (Fig. 6A, C). Thus, the stabilization of Cdc5 alone is not sufficient to block myosin complex disassembly.

We recently identified Iqg1 as an APC^{Cdh1} substrate (Ko *et. al.*, in press). As Iqg1 is required to recruit actin to the bud neck and to initiate actomyosin ring contraction, we speculated that its APC-dependent degradation might contribute to disassembly of the Myo1 complex. We therefore monitored Myo1-GFP in cells carrying a non-degradable mutant form of Iqg1, $\Delta 42$ -iqg1, which lacks the first 42 amino acids that contain its APC recognition sequence. Myo1-GFP dots were observed 10 min after ring contraction in 6 of 17 cells (35%; Fig. 6A, D). Although this dot frequency is similar to that of wild-type, we noted that the percentage of cells with 2 dots increased 2-fold from 9% of wild-type (Fig. 2B) to 19% of non-degradable Iqg1 cells (see Fig. 8F below). We also examined whether stabilization of Iqg1 affects its own disassembly in cells carrying a GFP-tagged $\Delta 42$ -iqg1. The $\Delta 42$ -iqg1-GFP ring contracted (4.8 +/- 0.7 min, n=24 cells) and disappeared like wild-type Iqg1-GFP (2 of 26 cells had dots 10 min after contraction) (Fig. 6A, E). Thus, stabilization of Iqg1 alone has minor, if any, effects on the disassembly of Myo1 or Iqg1.

To further assess the importance of Iqg1 destruction in the disassembly of myosin, we analyzed the Myo1 disassembly phenotype in *cdh1* Δ *iqg1* Δ double mutant cells. Cells lacking *IQG1* have substantially reduced Myo1-GFP signal at the bud neck, making time-lapse microscopy more difficult. To avoid photobleaching, we acquired images of Myo1-GFP every 5 min. Myosin ring contraction occurred in 16.5 min (+/- 5.7 min, n=47 cells), about 10-11 min longer than wild-type or *cdh1* Δ cells (Fig. 7A, Appendix Table 2). In 36 of the 61 cells (59%) in which a myosin ring contracted, Myo1-GFP dots were visible for more than 10 min after contraction (Fig. 7E). The number of dots per cell also decreased substantially compared to *cdh1* Δ cells. Only 11% of cells

contained a maximum of 3 or more dots compared to 58% of *cdh1Δ* cells (Fig. 2B, 7F). Thus, compared to *cdh1Δ* cells, fewer double mutant cells exhibited a myosin disassembly defect and the defect was less severe. We also analyzed the disassembly of Myo1 in an *iqg1Δ* cell and observed that ring contraction was similar to that in the double mutant (15.5 +/- 4.4 min, n=10 cells) (Fig. 7B, Appendix Table 2); however, Myo1 dots were present 10 min after ring contraction in only 3 of 13 cells (23%, Fig. 7E). In summary, deletion of *IQG1* seemed to destabilize the myosin ring and partially rescue the myosin disassembly defect in *cdh1Δ* cells. This may indicate that Iqg1 destruction contributes to myosin disassembly.

As eliminating Iqg1 allows partial disassembly of myosin foci in *cdh1Δ* cells, we tested whether the deletion of Myo1 affects the disassembly of Iqg1 foci in *cdh1Δ* cells. We analyzed the disappearance of Iqg1-GFP in a *myo1Δ* strain and a *cdh1Δ myo1Δ* double mutant. In only 5 of 24 *myo1Δ* cells (21%), Iqg1-GFP foci were visible more than 10 min after ring contraction (Fig. 7C, E), which is similar to the frequency of Iqg1-GFP foci in a wild-type background (Fig. 2A); deletion of *MYO1* therefore has little effect on Iqg1 disassembly. On the other hand, 47 of 82 (54%) *cdh1Δ myo1Δ* cells contained visible Iqg1-GFP dots 10 min after ring contraction (Fig. 7C, D, E), compared to 100% of *cdh1Δ* cells (Fig. 2A); 11% of *cdh1Δ myo1Δ* cells contained 3 or more dots (Fig. 7F), down from 60% of *cdh1Δ* cells (Fig. 2B). Thus, deletion of *MYO1*, like that of *IQG1*, partially suppresses the disassembly defect of *cdh1Δ* cells, suggesting that Myo1 somehow contributes to the stability of Iqg1 complexes in the absence of Cdh1. We do not believe, however, that Myo1 is an APC substrate. Although the Myo1 ring normally disappears after contraction when analyzed by microscopy, we find that the amount of

Myo1 protein in the cell remains constant throughout the cell cycle (data not shown), and Myo1 is not a substrate of APC^{Cdh1} in vitro (data not shown).

The presence of Iqg1 foci even in the absence of Myo1 in a *cdh1Δ* cell suggests that formation and maintenance of these complexes does not depend solely on myosin. Disassembly of the large macromolecular complex of Myo1, Mlc1, Mlc2, and Iqg1 therefore appears to involve multiple mechanisms.

Disassembly of the Myosin Complex requires multiple pathways.

A myosin disassembly phenotype has also been observed in cells lacking Mlc2. If Mlc2 and Cdh1 regulate myosin disassembly through the same pathway, then the disassembly defect in a *mlc2Δ cdh1Δ* double mutant should resemble that in one of the single mutants. To assess the regulatory interactions between Cdh1 and Mlc2, we monitored Myo1-GFP disassembly in live cells lacking both *CDH1* and *MLC2*. In all 19 cells observed, Myo1-GFP dots persisted for more than 10 min after ring contraction (Fig. 8A, 8E). Thus, as in *cdh1Δ* cells, 100% of double mutant cells displayed a myosin disassembly defect. However, further analysis revealed three significant differences in the phenotypes of *cdh1Δ* and *mlc2Δ cdh1Δ* cells: (1) In 47% of *mlc2Δ cdh1Δ* cells, myosin foci were observed away from the bud neck before ring contraction, whereas none were visible in *cdh1Δ* cells (Fig. 8A, Appendix Table 4); (2) The percentage of cells with 3 or more Myo1-GFP dots was 59% for *cdh1Δ* and 87% for the double mutant (Fig. 2B, 8F); and (3) Myo1-GFP dots were less mobile in the double mutant as compared to *cdh1Δ* cells. The percentage of cells in which Myo1 dots traveled toward the bud neck dropped from 65% in *cdh1Δ* cells to 11% in the double mutant (Appendix Table 2). We did not

observe an appreciable myosin disassembly defect in cells lacking Mlc2 alone (Fig. 8B, E). Nevertheless, the fact that the double mutant displayed a more severe disassembly defect than that seen in either single mutant suggests that Cdh1 and Mlc2 function in separate pathways to promote myosin ring disassembly.

These conclusions are supported by simple analysis of cytokinesis in these cells. We observed that about 5% of *mlc2Δ* cells were found in clusters of 3-4 cells, but the number of clustered cells increased 4-fold to 18% of *mlc2Δ cdh1Δ* cells (Appendix Fig. 1). As Iqg1 was the only APC^{Cdh1} substrate we found whose deletion partially rescued the myosin disassembly defect in a *cdh1Δ* cell, we next tested whether stabilization of Iqg1 in the absence of Mlc2 would produce a myosin disassembly defect. Analysis of Myo1-GFP in $\Delta 42$ -*iqg1 mlc2Δ* cells revealed that myosin did not disappear after ring contraction (Fig. 8C). In 14 of 16 cells (88%), myosin dots were visible at least 10 min after ring contraction (Fig. 8E). Although the majority of cells had myosin dots after 10 minutes, the number of dots per cell was less than that in a *cdh1Δ* cell: only 13% of $\Delta 42$ -*iqg1 mlc2Δ* cells had 3 or more dots after 10 min compared to 58% of *cdh1Δ* cells (Fig. 2B, 8F). Therefore, a cell containing a non-degradable version of Iqg1 and lacking Mlc2 has a myosin disassembly defect that is similar to but less severe than that in *cdh1Δ* cells.

Similar results were obtained when we examined the disassembly of Iqg1 itself in the absence of Mlc2. Like Myo1-GFP, $\Delta 42$ -*iqg1*-GFP contracted and did not disappear in *mlc2Δ* cells, and the fluorescent dot in these cells could be seen moving around the daughter cell (Fig. 8D). Iqg1-GFP dots were visible in 8 of 24 cells (33%) at least 10 min after ring contraction (Fig. 8E). In $\Delta 42$ -*iqg1*-GFP cells containing wild-type Mlc2, only

8% had Iqg1-GFP dots 10 min after contraction (Fig. 6A). Although deletion of *MLC2* in combination with non-degradable Iqg1 significantly disrupted Iqg1 disassembly, the phenotype was not as severe as that in a *cdh1Δ* strain, where 100% of cells had Iqg1 foci 10 min after contraction (Fig. 2A). A potential explanation for these results is that deletion of *MLC2* eliminates one mechanism of actomyosin ring disassembly, making disassembly more dependent on an alternate mechanism involving the degradation of Iqg1. However, stabilization of Iqg1 (even in the absence of Mlc2) does not completely phenocopy the *cdh1Δ* defect, indicating that additional regulatory mechanisms (requiring the destruction of other APC^{Cdh1} substrates) promote efficient actomyosin ring disassembly.

Functional interactions between the APC and septins in cytokinesis

Members of the septin family, including Cdc12, are also required for myosin contraction and disassembly. In a *cdc12-6* temperature-sensitive mutant growing near the restrictive temperature, Myo1 disassembly is slowed by about 5-10 minutes (Dobbelaere and Barral, 2004). To investigate potential functional interactions between APC^{Cdh1} and septins, we tested whether deletion of *CDH1* had any effect on the growth of the *cdc12-6* allele. The *cdc12-6* strain is inviable at 37°C and viable at 30°C. When *CDH1* is deleted from this strain, the restrictive temperature shifts down to 30°C (Fig. 9A). Analysis of the double mutant cells at 30°C revealed the same phenotype seen with *cdc12-6* cells at 37°C: chains of cells with multiple DNA masses (Fig. 9B).

We also investigated myosin disassembly at room temperature in the *cdc12-6 cdh1Δ* double mutant using live cell microscopy of Myo1-GFP, expressed from a low-

copy plasmid. In 8 of 9 cells (88%), Myo1-GFP foci were present more than 10 min after ring contraction (Fig. 9C). However, as in the *mlc2Δ cdh1Δ* double mutant, the number of Myo1 dots was greater in the *cdc12-6 cdh1Δ* double mutant than it was in *cdh1Δ* cells. The proportion of cells containing three or more dots increased 3-fold (from 20% to 63%) in the double mutant compared to *cdh1Δ* cells (Fig. 9D). Thus, septins and APC^{Cdh1} also appear to promote myosin disassembly through different pathways.

DISCUSSION

The experiments in this chapter explored how the disassembly of the actomyosin complex is regulated so that the cytokinesis machine is efficiently turned off after cell division. We began by investigating the function of a major cell cycle regulator, the APC, in the control of cytokinesis. In wild-type cells, the actomyosin ring contracts and then disassembles immediately after mitosis, and does not reform until the start of the following cell cycle. We observed that in cells defective for APC function, the actomyosin ring fails to efficiently disassemble. This disassembly defect was characterized by the presence of large foci immediately following ring contraction. These foci contained Myo1, Mlc2, Mlc1, and Iqg1, and seemed very dynamic as they moved around the cell and merged with each other. The foci were present during all of G1 and finally disappeared at the start of the following cell cycle. Our results suggest that in a wild-type cell, the activation of APC^{Cdh1} in late mitosis promotes the disassembly of the actomyosin ring after contraction. Our findings raise a number of interesting questions. First, what is the molecular nature of the myosin foci? Second, what is the identity of the APC^{Cdh1} substrates that must be degraded to promote efficient myosin disassembly? Third, what other pathways promote myosin disassembly in parallel to APC^{Cdh1}?

What are the myosin foci?

Two lines of evidence suggest that Myo1, Mlc2, Mlc1, and Iqg1 are associated in large macromolecular complexes after actomyosin ring contraction: (1) All of these proteins exhibited a similar behavior after ring contraction in *cdh1*Δ cells; and (2) Mcl1,

Mlc2, and Iqg1 all co-localize with every Myo1 focus. Some Mlc1 in *cdh1Δ* cells is also present in locations where no Myo1 is located. We speculate that these other sites represent Mlc1 bound to Sec2-containing secretory vesicles that are not associated with Myo1.

Thus far, we have identified 3 proteins that associate with Myo1 foci. The observation that foci are still present in *iqg1Δ cdh1Δ* and *myo1Δ cdh1Δ* cells suggests that the formation of these foci does not depend entirely on Iqg1 or Myo1. Mlc1 may be the cornerstone of the complex. Mlc1 binds to both Iqg1 and Myo1 and is known to associate with many other proteins (Sec2 and Myo2, for example). (Luo *et al.*, 2004) identified an *mlc1-11* mutant that no longer associates with Iqg1 and has diminished binding to Myo1. Therefore, if Mlc1 acts as the glue for these complexes, then the *mlc1-11* mutant may suppress the myosin disassembly defect in a *cdh1Δ* cell. If myosin disassembly is not affected by a *mlc1-11* mutant, then further studies to identify other members of this complex will help us understand how it is taken apart in a wild-type cell.

What APC^{Cdh1} substrates are degraded to promote efficient myosin disassembly?

Our evidence suggests that Iqg1 is the only known APC target whose destruction might contribute to disassembly of myosin ring complexes. Deletion of *IQG1* partially rescued the disassembly defect. The non-degradable version of Iqg1 did not have an appreciable effect on myosin disassembly by itself but did have a profound disassembly defect in the absence of *MLC2*. Degradation of Iqg1 by APC^{Cdh1} is therefore required for efficient myosin disassembly. The fact that the myosin disassembly defect in a *Δ42-iqg1 mlc2Δ* strain was not as severe as that in a *cdh1Δ* strain suggests that there must be

additional APC^{Cdh1} substrates whose degradation, in combination with that of Iqg1, promotes myosin disassembly. The identities of these other substrates remains unknown. As we described in Chapter 1, we screened over 100 cytokinesis proteins and Iqg1 was the only APC^{Cdh1} substrate identified. Although far from complete, the screen included all of the major players in cytokinesis.

In metazoans, the cytokinesis protein anillin has been reported to be a substrate of the APC. We found that the closest budding yeast homolog of anillin, Bud4, is degraded during G1 but is not a direct APC^{Cdh1} substrate *in vitro*. Although the exact substrates may not be conserved, the involvement of APC^{Cdh1} activity in cytokinesis seems to be conserved. In HeLa cells, for example, proteasome activity is required to terminate cytokinesis (Straight *et al.*, 2003).

What other pathways, parallel to APC^{Cdh1}, promote myosin disassembly?

Previous work suggests that Mlc2 and septins aid myosin disassembly. Our results support this model and further suggest that these proteins act in parallel to APC^{Cdh1}. The disassembly phenotype for both *cdh1Δ mlc2Δ* and *cdh1Δ cdc12-6* was more pronounced than that in either single mutant. Mlc2 may promote myosin disassembly by stimulating the transport of myosin along actin cables after ring contraction. Consistent with this possibility, we observed that deletion of *MLC2* decreased the motility of the myosin dots that move around *cdh1Δ* cells after ring contraction.

Temperature-sensitive septin mutants fail to localize Myo1 to the presumptive bud site. Instead, myosin co-localizes with multiple septin foci around the cell cortex (Roh *et al.*, 2002). In addition, Myo1 and Iqg1 are mislocalized near the bud neck as a

dots in the absence of Shs1, a non-essential component of the septin complex (Iwase et al, 2007). Therefore, it is possible that the synthetic lethality between *cdh1Δ* and *cdc12-6* is due to a two-pronged effect on myosin localization: that is, deletion of *CDH1* causes improper disassembly, and the *cdc12-6* mutation causes improper assembly. Although *MYO1* is not essential, the severe mislocalization of Myo1 could sequester other essential proteins such as Iqg1 and Mlc1. Preliminary data indicates that when *MYO1* is deleted from a *cdh1Δ cdc12-6* double mutant, the restrictive temperature shifts from 30°C to 37°C (data not shown). Thus, deleting *MYO1* may rescue the synthetic interaction between *cdh1Δ* and *cdc12-6*. Therefore, one role of myosin complex disassembly may be to disassociate these proteins so that in the next cell cycle, their association with the cytokinesis machine is properly regulated to occur at the right time and place.

These questions of myosin regulation by the APC and septins need further investigation. Some follow-up experiments that may either support or negate this model are: (1) Analyze the genetic interactions between *cdh1Δ* and other septin mutants. As previously mentioned, *shs1Δ* cells exhibit myosin mislocalization; therefore, crossing *cdh1Δ* to *shs1Δ* (and other septin mutants) may reveal similar genetic interactions. (2) Determine whether Mlc2 and septins function in the same or parallel pathways. Although the myosin disassembly defect in a *mlc2Δ* cell is less severe than that in a *cdh1Δ* cell, an *mlc2Δ* may display a genetic interaction with septins if they are genetically redundant. (3) As APC^{Cdh1} destruction of Iqg1 contributes to myosin disassembly, then non-degradable *Δ42-iqg1* may also exhibit a synthetic interaction with *cdc12-6*.

Myosin filament regulation.

Most of the work regarding myosin disassembly has focused on how phosphorylation regulates the self-assembly of bipolar myosin filaments. In higher eukaryotes, phosphorylation of myosin light chain promotes filament assembly, whereas in lower eukaryotes, phosphorylation of the heavy chain prevents filament assembly (Matsumura, 2005). In *Dictyostelium*, for example, phosphorylation of 3 threonines on myosin II causes thick filaments to disassemble. Substituting the threonines with alanine causes myosin to aggregate. In budding yeast, the C-terminal 26 amino acids of Myo1 are required for phosphorylation *in vivo* (Negron *et al.*, 1996); however, it is not known whether this regulates filament formation. Deletion of this C terminus does not prevent myosin localization to the bud neck or ring contraction (Lister *et al.*, 2006). As this region is not required for filament assembly, it may be required for disassembly. As in *Dictyostelium*, phosphorylation of myosin in yeast may promote filament disassembly. If this is true, then deletion of the C-terminal domain may disrupt myosin disassembly. Analyzing the disassembly of *myo1-26Δ*-GFP in a wild-type and sensitized backgrounds (*cdh1Δ*, *mlc2Δ*, *cdc12-6*, or *Δ42-igg1*) should provide more insight into the mechanisms by which the actomyosin ring is properly disassembled in a wild-type cell.

MATERIALS AND METHODS

Strains, Plasmids, Growth Conditions, and Genetic Methods

All strains were based on the W303 or S288C genetic background as indicated and were grown at 30 °C unless otherwise indicated. 2% glucose was used as carbon source except for experiments involving induction of gene expression under *GAL* promoter control, for which 2% raffinose plus 2% galactose was used. Standard procedures were used for growth of *Escherichia coli*, genetic manipulations, polymerase chain reaction (PCR), and other molecular biological procedures (Guthrie and Fink, 1991).

The strains and plasmids used in this study that were kindly shared by other laboratories are listed below: APC bypass strain (*apc2Δ pds1Δ clb5Δ SIC110X*) from David Toczyski (Thornton and Toczyski, 2003). *hsl1Δ swe1Δ cdh1Δ* strain from Mark Solomon (Burton and Solomon, 2001). TPM2-GFP and pGFP-Mlc1 plasmid from Mark Pellman. pGFP-Myo1 plasmid from Matt Lord (Lord *et al.*, 2005). *iqg1Δ*, *myo1Δ*, *cdc12-6* strains from John Pringle (Nishihama *et al.*, in press). mCherry plasmids from Peter Walter.

Non-degradable $\Delta 42$ -*iqg1-GFP* strain was made by transforming GFP-tag library (Huh *et al.*, 2003) *IQG1-GFP* strain with pGT04 (described in previous chapter).

Cluster Indices

To determine cell-cluster indices, 1 ml of the culture grown to Log phase was washed once with water by centrifugation, resuspended, sonicated briefly, and observed by DIC microscopy. For each strain, 400 cell clusters were counted.

Fixed Microscopy

Visualization of F-actin, Myo1p-GFP, and DNA in the same cells was done as described in (Bi *et al.*, 1998). Log phase growing cells were pelleted by centrifugation for 30 sec in a nanofuge and then fixed by resuspending the cell pellet in ice-cold 70% ethanol followed by incubation on ice for 10 min. Cells were then incubated at room temperature for 2 min with 20U/ml (0.66uM) TRITC-phalloidin (Invitrogen) in PBS containing 10 mg/ml BSA. Cells were then washed three times with PBS by centrifugation and then resuspended in mounting medium containing 1 µg/ml 4',6-Diamidino-2-phenylindole dihydrochloride (DAPI). 2-3 µl of this suspension were placed on a slide, covered with a coverslip, and then pressed with a weight (usually a centrifuge rotor) for 10 min before microscopic examination.

Fluorescence and differential interference contrast (DIC) microscopy was performed using an Axiovert 200M microscope (Carl Zeiss, Jena Germany), 63x NA 1.4 oil immersion DIC objective (Plan-Apochromat, Zeiss), equipped with an X-cite 120 mercury arc lamp (EXFO) and an Orca ER camera (Hamamatsu, Bridgewater, NJ). MetaMorph (Molecular Devices, Sunnyvale, CA) was used for data collection. 7 images in the GFP (750ms) and Texas Red (50ms) filters, 1x1 binning, were acquired at 0.5um intervals, which were then projected into one image by maximum intensity in MetaMorph. The corresponding images were paired with the DAPI and DIC images. Contrast was enhanced using ImageJ (<http://rsb.info.nih.gov/ij/>) and Photoshop (Adobe Systems Corp., San Jose, CA).

Live Microscopy

Live microscopy was done with the same microscope and imaging software described above. For all time-lapse movies, Log phase cells grown at room temperature in minimal SD media (supplemented with 0.01% Ade/Trp) to minimize background fluorescence. The cells were adhered with Concavalin A (Sigma) on 35mM glass bottom Petri dishes (MaTek, Cat. No. P35G-1,5-14-C). Briefly, 300ul of 50ug/ml in PBS pH 7.4 Concavalin A was incubated for 10 min, and washed 3 times with PBS pH 7.4. Once dried, 300ul of cell culture was added for at least 30 min at room temperature for complete adhesion to the dish. Cells were washed 3 times with minimal SD media. All live cell experiments were performed at RT.

Images were acquired using Metamorph. Briefly, movies lasted 30 minutes and images were taken at 1 min intervals (unless otherwise indicated) at multiple stage positions (3-5). For GFP and mCherry, image acquisition ranged from 300-750ms depending on fluorescence intensity with 1x1 binning. Maximum projections of the fluorescence images were generated by acquiring 7 images at 0.5um intervals for each stage position. Power levels of the mercury arc lamp (EXFO) were lowered to minimize photo-toxicity.

Image analysis and quantification

Ring contraction

All quantification was performed manually using ImageJ. Briefly, for each projected stack of images, every cell that showed ring contraction given a number. Only

the cells where the start and end of ring contraction was visible were included to calculate the average time of ring contraction.

Ring disassembly

For disassembly, only cells in which ring contraction ended with at least 10 min left in the movie were included. If a GFP dot was visible after the 10 min time point, then it was marked as GFP visible > 10 min..

Myo1 movement

To measure Myo1 movement toward bud neck, only cells that had a GFP signal visible 10 min after the end of ring contraction were included. If GFP dots that were seen moving in the direction of the bud neck (in most cases it merged with a dot at the bud neck), then it was marked as movement toward the bud neck.

Myo1 dots per cell

To estimate the number of GFP dots per cell, the maximum number of GFP foci were counted only in cells for which a GFP signal was visible 10 min after ring contraction ended. Dots visible in both the mother and daughter cells were added together to calculate the maximum number of dots.

GFP-mCherry colocalization

For co-localization quantification, only cells in which GFP foci were present after 10 minutes were analyzed. The co-localization of each GFP and mCherry dot was manually monitored at each time point. Only cells in which GFP-mCherry co-localization was constant (from the end of ring contraction until the end of the time-lapse) were counted as positives.

Myo1 dot outside bud neck

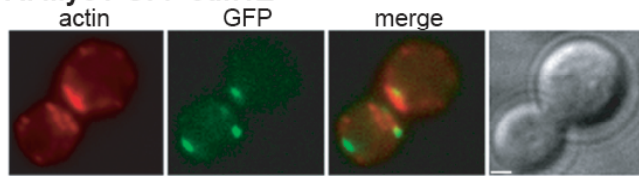
If a GFP dot was visible at any time before ring contraction began during the 30 minute time-lapse, then the cell was counted as a positive for having a GFP dot outside bud neck before contraction.

FIGURES

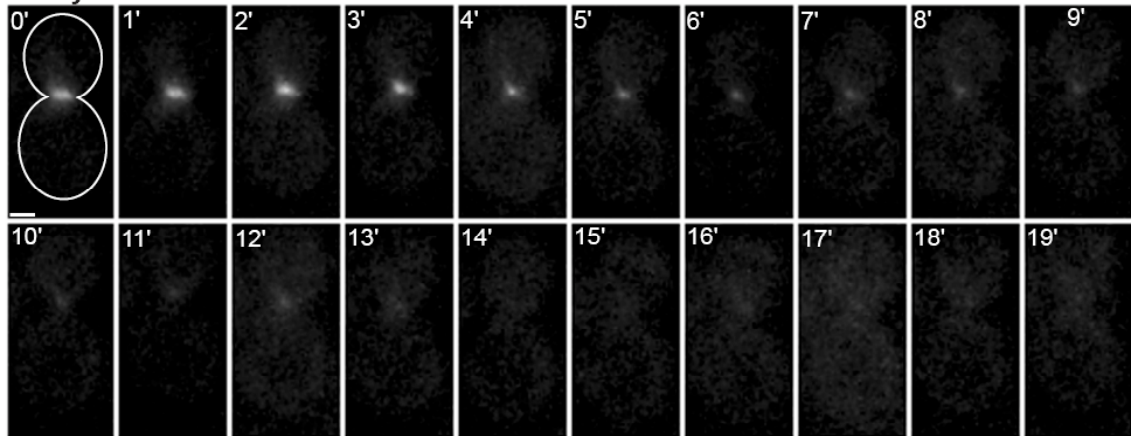
Figure 1. Cdh1 is required for normal disassembly of the actomyosin ring. (A) Representative images of a Myo1-GFP *cdh1* Δ cell fixed with ethanol and stained with TRITC-Phalloidin (red) to visualize actin filaments. Myo1-GFP is shown in green. The presence of large actin patches at the bud neck suggests recent completion of cytokinesis. (B) Time-lapse images of a Myo1-GFP cell in an asynchronous population, captured by epifluorescence microscopy. Images were taken at one-minute intervals, and time point 0 marks the initiation of ring contraction. The cell outline is drawn in the first panel. (C) Time-lapse images of a Myo1-GFP *cdh1* Δ cell. A Myo1-GFP dot moving toward the bud neck is marked with an asterisk in panels 23'-26'. (D) Myo1-GFP dots persist until formation of a new myosin ring and bud in *cdh1* Δ cells. Images of Myo1-GFP *cdh1* Δ were acquired every 10 minutes to observe myosin dots throughout G1 up to the formation of myosin ring and budding. Bar, 1 μ m.

Figure 1.

A. Myo1-GFP *cdh1* Δ



B. Myo1-GFP



C. Myo1-GFP *cdh1* Δ

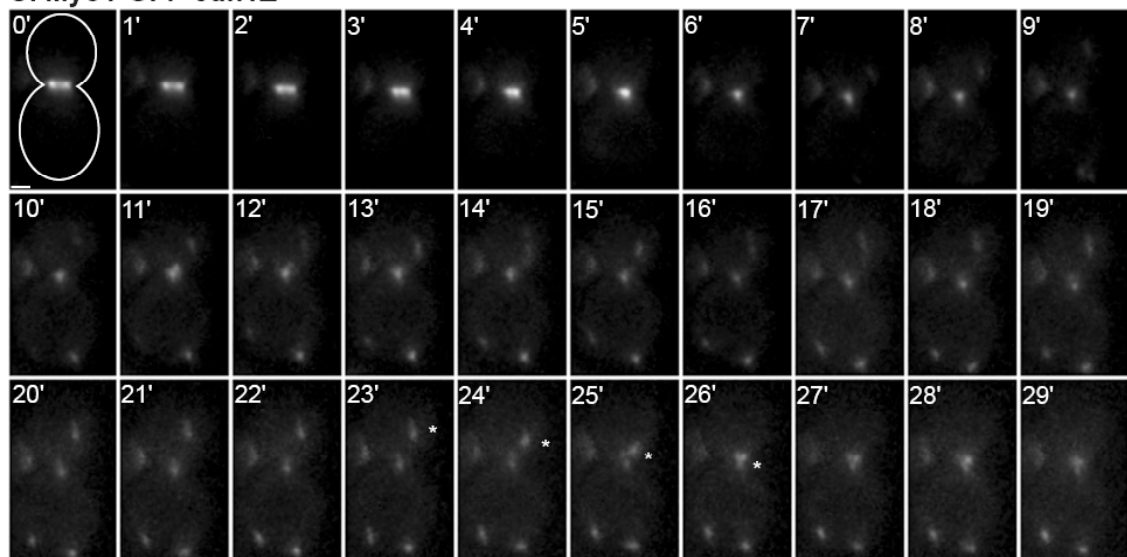


Figure 2. Myo1, Mlc2, Mlc1, and Iqg1 exhibit similar disassembly defects in APC mutant cells. (A) The percentage of cells with visible GFP dots at least 10 minutes after ring contraction was counted for each of the indicated strains. The exact percentages, and number of cells counted, are presented in Appendix Table 2. (B) The maximum number of dots per cell, at least 10 minutes after ring contraction, was calculated for the indicated strains.

Figure 2.

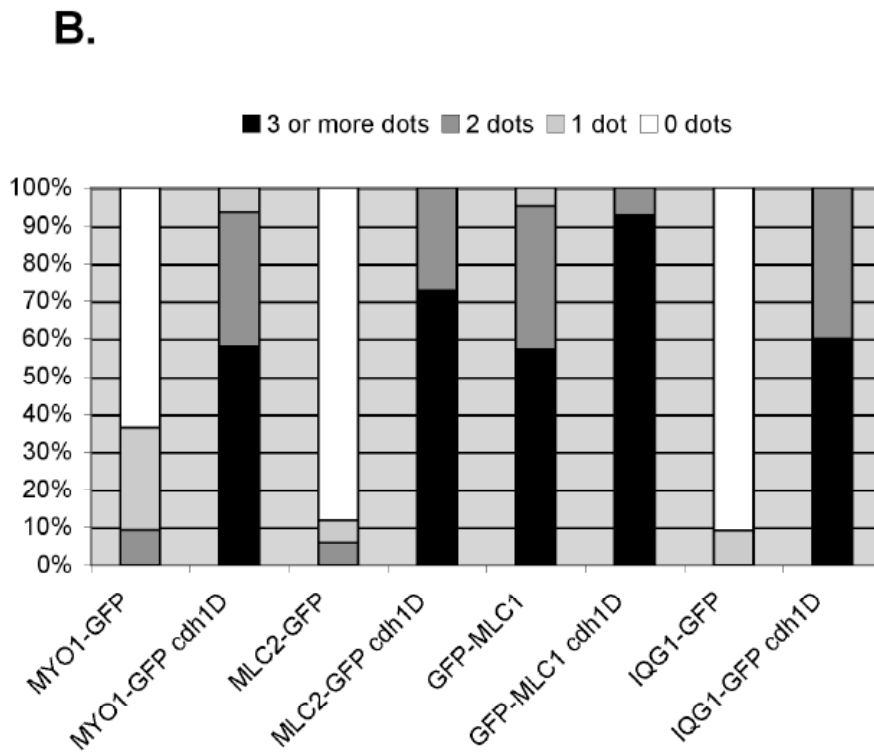
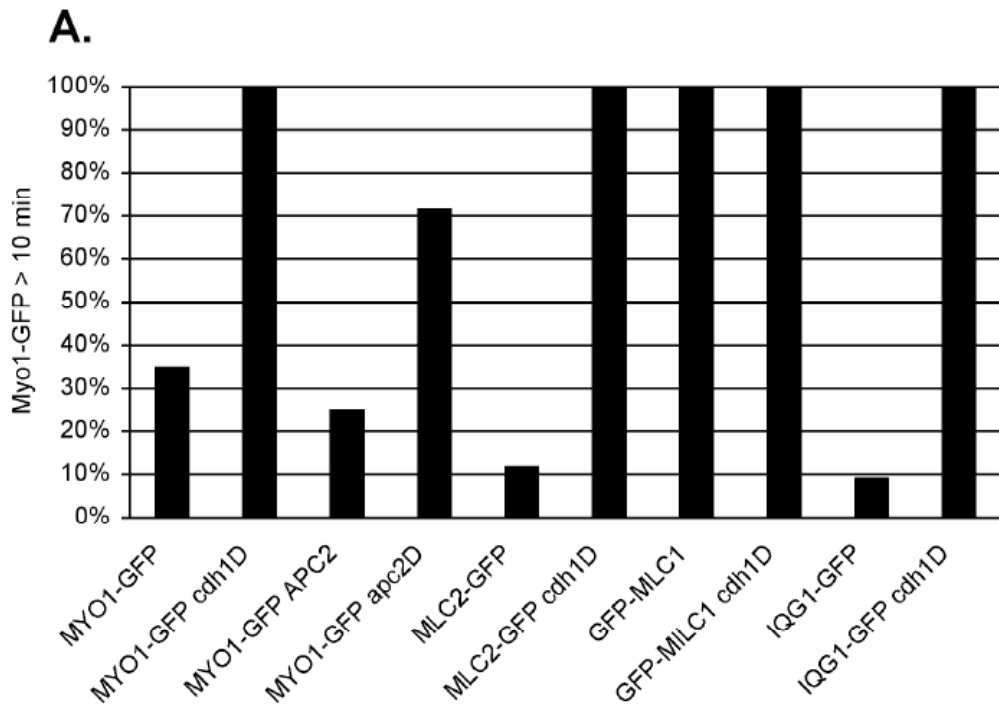


Figure 3. APC activity is required for myosin ring disassembly. Time-lapse images of Myo1-GFP were acquired in a strain (*pds1Δ clb5Δ 10XSIC1*) that can survive without the APC. This strain serves as the parental (wild-type *APC2*) control. (B) Images were acquired in a strain lacking *APC2* to abolish all APC activity. Images were taken at one-minute intervals, and time point 0 marks the initiation of ring contraction. The cell outline is drawn in the first panel. Bar, 1 μm .

Figure 3.

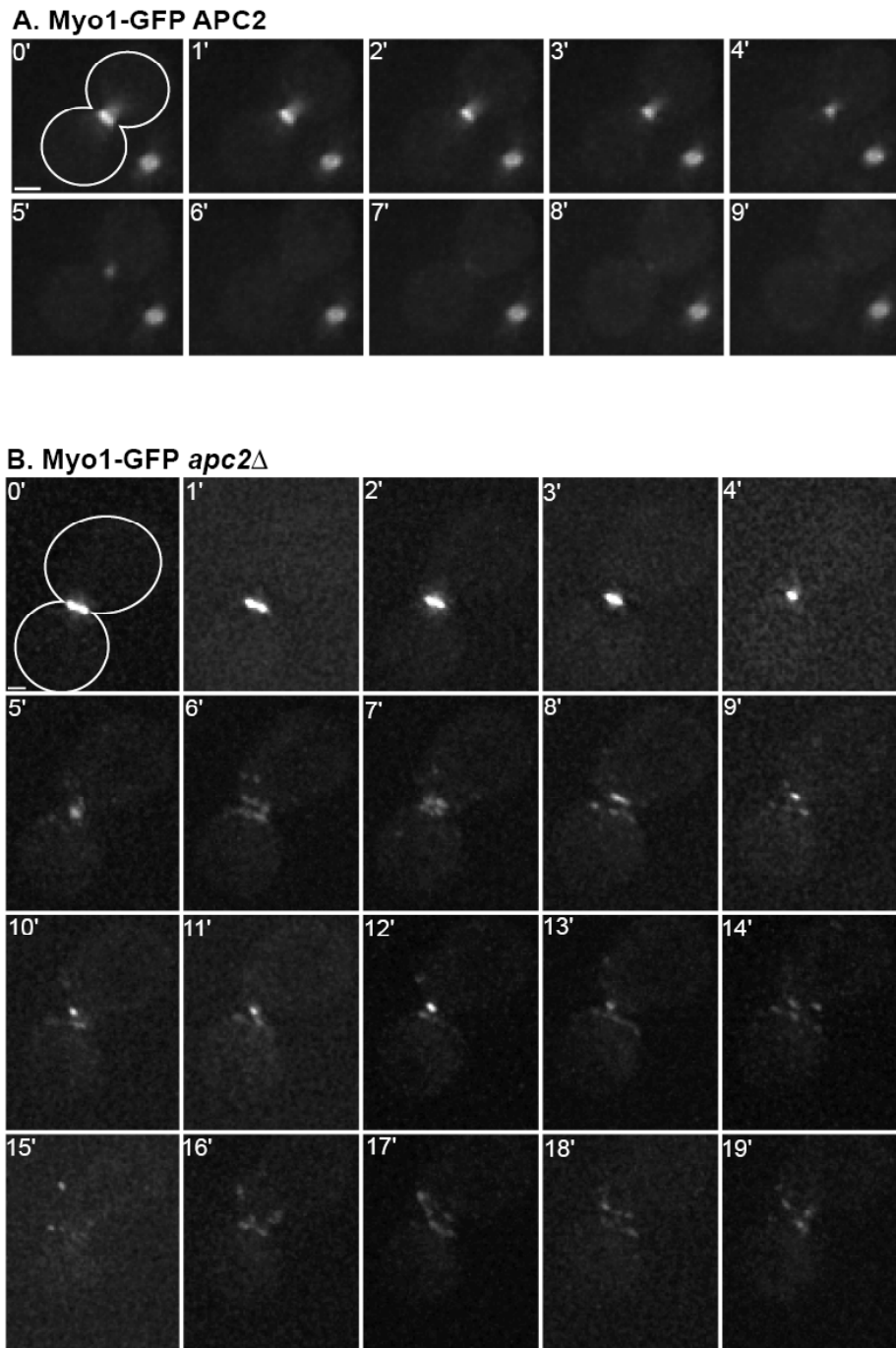


Figure 4. APC^{Cdh1} is required to disassemble the myosin light chains Mlc2 and Mlc1 and the IQGAP, Iqg1. Time-lapse images were acquired at one-minute intervals in strains carrying GFP-tagged proteins as follows: (A) Mlc2-GFP, (B) Mlc2-GFP *cdh1* Δ , (C) GFP-Mlc1, (D) GFP-Mlc1 *cdh1* Δ , (E) Iqg1-GFP, and (F) Iqg1-GFP *cdh1* Δ . Time point 0 marks the initiation of ring contraction; the cell outline is drawn in the first panel. Bar, 1 μ m.

Figure 4.

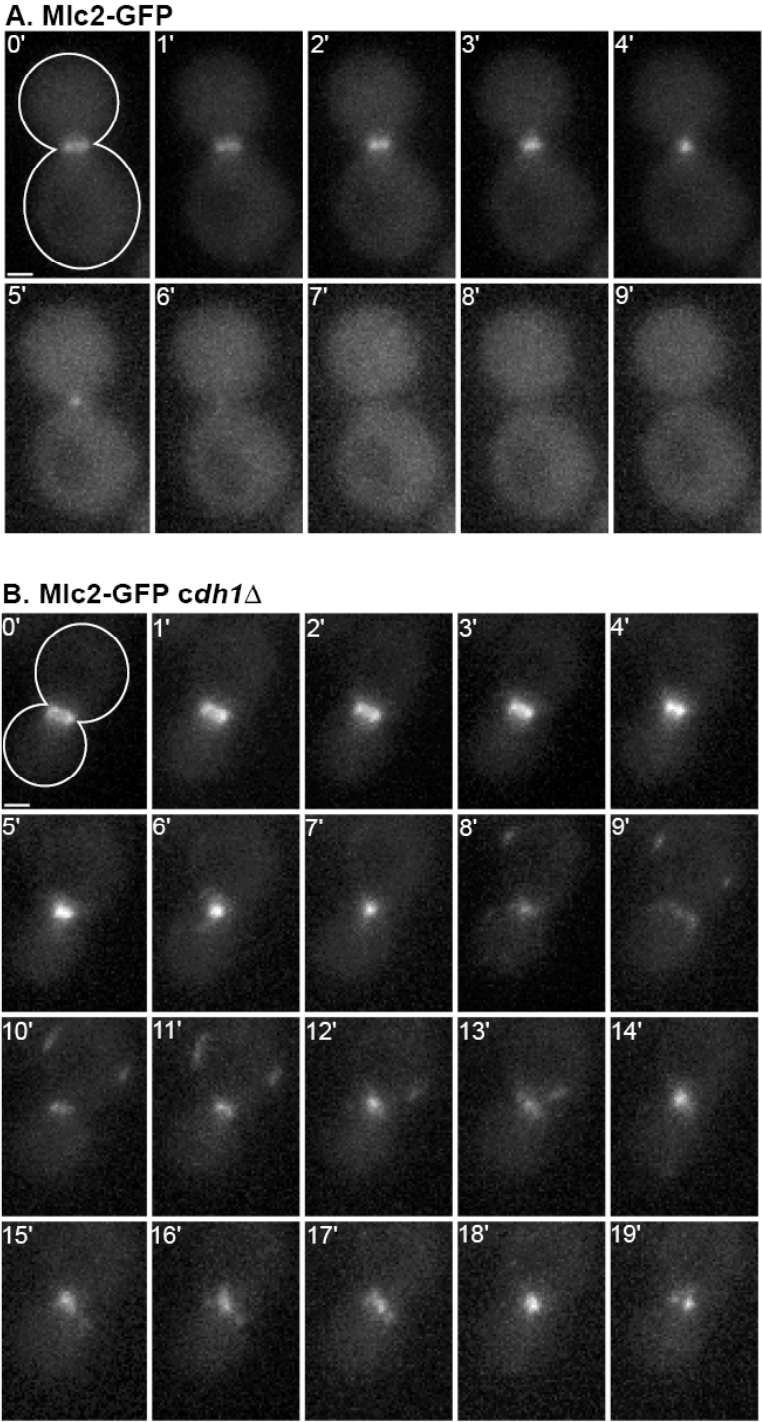
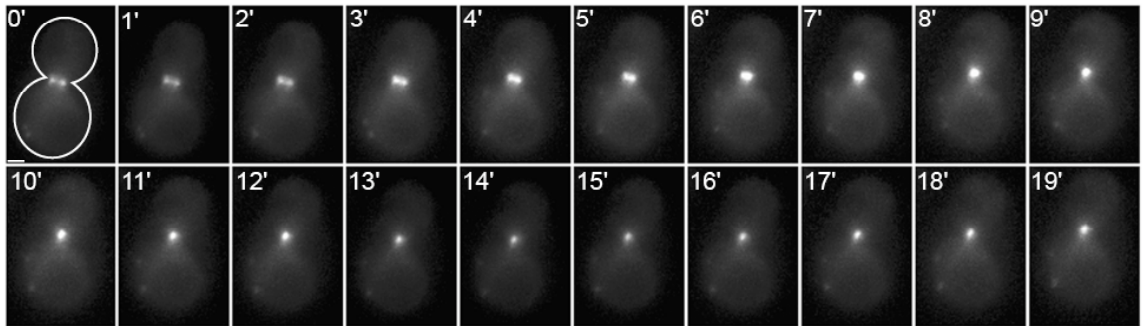


Figure 4.

C. GFP-Mlc1



D. GFP-Mlc1 *cdh1* Δ

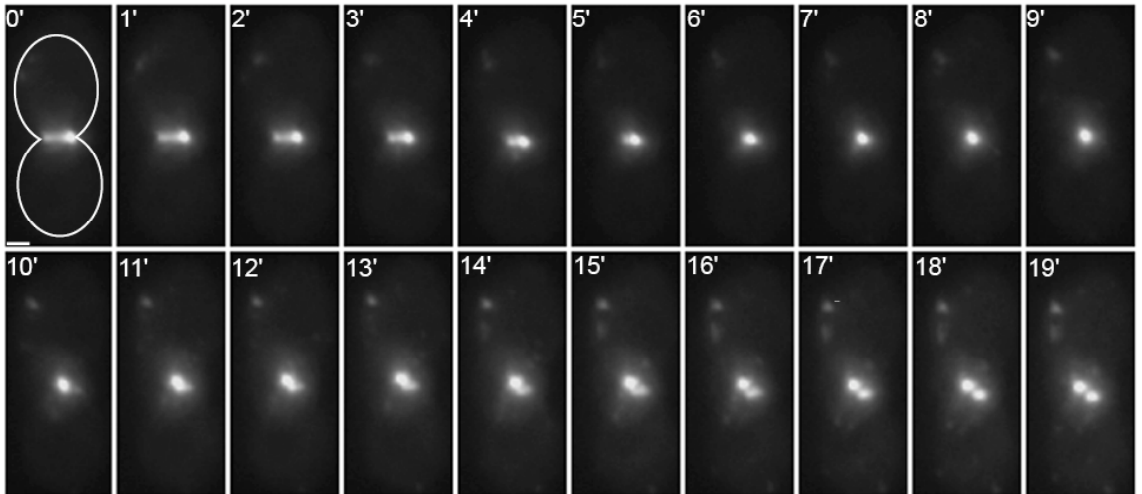


Figure 4.

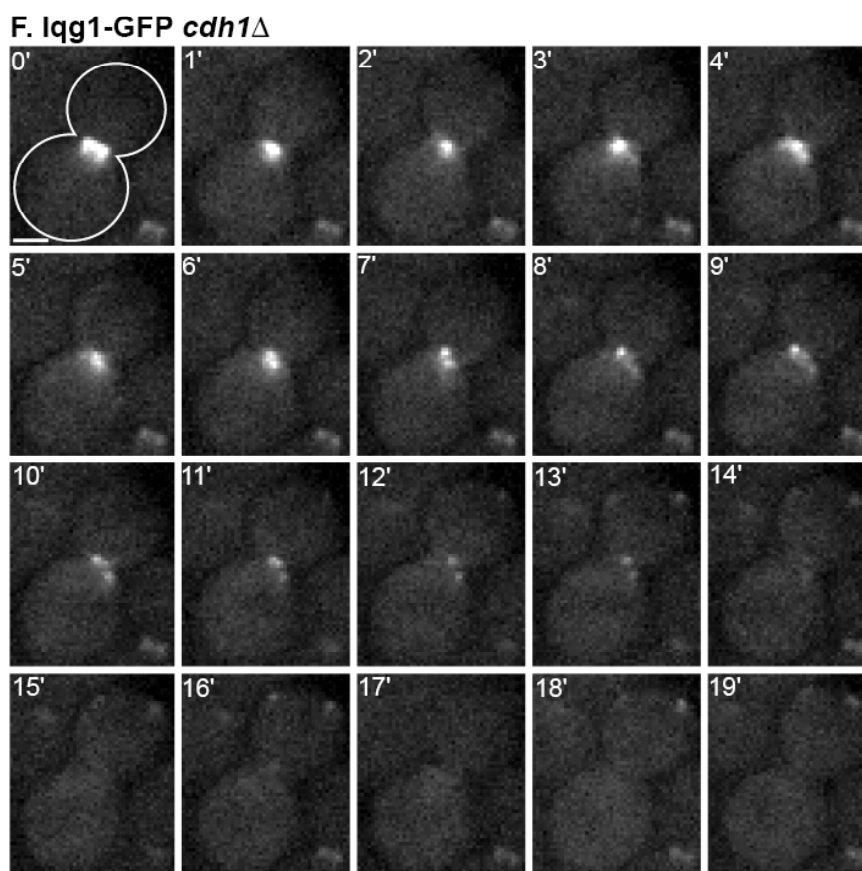
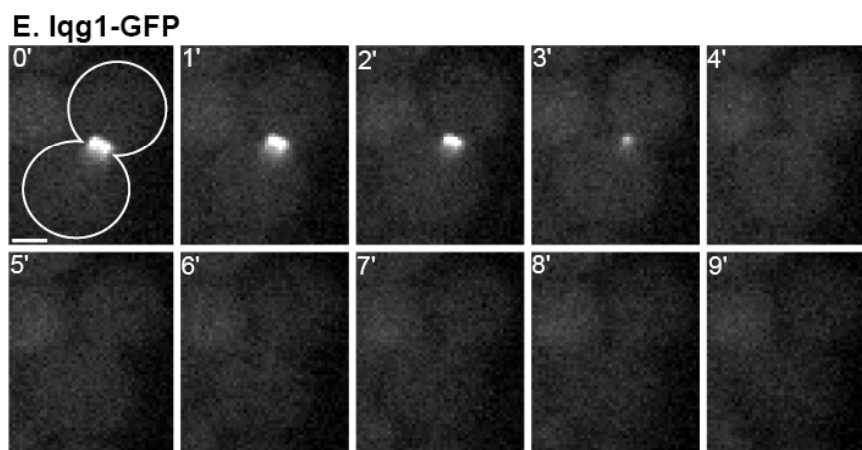
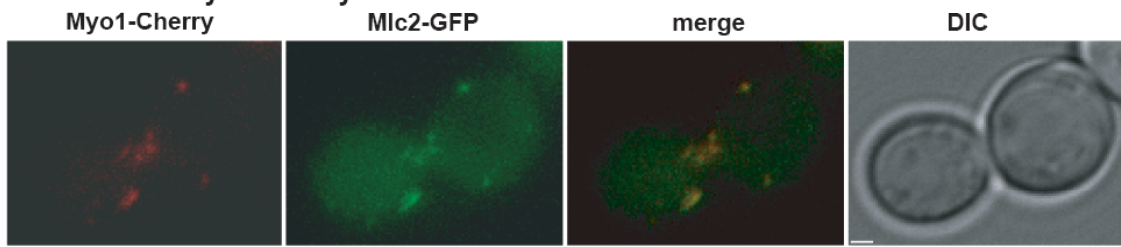


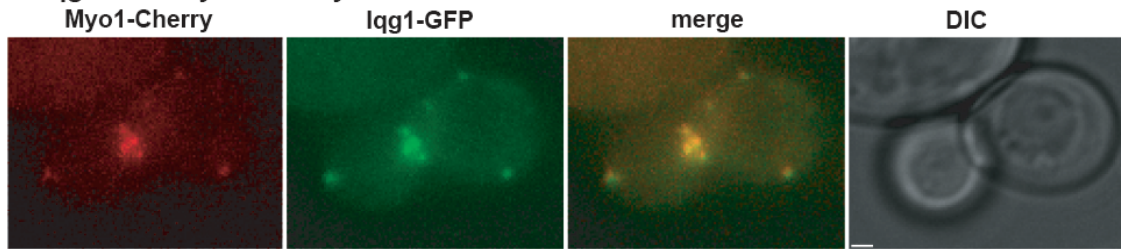
Figure 5. Myo1 co-localizes with Mlc2, Mlc1, and Iqg1 in *cdh1*Δ cells. Representative images of Myo1-Cherry (red) and (A) Mlc2-GFP, (B) Iqg1-GFP, (C) GFP-Mlc1, and (D) Sec2-GFP. The asterisks in C indicates faint GFP-Mlc1 dots for which no Myo1-Cherry dots are present. All GFP images are shown in green. All images are a selected time point from time-lapse series in Supplementary Figures 2-5. Bar, 1 μm.

Figure 5.

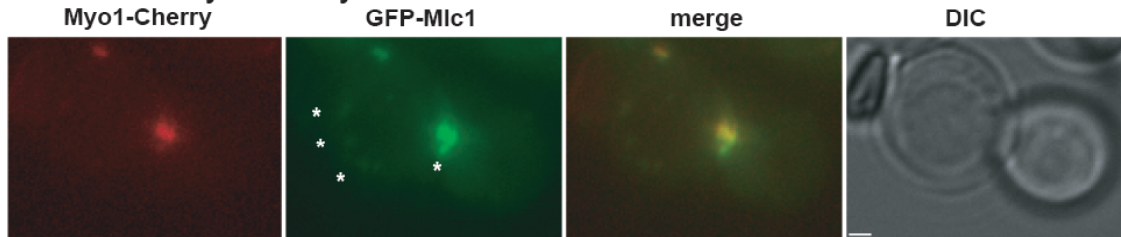
A. Mlc2-GFP Myo1-Cherry *cdh1* Δ



B. Iqg1-GFP Myo1-Cherry *cdh1* Δ



C. GFP-Mlc1 Myo1-Cherry *cdh1* Δ



D. Sec2-GFP Myo1-Cherry *cdh1* Δ

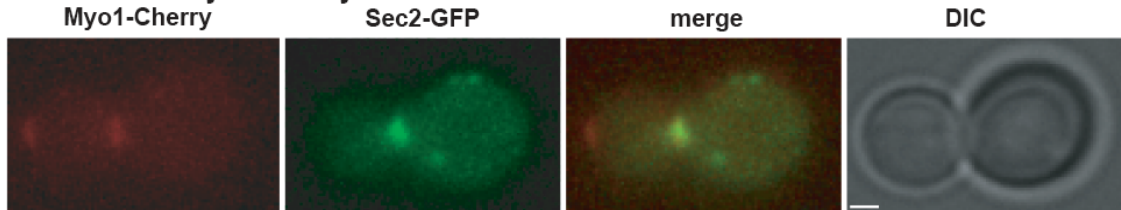


Figure 6. Deletion or stabilization of several APC^{Cdh1} substrates does not affect myosin disassembly. (A) Percentage of cells with visible GFP dots at least 10 minutes after ring contraction for the indicated strains. Images for some strains are shown in later panels. The exact percentage for each strain is provided in Appendix Table 2. (B) Overexpression of the CDK inhibitor Sic1 does not rescue the myosin disassembly defect in *cdh1Δ* cells. Time-lapse images of Myo1-GFP *GAL-SIC1 cdh1Δ* cells, 3 h after addition of galactose to induce expression of *SIC1*. (C, D) Stabilization of the APC^{Cdh1} substrates Cdc5 and Iqg1 does not affect myosin disassembly. Time-lapse series of Myo1-GFP in cells expressing non-degradable $\Delta 5-70$ -*cdc5* (C) or non-degradable $\Delta 42$ -*iqg1* (D). (E) Iqg1 disassembly does not depend on its degradation by the APC^{Cdh1}. Time-lapse images of $\Delta 42$ -*iqg1*-GFP were taken at one-minute intervals, and time point 0 marks the initiation of ring contraction. The cell outline is drawn in the first panel. Bar, 1 μ m.

Figure 6.

A.

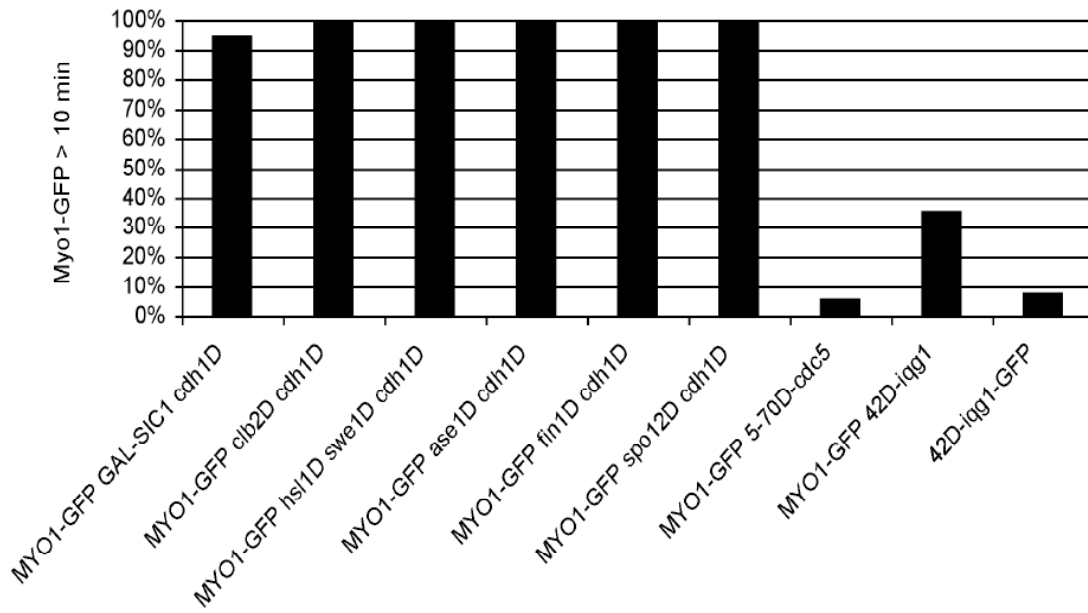
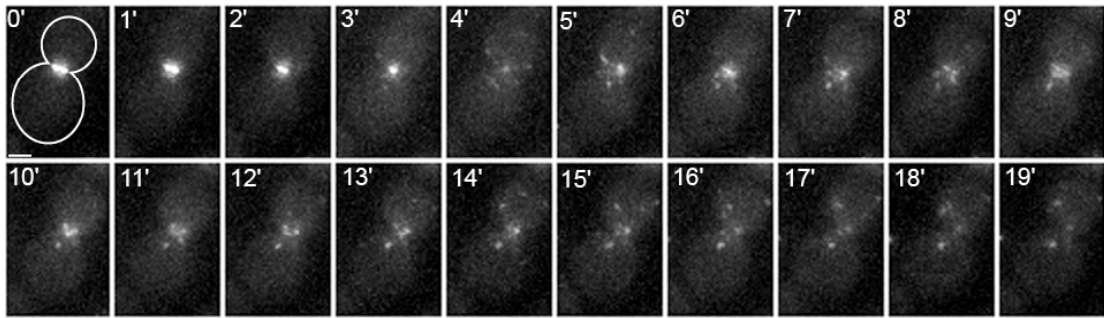
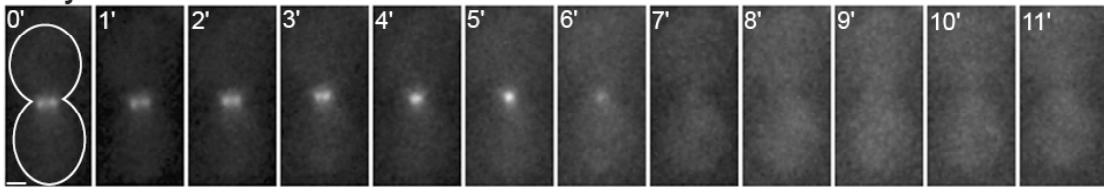


Figure 6.

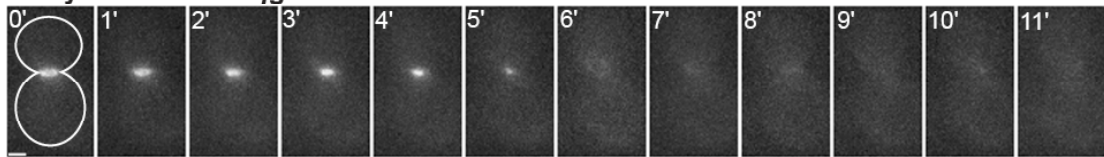
B. Myo1-GFP Gal-Sic1 *cdh1*Δ



C. Myo1-GFP Δ5-70-*cdc5*



D. Myo1-GFP Δ42-*iqg1*



E. Δ42-*iqg1*-GFP

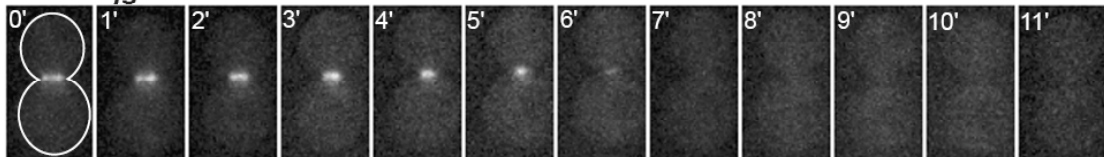
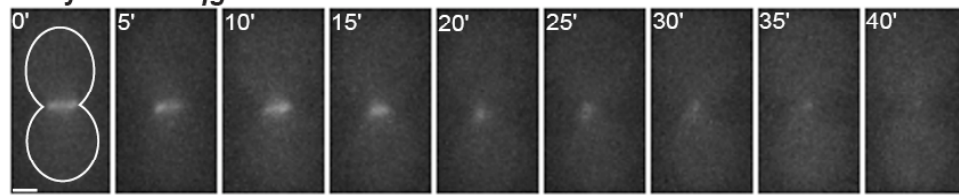


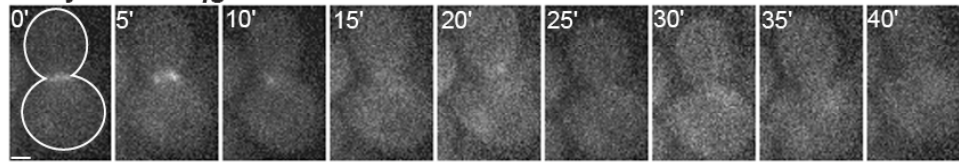
Figure 7. Deletion of *IQG1* or *MYO1* partially rescues the disassembly defect in *cdh1Δ* cells. All images were acquired every 5 minutes to decrease photobleaching of the weak Myo1-GFP or Iqg1-GFP signals. Time-lapse images were acquired of the following strains: (A) Myo1-GFP *iqg1Δ cdh1Δ*, (B) Myo1-GFP *iqg1Δ*, (C) Iqg1-GFP *myo1Δ*, and (D) Iqg1-GFP *myo1Δ cdh1Δ*. Time 0 indicates initiation of ring contraction. (E) Percentage of cells with visible GFP dots at least 10 min after ring contraction for the indicated strains. The exact percentage for each strain is provided in Appendix Table 2. (F) Maximum number of dots per cell at least 10 min after ring contraction. The *MYO1-GFP cdh1Δ* data from Fig. 2B is included here for convenience. Bar, 1 μ m.

Figure 7.

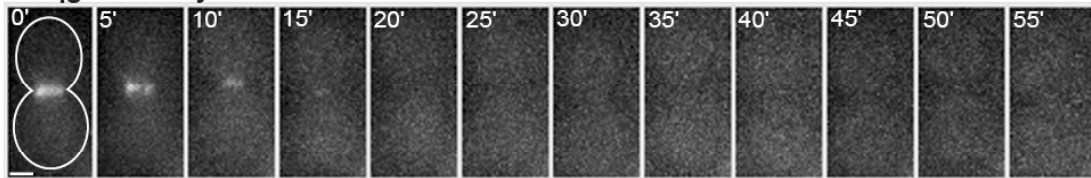
A. Myo1-GFP *iqg1* Δ *cdh1* Δ



B. Myo1-GFP *iqg1* Δ



C. *iqg1*-GFP *myo1* Δ



D. *iqg1*-GFP *myo1* Δ *cdh1* Δ

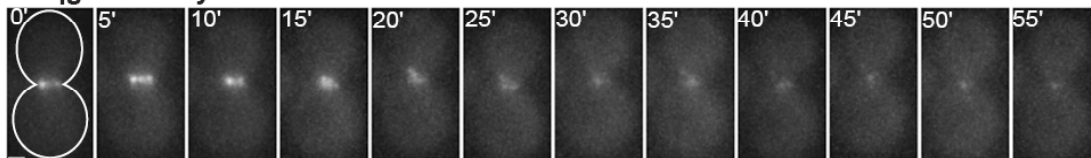
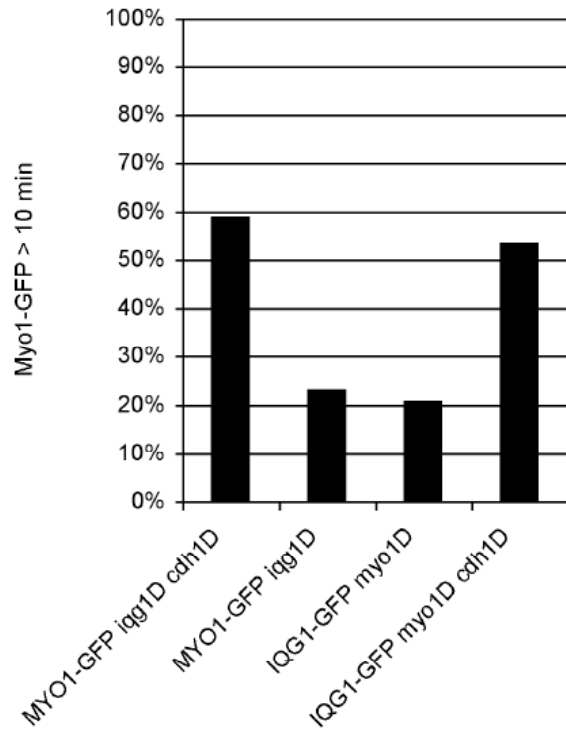


Figure 7.

E.



F.

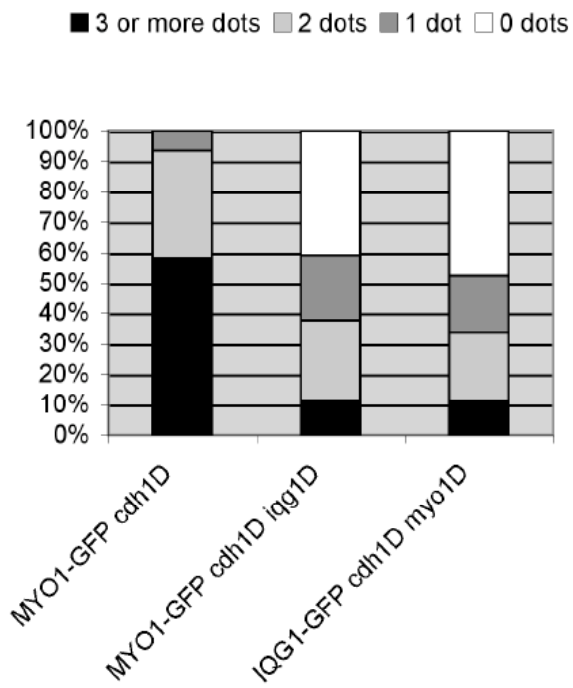
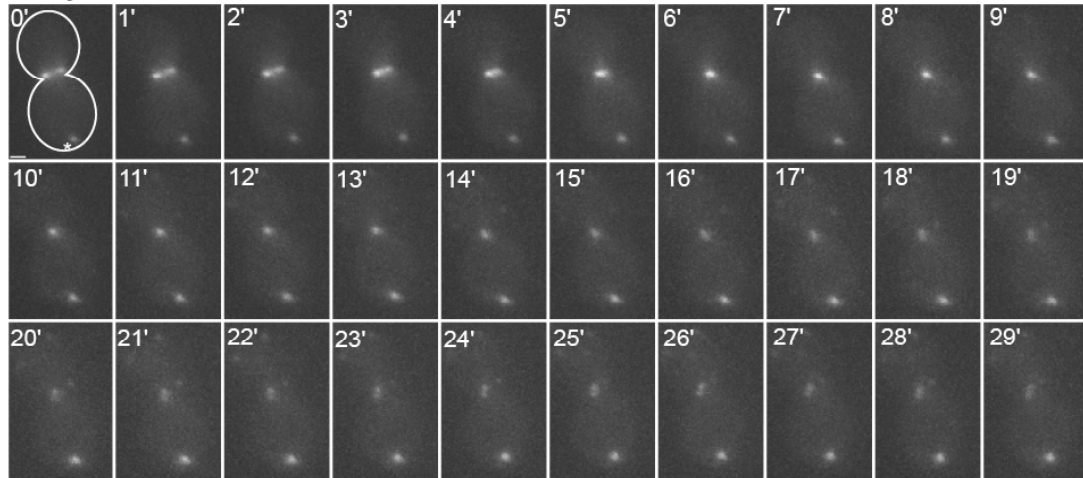


Figure 8. Mlc2 and APC^{Cdh1} function together to disassemble the actomyosin ring.

Time-lapse images of (A) Myo1-GFP *mlc2Δ cdh1Δ* and (B) Myo1-GFP *mlc2Δ* cells acquired every minute; time 0 indicates initiation of ring contraction. The asterisk in (A, time 0) indicates a Myo1 dot present before ring contraction. (C) Deletion of *MLC2* in combination with non-degradable $\Delta 42$ -*iqg1* inhibits myosin disassembly. Time-lapse images of a Myo1-GFP $\Delta 42$ -*iqg1 mlc2Δ* cell acquired every minute. (D) Non-degradable $\Delta 42$ -*iqg1*-GFP disassembly is also inhibited by deletion of *MLC2*. Time-lapse images of a $\Delta 42$ -*iqg1*-GFP *mlc2Δ* cell acquired every minute. (E) Percentage of cells with visible GFP dots at least 10 min after ring contraction for the indicated strains. The exact percentage for each strain is shown in Appendix Table 2. (F) Maximum number of dots per cell at least 10 min after ring contraction. The *MYO1-GFP cdh1Δ* data from Fig. 2B is included here for convenience. Bar, 1 μ m.

Figure 8.

A. Myo1-GFP *mlc2* Δ *cdh1* Δ



B. Myo1-GFP *mlc2* Δ

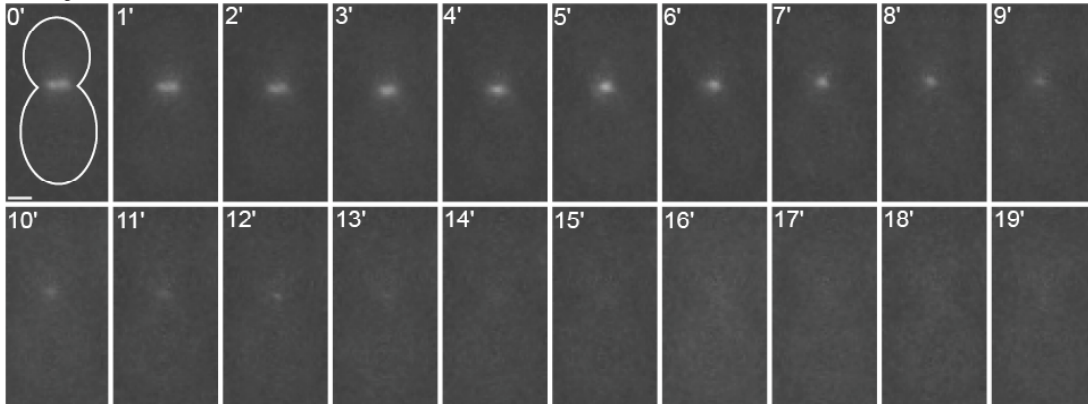
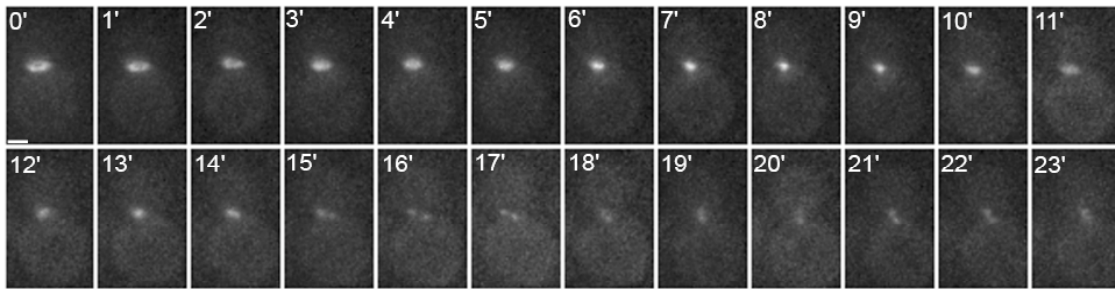


Figure 8.

C. Myo1-GFP $\Delta 42$ -*iqg1* *mlc2* Δ



D. $\Delta 42$ -*iqg1*-GFP *mlc2* Δ

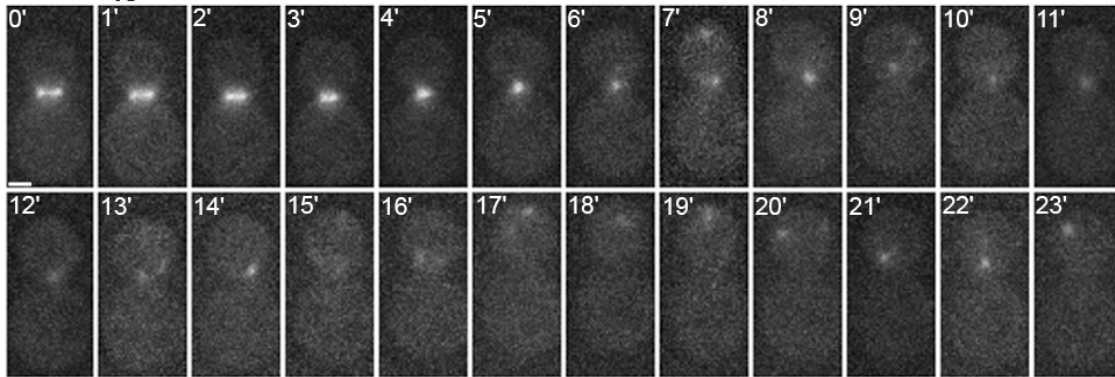
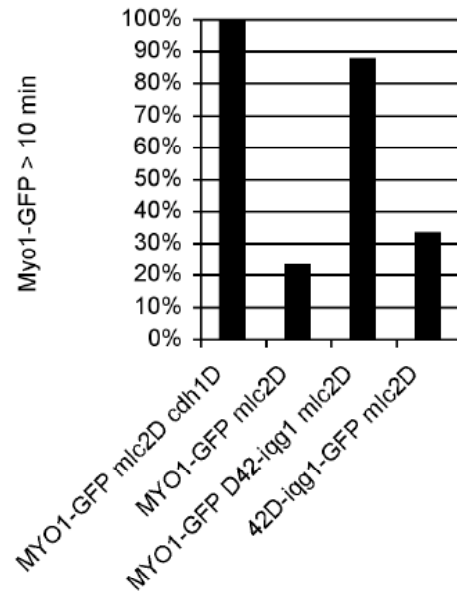


Figure 8.

E.



F.

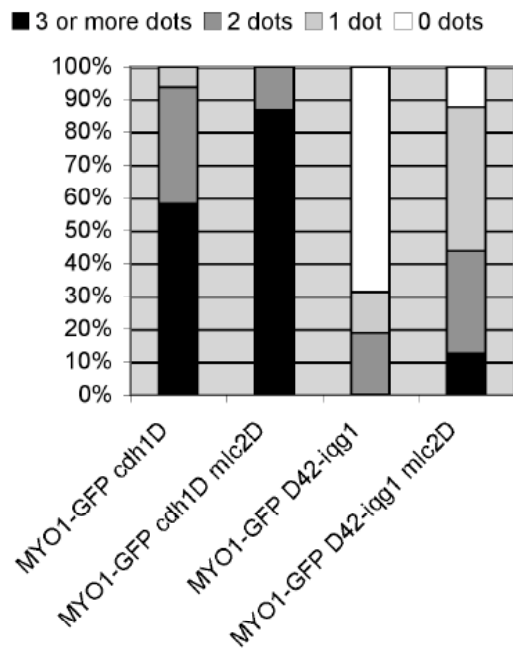
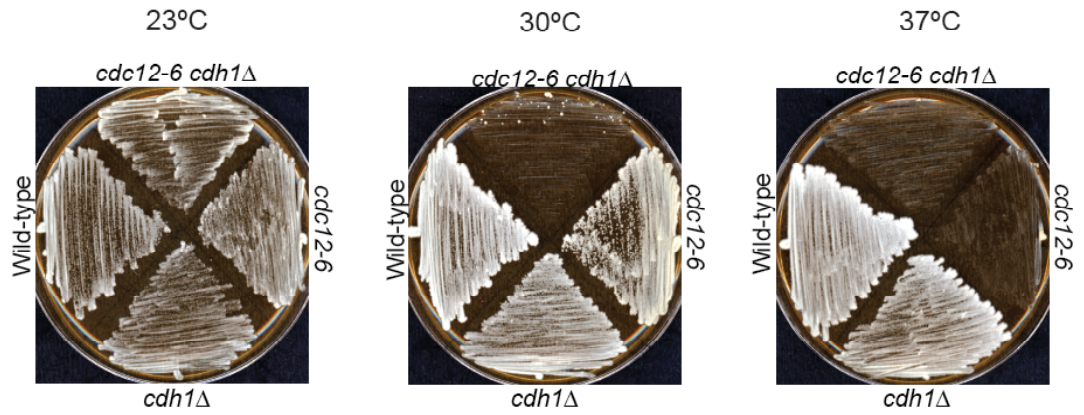


Figure 9. Deleting *CDH1* lowers the restrictive temperature of a septin mutant. (A) Wild-type, *cdh1* Δ , *cdc12-6*, and *cdc12-6 cdh1* Δ cells were patched on YPD agarose plates and grown at the indicated temperatures. (B) *cdc12-6 cdh1* Δ cells at 30°C die as chains of cells with multiple DNA masses. Representative images of wild-type, *cdh1* Δ , *cdc12-6*, and *cdc12-6 cdh1* Δ cells were stained with DAPI to observe DNA masses and visualized by DIC microscopy. (C) Percentage of cells with visible GFP dots at least 10 min after ring contraction for the indicated strains. The exact percentage for each strain is shown in Appendix Table 2. (D) Maximum number of dots per cell at least 10 min after ring contraction. Bar, 1 μ m.

Figure 9.

A.



B.

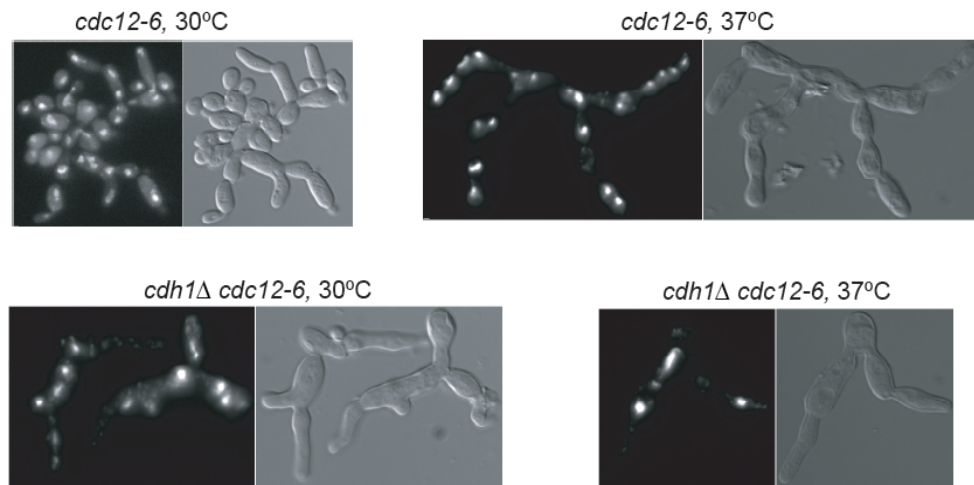
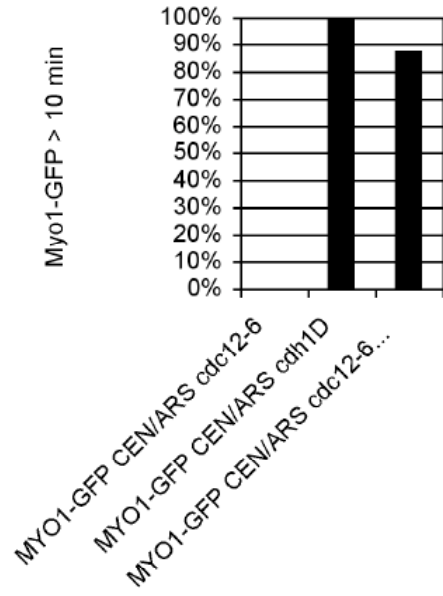
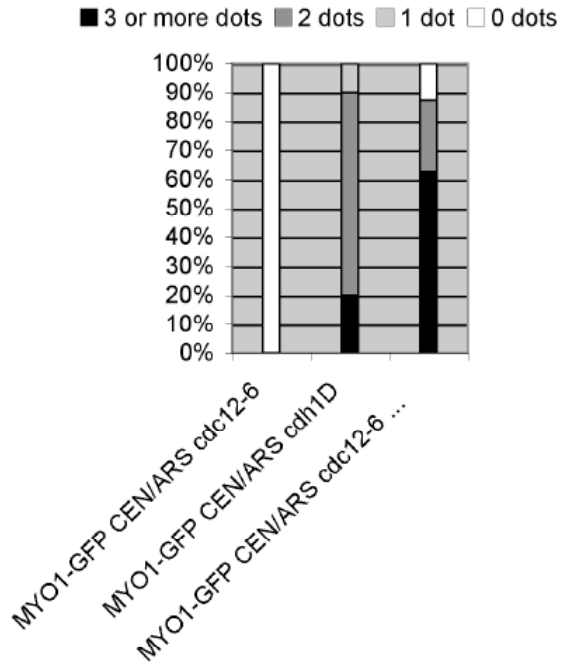


Figure 9.

C.



D.



APPENDIX

Figure 1. *cdh1*Δ and *mlc2*Δ cell clustering is enhanced in a *mlc2*Δ *cdh1*Δ double mutant. For each of the indicated strains, 400 cells were counted and clusters were defined as groups of 3 or more cells after brief sonication, as described in Materials and Methods.

Figure 1.

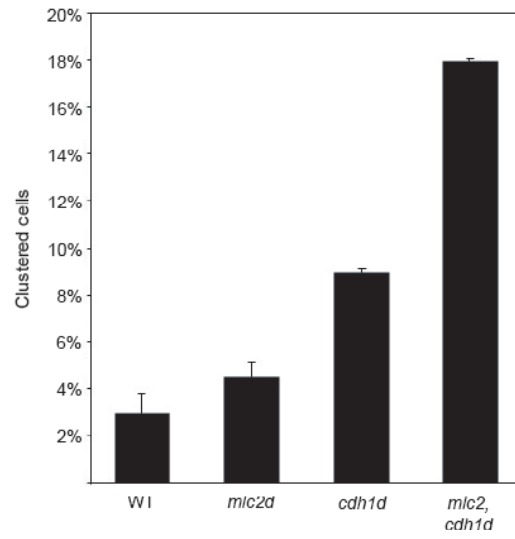
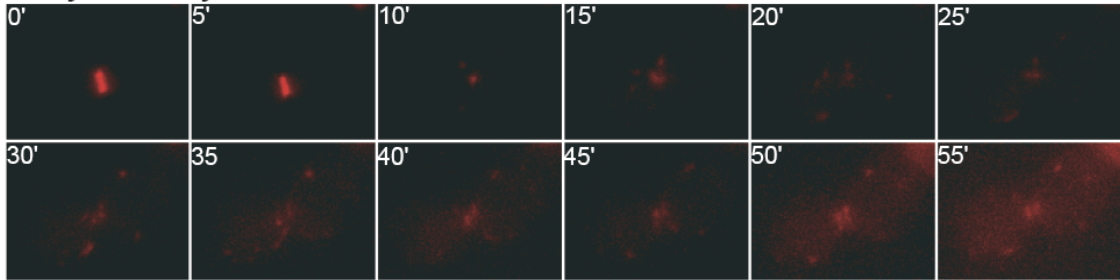


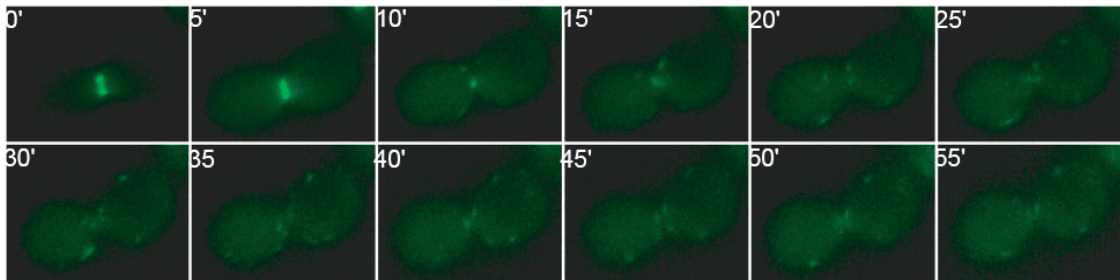
Figure 2. Myo1 and Mlc2 co-localize after ring contraction in *cdh1Δ* cells. Time-lapse images of a Myo1-Cherry Mlc2-GFP *cdh1Δ* cell, showing: (A) Myo1-Cherry (red); (B) Mlc2-GFP (green); (C) merged composite of Myo1-Cherry and Mlc2-GFP; and (D) corresponding DIC images. Bar, 1 μm .

Figure 2.

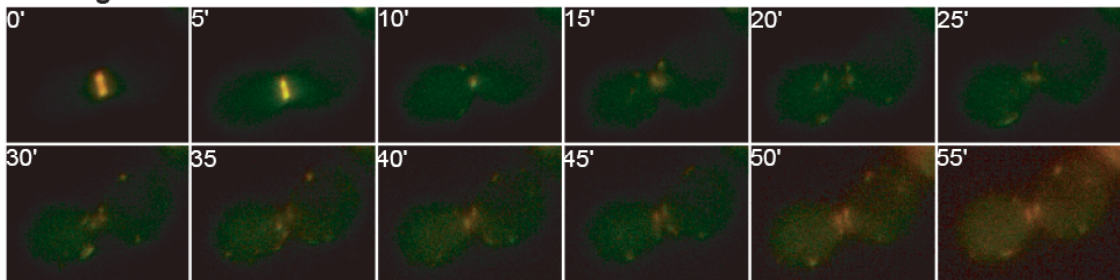
A. Myo1-Cherry



B. Mlc2-GFP



C. merge



D. DIC

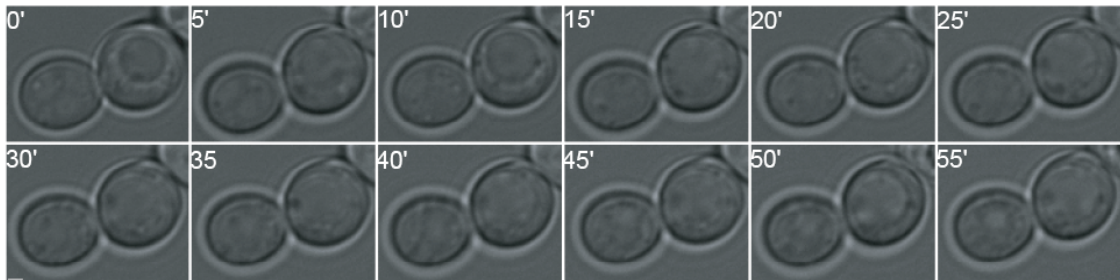
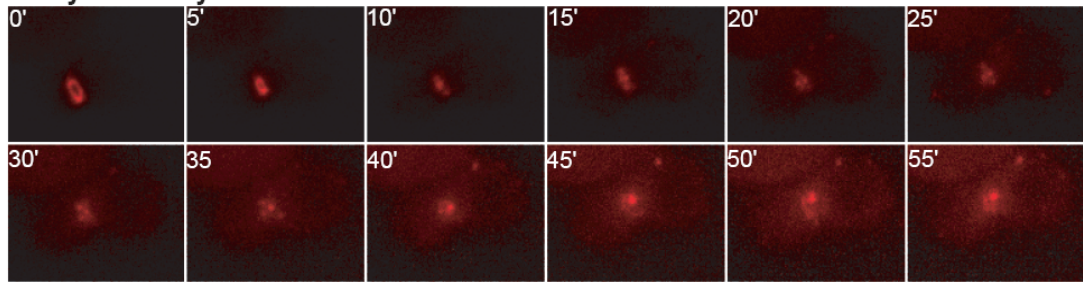


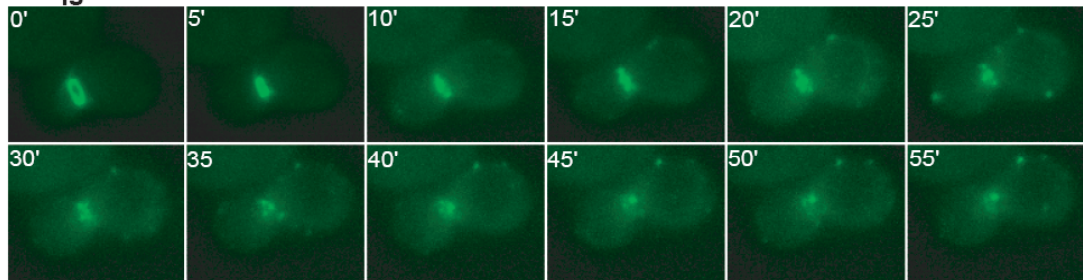
Figure 3. Myo1 and Iqg1 co-localize after ring contraction in *cdh1Δ* cells. Time-lapse images of a Myo1-Cherry Iqg1-GFP *cdh1Δ* cell, showing: (A) Myo1-Cherry (red); (B) Iqg1-GFP (green); (C) merged composite; and (D) corresponding DIC images. Bar, 1 μm .

Figure 3.

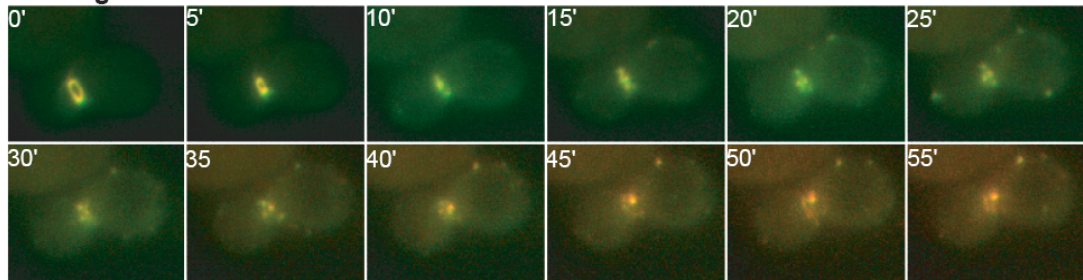
A. Myo1-Cherry



B. Iqg1-GFP



C. merge



D. DIC

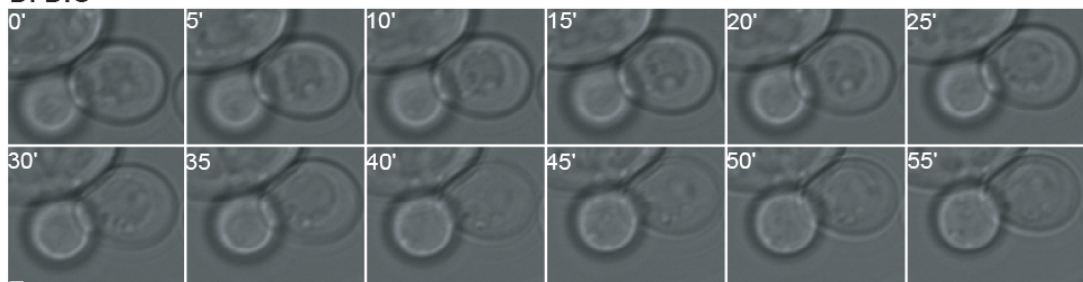
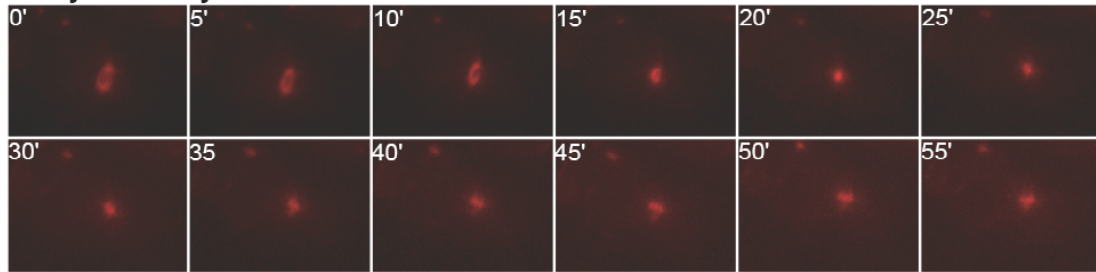


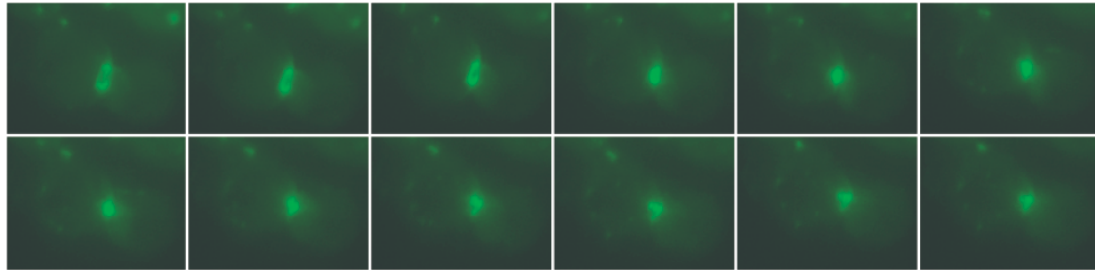
Figure 4. Myo1 and Mlc1 co-localize after ring contraction in *cdh1*Δ cells. Time lapse images of Myo1-Cherry GFP-Mlc1 *cdh1*Δ cells, showing: (A) Myo1-Cherry (red); (B) GFP-Mlc1 (green); (C) merged composite; and (D) corresponding DIC images. Bar, 1 μm.

Figure 4.

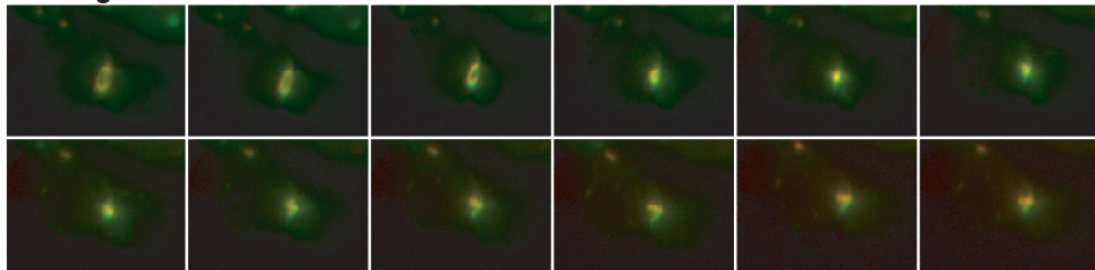
A. Myo1-Cherry



B. GFP-Mlc1



C. merge



D. DIC

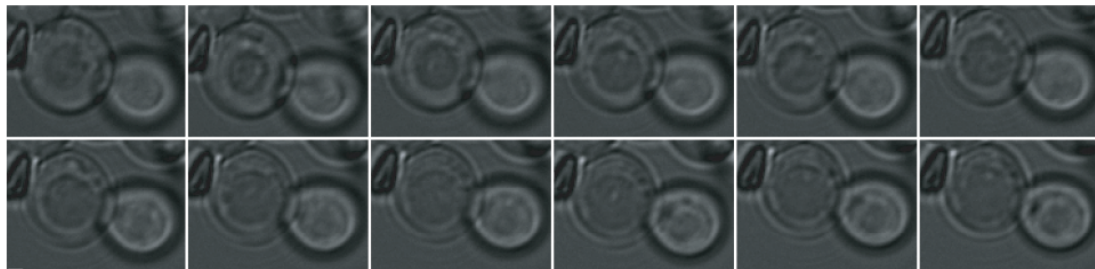


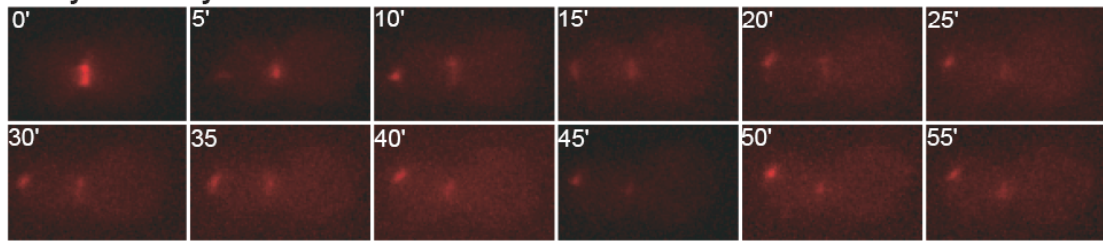
Figure 5. Myo1 and Sec2 do not co-localize after ring contraction in *cdh1*Δ cells.

Time-lapse images of a Myo1-Cherry Sec2-GFP *cdh1*Δ cell, showing: (A) Myo1-Cherry (red); (B) Sec2-GFP (green); (C) merged composite; and (D) corresponding DIC images.

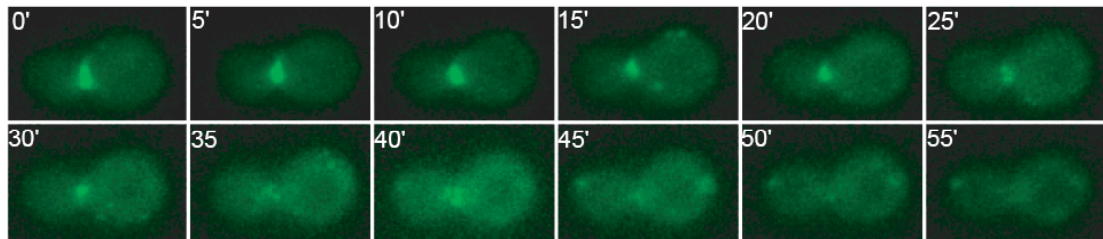
Bar, 1 μm.

Figure 5.

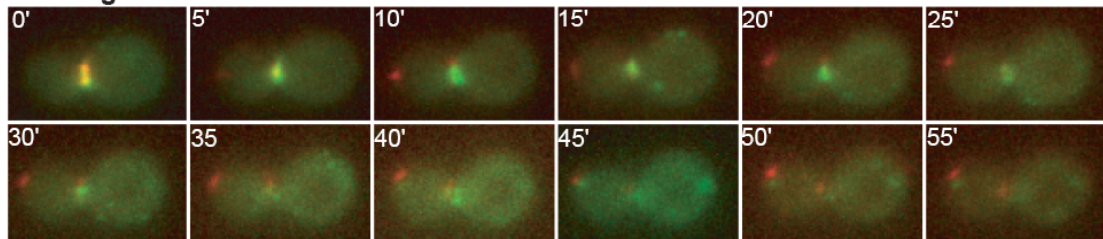
A. Myo1-Cherry



B. Sec2-GFP



C. merge



D. DIC

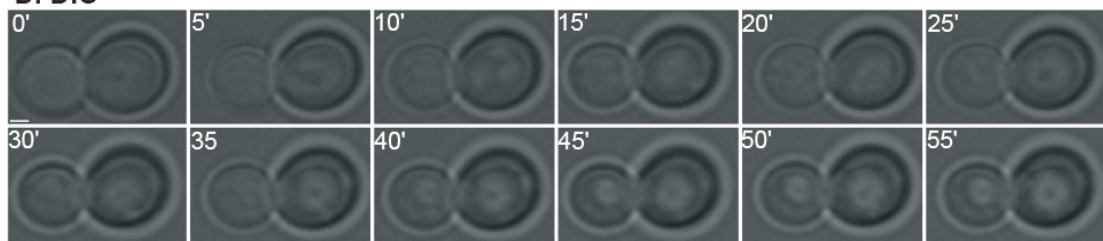


Table 1. Cell cycle abundance of cytokinesis proteins. The 103 cytokinesis proteins that were tested in the cell cycle arrest screen (described in Materials and Methods) are shown with their corresponding transcription peak; number of potential Cdk1 sites; D-box and KEN sequences; Western blots illustrating their abundance in G1 and G2/M arrested cells; and a brief description of protein function from SGD. A “y” or “n” (indicating yes or no) are in the columns labeled visible band, absent_G1 & present_G2/M, and band shift. The first 7 proteins are also shown in Chapter 2 Fig. 1.

Table 1

protein	peak	Cdk1 sites	D-box	KEN	visible band	absent_G1 & present_G2/M	band shift	Log-G1-G2/M	positive repeat G1-G2/M-G1-G2/M	SGD Function
CDC5	G2/M	1	0	1	y	y	y/n			Serine/threonine protein kinase required for exit from mitosis; may be involved in operation of the mitotic spindle, member of the polo family of protein kinases
IQG1	G2/M	4	2	2	y	y	y			Essential protein required for determination of budding pattern, promotes localization of axial markers Bud4p and Cdc12p and functionally interacts with Sec3p, localizes to the contractile ring during anaphase, member of the IQGAP family
HOF1	G2/M	0	1	1	y	y	y			Bud neck-localized, SH3 domain-containing protein required for cytokinesis; regulates actomyosin ring dynamics and septin localization; interacts with the formins, Bni1p and Dnr1p, and with Cyk3p, Vrp1p, and Dn5p
MOB1	G2/M	2	0	0	y	y	n			Component of the mitotic exit network; associates with and is required for the activation and Cdc15p-dependent phosphorylation of the Dbf2p kinase; required for cytokinesis and cell separation
BUD4	G2/M	6	0	0	y	y	n			Protein involved in bud-site selection and required for axial budding pattern; localizes with septins to bud neck in mitosis and may constitute an axial landmark for next round of budding, potential Cdc28p substrate
TEM1	G2/M	0	0	0	y	y	n			GTP-binding protein of the ras superfamily involved in termination of M-phase; controls actomyosin and septin dynamics during cytokinesis
ELM1	S/G2	1	0	1	y	y	n			Serine/threonine protein kinase that regulates cellular morphogenesis, septin behavior, and cytokinesis; required for the regulation of other kinases; forms part of the bud neck ring
BUD2		1	0	0	y	y	n			GTPase activating factor for Rsr1p/Bud1p required for both axial and bipolar budding patterns; mutants exhibit random budding in all cell types
BUD3	S/G2	5	0	1	y	y/n	y		not visible	Protein involved in bud-site selection and required for axial budding pattern; localizes with septins to bud neck in mitosis and may constitute an axial landmark for next round of budding
EXO84		5	1	0	y	y/n	n		not visible	Essential protein with dual roles in spliceosome assembly and exocytosis; the exocyst complex (Sec3p, Sec5p, Sec6p, Sec8p, Sec10p, Sec15p, Exo70p, and Exo84p) mediates polarized targeting of secretory vesicles to active sites of exocytosis
ROM1		0	1	0	y	y/n	n		not visible	GDP/GTP exchange protein (GEP) for Rho1p; mutations are synthetically lethal with mutations in rom2, which also encodes a GEP
PRK1		3	1	0	y	y/n	y			Protein serine/threonine kinase; regulates the organization and function of the actin cytoskeleton through the phosphorylation of the Pan1p-Sla1p-End3p protein complex
SEC5		0	2	2	y	y/n	n		not test	Essential 107kDa subunit of the exocyst complex (Sec3p, Sec5p, Sec6p, Sec8p, Sec10p, Sec15p, Exo70p, and Exo84p), which has the essential function of mediating polarized targeting of secretory vesicles to active sites of exocytosis
SEC10		0	0	0	y	n	y			Essential 100kDa subunit of the exocyst complex (Sec3p, Sec5p, Sec6p, Sec8p, Sec10p, Sec15p, Exo70p, and Exo84p), which has the essential function of mediating polarized targeting of secretory vesicles to active sites of exocytosis
CDC3		0	0	0	y	n	y			Component of the septin ring of the mother-bud neck that is required for cytokinesis; septins recruit proteins to the neck and can act as a barrier to diffusion at the membrane, and they comprise the 10nm filaments seen with EM
CDC11		0	0	0	y	n	y			Component of the septin ring of the mother-bud neck that is required for cytokinesis; septins recruit proteins to the neck and can act as a barrier to diffusion at the membrane, and they comprise the 10nm filaments seen with EM

Table 1

protein	peak	Cdk1 sites	D-box	KEN	visible band	absent_G1 & present_G2/M	band shift	Log-G1-G2/M	positive repeat G1-G2/M-G1-G2/M	SGD Function
SHS1		1	0	1	y	n	y			One of five related septins (Cdc3p, Cdc10p, Cdc11p, Cdc12p, Shs1p) that form a cortical filamentous collar at the mother-bud neck which is necessary for normal morphogenesis and cytokinesis
GIN4	G1/S	2	0	0	y	n	y			Protein kinase involved in bud growth and assembly of the septin ring, proposed to have kinase-dependent and kinase-independent activities; undergoes autophosphorylation; similar to Kcc4p and Hsl1p
SAC7		2	0	0	y	n	y			GTPase activating protein (GAP) for Rho1p, involved in signaling to the actin cytoskeleton, null mutations suppress tor2 mutations and temperature sensitive mutations in actin; potential Cdc28p substrate
HKR1		1	0	1	y	n	y			Serine/threonine rich cell surface protein; osmosensor; involved in the regulation of cell wall beta-1,3 glucan synthesis, bud site selection and hyperosmotic response, overexpression confers resistance to Hansenula mrakii killer toxin HM-1
CDC15		5	0	0	y	n	y			Protein kinase of the Mitotic Exit Network that is localized to the spindle pole bodies at late anaphase; promotes mitotic exit by directly switching on the kinase activity of Dbf2p
BUD7		1	1	1	y	n	y			Member of the Chs5p-Arf1p-binding proteins (ChAPs), a group of 4 related, interacting proteins (Bch1p, Fmp50p, Bud7p, Chs6p) that mediate export of specific cargo proteins, including chitin synthase Chs3p, from the Golgi to plasma membrane
DBF2	G2/M	2	0	0	y	n	y			Ser/Thr kinase involved in transcription and stress response; functions as part of a network of genes in exit from mitosis; localization is cell cycle regulated, activated by Cdc15p during the exit from mitosis
BFA1		1	0	0	y	n	y			Component of the GTPase-activating Bfa1p-Bub2p complex involved in multiple cell cycle checkpoint pathways that control exit from mitosis
YCK1	S/G2	1	0	0	y	n	y			Palmitoylated, plasma membrane-bound casein kinase I isoform; shares redundant functions with Yck2p in morphogenesis, proper septin assembly, endocytic trafficking; provides an essential function overlapping with that of Yck2p
BEM3		5	0	0	y	n	y			Rho GTPase activating protein (RhoGAP) involved in control of the cytoskeleton organization; targets the essential Rho-GTPase Cdc42p, which controls establishment and maintenance of cell polarity, including bud-site assembly
SPA2		2	0	1	y	n	y			Component of the polarisome, which functions in actin cytoskeletal organization during polarized growth; acts as a scaffold for Mkk1p and Mpk1p cell wall integrity signaling components; potential Cdc28p substrate
BEM2		1	0	0	y	n	y			Rho GTPase activating protein (RhoGAP) involved in the control of cytoskeleton organization and cellular morphogenesis; required for bud emergence
PAN1		0	1	0	y	n	y			Part of actin cytoskeleton-regulatory complex Pan1p-Sla1p-End3p, associates with actin patches on the cell cortex; promotes protein-protein interactions essential for endocytosis; previously thought to be a subunit of poly(A) ribonuclease
CLA4		0	0	0	y	n	y			Cdc42p activated signal transducing kinase of the PAK (p21-activated kinase) family, involved in septin ring assembly and cytokinesis; directly phosphorylates septins Cdc3p and Cdc10p; other yeast PAK family members are Ste20p and Skn1p
SEC15		0	1	0	y	n	y/n			Essential 113kDa subunit of the exocyst complex (Sec3p, Sec5p, Sec6p, Sec8p, Sec10p, Sec15p, Exo70p, and Exo84p), which mediates polarized targeting of vesicles to active sites of exocytosis; Sec15p associates with Sec4p and vesicles
BNI4	G1	4	1	0	y	n	y/n			Targeting subunit for Glc7p protein phosphatase, localized to the bud neck, required for localization of chitin synthase III to the bud neck via interaction with the chitin synthase III regulatory subunit Skt5p

Table 1

protein	Cdk1 peak	D-sites	box	KEN	visible band	absent_G1 & present_G2/M	band shift	Log-G1-G2/M	positive repeat G1-G2/M-G1-G2/M	SGD Function
BUD8	2	0	0	0	y	n	y/n			Actin- and formin-interacting protein, involved in actin cable nucleation and polarized cell growth; isolated as bipolar budding mutant, potential Cdc28p substrate
CDC14	0	0	0	0	y	n	y/n			Protein phosphatase required for mitotic exit; located in the nucleolus until liberated by the FEAR and Mitotic Exit Network in anaphase, enabling it to act on key substrates to effect a decrease in CDK/B-cyclin activity and mitotic exit
MYO1	G2/M	0	2	2	y	n	n			Type II myosin heavy chain, required for wild-type cytokinesis and cell separation; localizes to the actomyosin ring; binds to myosin light chains Mlc1p and Mlc2p through its IQ1 and IQ2 motifs respectively
BUD5	0	0	0	0	y	n	n			GTP/GDP exchange factor for Rsr1p (Bud1p) required for both axial and bipolar budding patterns; mutants exhibit random budding in all cell types
BUB2	S/G2	0	0	0	0	y	n	n		Mitotic exit network regulator, forms GTPase-activating Bfa1p-Bub2p complex that binds Tem1p and spindle pole bodies, blocks cell cycle progression before anaphase in response to spindle and kinetochore damage
SKT5	M/G1	0	1	1	y	n	n			Activator of Chs3p (chitin synthase III), recruits Chs3p to the bud neck via interaction with Bni4p; has similarity to Shc1p, which activates Chs3p during sporulation
BUD20	0	0	0	0	y	n	n			Protein involved in bud-site selection; diploid mutants display a random budding pattern instead of the wild-type bipolar pattern
BUD17	0	0	0	0	y	n	n			Protein involved in bud-site selection; diploid mutants display a random budding pattern instead of the wild-type bipolar pattern
SEC6	0	0	0	0	y	n	n			Essential 88kDa subunit of the exocyst complex, which mediates polarized targeting of secretory vesicles to active sites of exocytosis; dimeric form of Sec6p interacts with Sec9p in vitro and inhibits t-SNARE assembly
CDC10	S/G2	0	0	1	y	n	n			Component of the septin ring of the mother-bud neck that is required for cytokinesis; septins recruit proteins to the neck and can act as a barrier to diffusion at the membrane, and they comprise the 10nm filaments seen with EM
NAP1	0	0	0	0	y	n	n			Protein that interacts with mitotic cyclin Ctb2p; required for the regulation of microtubule dynamics during mitosis; controls bud morphogenesis; involved in the transport of H2A and H2B histones to the nucleus
BFR1	1	0	1	1	y	n	n			Component of mRNP complexes associated with polyribosomes; implicated in secretion and nuclear segregation; multicopy suppressor of BFA (Brefeldin A) sensitivity
CTS1	G1	1	0	0	0	y	n	n		Endochitinase, required for cell separation after mitosis; transcriptional activation during late G and early M cell cycle phases is mediated by transcription factor Ace2p
YCK2	0	0	0	0	y	n	n			Palmitoylated, plasma membrane-bound casein kinase I isoform; shares redundant functions with Yck1p in morphogenesis, proper septin assembly, endocytic trafficking; provides an essential function overlapping with that of Yck1p
LAS17	0	0	0	0	y	n	n			Actin assembly factor, activates the Arp2/3 protein complex that nucleates branched actin filaments; localizes with the Arp2/3 complex to actin patches; homolog of the human Wiskott-Aldrich syndrome protein (WASP)
PWP2	0	0	0	0	y	n	n			Conserved 90S pre-ribosomal component essential for proper endonucleolytic cleavage of the 35 S rRNA precursor at A0, A1, and A2 sites; contains eight WD-repeats; PWP2 deletion leads to defects in cell cycle and bud morphogenesis

Table 1

protein	Cdk1 peak	D-sites	box	KEN	visible band	absent_G1 & present_G2/M	band shift	Log-G1-G2/M	positive repeat G1-G2/M-G1-G2/M	SGD Function
MYO2	1	0	1	y	n	n				One of two type V myosin motors (along with MYO4) involved in actin-based transport of cargos; required for the polarized delivery of secretory vesicles, the vacuole, late Golgi elements, peroxisomes, and the mitotic spindle
RAX2	G2/M	1	0	0	y	n	n			N-glycosylated protein involved in the maintenance of bud site selection during bipolar budding; localization requires Rax1p
CHS3	0	1	0	y	n	n				Chitin synthase III, catalyzes the transfer of N-acetylglucosamine (GlcNAc) to chitin; required for synthesis of the majority of cell wall chitin, the chitin ring during bud emergence, and spore wall chitosan
PIK1	0	0	1	y	n	n				Phosphatidylinositol 4-kinase; catalyzes first step in the biosynthesis of phosphatidylinositol-4,5-bisphosphate; may control cytokinesis through the actin cytoskeleton
ARK1	1	1	0	y	n	n				Serine/threonine protein kinase involved in regulation of the cortical actin cytoskeleton; involved in control of endocytosis
EXO70	0	0	0	y	n	n				Essential 70kDa subunit of the exocyst complex (Sec3p, Sec5p, Sec6p, Sec8p, Sec10p, Sec15p, Exo70p, and Exo84p), which has the essential function of mediating polarized targeting of secretory vesicles to active sites of exocytosis
BUD22	0	0	0	y	n	n				Protein involved in bud-site selection; diploid mutants display a random budding pattern instead of the wild-type bipolar pattern
MMM1	0	0	0	y	n	n				Mitochondrial outer membrane protein, component of the Mdm10-Mdm12-Mmm1 complex involved in import and assembly of outer membrane beta-barrel proteins
END3	0	1	0	y	n	n				EH domain-containing protein involved in endocytosis, actin cytoskeletal organization and cell wall morphogenesis; forms a complex with Sla1p and Pan1p
BUD23	0	0	0	y	n	n				Protein involved in bud-site selection; diploid mutants display a random budding pattern instead of the wild-type bipolar pattern
BUD32	0	0	0	y	n	n				Protein kinase proposed to be involved in bud-site selection, telomere uncapping and elongation, and transcription; component of the EKC/KEOPS protein complex with Kae1p, Cgi121p, Pcc1p, and Gon7p
RDI1	0	0	1	y	n	n				Rho GDP dissociation inhibitor involved in the localization and regulation of Cdc42p
BUD31	0	0	0	y	n	n				Protein involved in bud-site selection; analysis of integrated high-throughput datasets predicts an involvement in RNA splicing; diploid mutants display a random budding pattern instead of the wild-type bipolar pattern
HYM1	0	0	0	y	n	n				Component of the RAM signaling network that is involved in regulation of Ace2p activity and cellular morphogenesis, interacts with Kic1p and Sog2p, localizes to sites of polarized growth during budding and during the mating response
THP1	0	0	0	y	n	n				Nuclear pore-associated protein, forms a complex with Sac3p that is involved in transcription and in mRNA export from the nucleus; contains a PAM domain implicated in protein-protein binding
BUD27				y	n	n				Protein involved in bud-site selection, nutrient signaling, and gene expression controlled by the TOR kinase; diploid mutants display a random budding pattern instead of the wild-type bipolar pattern

Table 1















protein	peak	Cdk1 sites	D-box	KEN	visible band	absent_G1 & present_G2/M	band shift	Log-G1-G2/M	positive repeat G1-G2/M-G1-G2/M	SGD Function
CYK3	M/G1	1	0	0	y	n	n			H3-domain protein located in the mother-bud neck and the cytokinetic actin ring; mutant phenotype and genetic interactions suggest a role in cytokinesis
STE20		5	0	0	y	n	n			Signal transducing kinase of the PAK (p21-activated kinase) family, involved in pheromone response and pseudohyphal/invasive growth pathways, activated by Cdc42p; binds Ste4p at a GBB motif present in noncatalytic domains of PAK kinases
KCC4	G1	2	0	1	y	n	n			Protein kinase of the bud neck involved in the septin checkpoint, associates with septin proteins, negatively regulates Swe1p by phosphorylation, shows structural homology to bud neck kinases Gin4p and Hsl1p
DSE4					y	n	n			Daughter cell-specific secreted protein with similarity to glucanases, degrades cell wall from the daughter side causing daughter to separate from mother
SEC3		2	0	1	y	n	n			Non-essential subunit of the exocyst complex (Sec3p, Sec5p, Sec6p, Sec8p, Sec10p, Sec15p, Exo70p, Exo84p) which mediates targeting of post-Golgi vesicles to sites of active exocytosis; Sec3p specifically is a spatial landmark for secretion
BNR1		2	1	1	y	n	n			Formin, nucleates the formation of linear actin filaments, involved in cell processes such as budding and mitotic spindle orientation which require the formation of polarized actin cables, functionally redundant with BNI1
BNI1		3	0	2	y	n	n			Formin, nucleates the formation of linear actin filaments, involved in cell processes such as budding and mitotic spindle orientation which require the formation of polarized actin cables, functionally redundant with BNR1
NUM1	S/G2	2	0	13	y	n	n			Protein required for nuclear migration, localizes to the mother cell cortex and the bud tip, may mediate interactions of dynein and cytoplasmic microtubules with the cell cortex
BUD16		0	0	0	y	n	n			Protein involved in bud-site selection and telomere maintenance, diploid mutants display a random budding pattern instead of the wild-type bipolar pattern; has similarity to pyridoxal kinases
SPC34	S	0	0	0	y	n	n			Essential subunit of the Dam1 complex (aka DASH complex), couples kinetochores to the force produced by MT depolymerization thereby aiding in chromosome segregation; also localized to nuclear side of spindle pole body
BUD25					y	n	n			Protein involved in bud-site selection; diploid mutants display a random budding pattern instead of the wild-type bipolar pattern
SPR28		0	0	0	y	n	n			Sporulation-specific homolog of the yeast CDC3/10/11/12 family of bud neck microfilament genes; meiotic septin expressed at high levels during meiotic divisions and ascospore formation
ROM2		2	0	0	y	n	n			GDP/GTP exchange protein (GEP) for Rho1p and Rho2p; mutations are synthetically lethal with mutations in rom1, which also encodes a GEP
GLC7					y	n	n			Catalytic subunit of type 1 serine/threonine protein phosphatase, involved in many processes including glycogen metabolism, sporulation, and mitosis; interacts with multiple regulatory subunits; predominantly isolated with Sds22p
NFI1		0	0	0	n					SUMO ligase, catalyzes the covalent attachment of SUMO (Smt3p) to proteins; involved in maintenance of proper telomere length
AME1		0	0	0	n					Essential kinetochore protein associated with microtubules and spindle pole bodies; component of the kinetochore sub-complex COMA (Cif19p, Okp1p, Mcm21p, Ame1p); involved in spindle checkpoint maintenance

Table 1

protein	peak	Cdk1 sites	D-box	KEN	visible band	absent_G1 & present_G2/M	band shift	Log-G1-G2/M	positive repeat G1-G2/M-G1-G2/M	SGD Function
MLC2					n					Regulatory light chain for the type II myosin, Myo1p; binds to an IQ motif of Myo1p; localization to the bud neck depends on Myo1p; involved in the disassembly of the Myo1p ring
CDC12		0	1	0	n					Component of the septin ring of the mother-bud neck that is required for cytokinesis; septins recruit proteins to the neck and can act as a barrier to diffusion at the membrane, and they comprise the 10nm filaments seen with EM
BUD9	G1	0	0	0	n					Protein involved in bud-site selection; diploid mutants display a unipolar budding pattern instead of the wild-type bipolar pattern, and bud at the distal pole
AXL2	G1	1	0	0	n					Integral plasma membrane protein required for axial budding in haploid cells, localizes to the incipient bud site and bud neck; glycosylated by Pm4p; potential Cdc28p substrate
AXL1		0	1	0	n					Haploid specific endoprotease that performs one of two N-terminal cleavages during maturation of a-factor mating pheromone; required for axial budding pattern of haploid cells
HSL1	G1	2	2	3	n					Nim1p-related protein kinase that regulates the morphogenesis and septin checkpoints; associates with the assembled septin filament; required along with Hsi7p for bud neck recruitment, phosphorylation, and degradation of Swe1p
PIP2		0	0	1	n					Autoregulatory oleate-specific transcriptional activator of peroxisome proliferation; contains Zn(2)-Cys(6) cluster domain, forms heterodimer with Oaf1p; binds oleate response elements (OREs), activates beta-oxidation genes
DSE2					n					Daughter cell-specific secreted protein with similarity to glucanases, degrades cell wall from the daughter side causing daughter to separate from mother; expression is repressed by cAMP
RSR1	G1	0	0	0	n					GTP-binding protein of the ras superfamily required for bud site selection, morphological changes in response to mating pheromone, and efficient cell fusion; localized to the plasma membrane; significantly similar to mammalian Rap GTPases
BUD19		0	0	0	n					Dubious open reading frame, unlikely to encode a protein; not conserved in closely related Saccharomyces species; 88% of ORF overlaps the verified gene RPL39; diploid mutant displays a weak budding pattern phenotype in a systematic assay
YOR300V		0	0	1	n					Dubious open reading frame, unlikely to encode a protein; overlaps with verified gene BUD7/YOR299W; mutation affects bipolar budding and bud site selection, though phenotype could be due to the mutation's effects on BUD7
PFY1		0	0	0	n					Profilin, actin- and phosphatidylinositol 4,5-bisphosphate-binding protein, plays a role in cytoskeleton organization, required for normal timing of actin polymerization in response to thermal stress; localizes to plasma membrane and cytosol
BUD28		0	0	0	n					Dubious open reading frame, unlikely to encode a protein; not conserved in closely related Saccharomyces species; 98% of ORF overlaps the verified gene RPL22A; diploid mutant displays a weak budding pattern phenotype in a systematic assay
CDC42		0	0	0	n					Small rho-like GTPase, essential for establishment and maintenance of cell polarity; mutants have defects in the organization of actin and septins
BUD13		0	0	0	n					Subunit of the RES complex, which is required for nuclear pre-mRNA retention and splicing; involved in bud-site selection; diploid mutants display a unipolar budding pattern instead of the wild-type bipolar pattern
BNI5	G1	0	0	0	n					Protein involved in organization of septins at the mother-bud neck; may interact directly with the Cdc11p septin, localizes to bud neck in a septin-dependent manner

Table 1

protein	peak	Cdk1 sites	D-box	KEN	visible band	absent_G1 & present_G2/M	band shift	Log-G1-G2/M	positive repeat G1-G2/M-G1-G2/M	SGD Function
RAX1		0	0	0	n					Protein involved in bud site selection during bipolar budding; localization requires Rax2p; has similarity to members of the insulin-related peptide superfamily
CST9		2	0	0	n					SUMO E3 ligase; required for synaptonemal complex formation; localizes to synapsis initiation sites on meiotic chromosomes; potential Cdc28p substrate
BUD8	G2/M	2	0	0	n					Protein involved in bud-site selection; diploid mutants display a unipolar budding pattern instead of the wild-type bipolar pattern, and bud at the proximal pole
GPI1		0	0	0	n					Membrane protein involved in the synthesis of N-acetylglucosaminyl phosphatidylinositol (GlcNAc-PI), the first intermediate in the synthesis of glycosylphosphatidylinositol (GPI) anchors; human and mouse GPI1p are functional homologs
EGT2	M/G1	0	0	0	n					Glycosylphosphatidylinositol (GPI)-anchored cell wall endoglycanase required for proper cell separation after cytokinesis; expression is activated by Swi5p and lightly regulated in a cell cycle-dependent manner
CHS2	G2/M	4	0	0	n					Chitin synthase II, requires activation from zymogenic form in order to catalyze the transfer of N-acetylglucosamine (GlcNAc) to chitin; required for the synthesis of chitin in the primary septum during cytokinesis
SEC8		0	0	1	n					Essential 121kDa subunit of the exocyst complex (Sec3p, Sec5p, Sec6p, Sec8p, Sec10p, Sec15p, Exo70p, and Exo84p), which has the essential function of mediating polarized targeting of secretory vesicles to active sites of exocytosis
BUD26		0	0	0						Dubious open reading frame, unlikely to encode a protein; not conserved in closely related Saccharomyces species; 1% of ORF overlaps the verified gene SNU56; diploid mutant displays a weak budding pattern phenotype in a systematic assay
MLC1		0	0	0						Essential light chain for Myo1p, light chain for Myo2p; stabilizes Myo2p by binding to the neck region; interacts with Myo1p, Iqg1p, and Myo2p to coordinate formation and contraction of the actomyosin ring with targeted membrane deposition
BUD30										Dubious open reading frame, unlikely to encode a protein; not conserved in closely related Saccharomyces species; 98% of ORF overlaps the verified gene RPC53; diploid mutant displays a weak budding pattern phenotype in a systematic assay
RHO1		0	0	0						GTP-binding protein of the rho subfamily of Ras-like proteins, involved in establishment of cell polarity; regulates protein kinase C (Pkc1p) and the cell wall synthesizing enzyme 1,3-beta-glucan synthase (Fks1p and Gsc2p)
SEC4		0	0	0						Secretory vesicle-associated Rab GTPase essential for exocytosis; associates with the exocyst component Sec15p and may regulate polarized delivery of transport vesicles to the exocyst at the plasma membrane
ACT1		0	0	0						Actin, structural protein involved in cell polarization, endocytosis, and other cytoskeletal functions
3PR3		0	1	1						Sporulation-specific homolog of the yeast CDC3/10/11/12 family of bud neck microfilament genes; septin protein involved in sporulation; regulated by ABF1

Table 2. Microscopy data of ring contraction, disassembly, and dot mobility for all strains analyzed. This table contains all of the tabulated microscopy data as described in Materials and Methods. The strains are grouped according to the charts in the text.

Table 2

genotype	ring contraction (min)	standard dev.	# cells counted	GFP visible > 10 min	# cells counted	Myo1 movement toward bud neck	# cells counted
<i>MYO1-GFP</i>	5.7	1.1	39	35%	46	n.a.	
<i>MYO1-GFP cdh1Δ</i>	6.5	1.3	27	100%	33	64%	33
<i>MYO1-GFP APC2</i>	6.3	2.3	3	25%	4	n.a.	
<i>MYO1-GFP apc2Δ</i>	5.1	1.0	10	71%	7	n.a.	
<i>MLC2-GFP</i>	5.1	1.2	14	12%	17	n.a.	
<i>MLC2-GFP cdh1Δ</i>	6.9	1.7	15	100%	11	36%	11
<i>GFP-MLC1</i>	5.7	1.1	24	100%	22	14%	21
<i>GFP-MLC1 cdh1Δ</i>	6.2	1.6	14	100%	19	63%	16
<i>IQG1-GFP</i>	4.6	1.0	7	9%	11	0%	
<i>IQG1-GFP cdh1Δ</i>	5.3	1.5	8	100%	9	11%	9
<i>MYO1-GFP GAL-SIC1 cdh1Δ</i>	5.1	1.2	18	95%	19	n.a.	
<i>MYO1-GFP clb2Δ cdh1Δ</i>	9.1	1.5	16	100%	12	50%	12
<i>MYO1-GFP hsl1Δ swe1Δ cdh1Δ</i>	7.6	1.7	10	100%	11	64%	11
<i>MYO1-GFP ase1Δ cdh1Δ</i>	6.3	1.0	13	100%	18	89%	18
<i>MYO1-GFP fin1Δ cdh1Δ</i>	8.7	1.5	7	100%	9	63%	8
<i>MYO1-GFP spo12Δ cdh1Δ</i>	5.9	1.0	12	100%	15	67%	15
<i>MYO1-GFP 5-70Δ-cdc5</i>	6.1	1.5	15	6%	17	n.a.	
<i>MYO1-GFP 42Δ-iqg1</i>	5.7	1.3	20	35%	17	n.a.	
<i>42Δ-iqg1-GFP</i>	4.8	0.7	24	8%	26	n.a.	
<i>MYO1-GFP iqg1Δ cdh1Δ</i>	17	5.6	47	59%	61	n.a.	
<i>MYO1-GFP iqg1Δ</i>	16	4.4	10	23%	13	n.a.	
<i>IQG1-GFP myo1Δ</i>	17	8.9	16	21%	24	n.a.	
<i>IQG1-GFP myo1Δ cdh1Δ</i>	21	7.9	44	54%	82	n.a.	
<i>MYO1-GFP mlc2Δ cdh1Δ</i>	5.5	1.0	15	100%	19	11%	19
<i>MYO1-GFP mlc2Δ</i>	6.1	1.1	26	23%	26	n.a.	
<i>MYO1-GFP Δ42-iqg1 mlc2Δ</i>	6.4	1.6	20	88%	16	7%	14
<i>42Δ-iqg1-GFP mlc2Δ</i>	5.0	1.1	24	33%	24	n.a.	
<i>MYO1-GFP CEN/ARS cdc12-6</i>	5.2	1.7	14	0%	15	n.a.	
<i>MYO1-GFP CEN/ARS cdh1Δ</i>	5.7	0.8	12	100%	11	55%	11
<i>MYO1-GFP CEN/ARS cdc12-6 cdh1Δ</i>	6.2	1.4	9	88%	9	29%	8

Table 3. Myo1-GFP co-localizes with Mlc2, Iqg1, Mlc1. This table displays the percentage of GFP and Cherry co-localization for the indicated strains. The number of cells in which Myo1-Cherry was visible after 10 minutes (as described in Materials and Methods) are shown for each strain.

Table 3

genotype	co-localization	# Myo1-Cherry cells
<i>MLC2-GFP MYO1-Cherry cdh1Δ</i>	100%	8
<i>IQG1-GFP MYO1-Cherry cdh1Δ</i>	100%	14
<i>GFP-MLC1 MYO1-Cherry cdh1Δ</i>	73%	11
<i>SEC2-GFP MYO1-Cherry cdh1Δ</i>	13%	8

Table 4. Myo1 dots outside bud neck in *mlc2Δ cdh1Δ* strains. The percentage of cells in which a Myo1-GFP dot was visible outside of the bud neck before ring contraction are displayed. Only in the double *mlc2Δ cdh1Δ* cells were dots present before ring contraction.

Table 4

genotype	dot outside budneck before contraction
<i>MYO1-GFP</i>	0%
<i>MYO1-GFP cdh1Δ</i>	0%
<i>MYO1-GFP cdh1Δ mlc2Δ</i>	47%

BIBLIOGRAPHY

Amon, A. (1997). Regulation of B-type cyclin proteolysis by Cdc28-associated kinases in budding yeast. *EMBO J.* 16, 2693-2702.

Amon, A., Irniger, S., and Nasmyth, K. (1994). Closing the cell cycle circle in yeast: G2 cyclin proteolysis initiated at mitosis persists until the activation of G1 cyclins in the next cycle. *Cell* 77, 1037-1050.

Bardin, A.J., and Amon, A. (2001). Men and sin: what's the difference? *Nat Rev Mol Cell Biol* 2, 815-826.

Bi, E., Maddox, P., Lew, D.J., Salmon, E.D., McMillan, J.N., Yeh, E., and Pringle, J.R. (1998). Involvement of an actomyosin contractile ring in *Saccharomyces cerevisiae* cytokinesis. *J Cell Biol* 142, 1301-1312.

Blondel, M., Bach, S., Bamps, S., Dobbelaere, J., Wiget, P., Longaretti, C., Barral, Y., Meijer, L., and Peter, M. (2005). Degradation of Hof1 by SCF(Grr1) is important for actomyosin contraction during cytokinesis in yeast. *Embo J* 24, 1440-1452.

Boyne, J.R., Yosuf, H.M., Bieganowski, P., Brenner, C., and Price, C. (2000). Yeast myosin light chain, Mlc1p, interacts with both IQGAP and class II myosin to effect cytokinesis. *J Cell Sci* 113 Pt 24, 4533-4543.

Brandeis, M., and Hunt, T. (1996). The proteolysis of mitotic cyclins in mammalian cells persists from the end of mitosis until the onset of S phase. *EMBO J.* 15, 5280-5289.

Brill, S., Li, S., Lyman, C.W., Church, D.M., Wasmuth, J.J., Weissbach, L., Bernards, A., and Snijders, A.J. (1996). The Ras GTPase-activating-protein-related human protein

IQGAP2 harbors a potential actin binding domain and interacts with calmodulin and Rho family GTPases. *Mol Cell Biol* *16*, 4869-4878.

Brown, M.D., and Sacks, D.B. (2006). IQGAP1 in cellular signaling: bridging the GAP. *Trends Cell Biol* *16*, 242-249.

Burton, J.L., and Solomon, M.J. (2001). D box and KEN box motifs in budding yeast Hsl1p are required for APC-mediated degradation and direct binding to Cdc20p and Cdh1p. *Genes Dev* *15*, 2381-2395.

Cabib, E., Roh, D.H., Schmidt, M., Crotti, L.B., and Varma, A. (2001). The yeast cell wall and septum as paradigms of cell growth and morphogenesis. *J Biol Chem* *276*, 19679-19682.

Carroll, C.W., and Morgan, D.O. (2002). The Doc1 subunit is a processivity factor for the anaphase-promoting complex. *Nat. Cell Biol.* *4*, 880-887.

Carroll, C.W., and Morgan, D.O. (2005). Enzymology of the Anaphase-Promoting Complex. *Meth. Enzymol.* *398*, 219-230.

Charles, J.F., Jaspersen, S.L., Tinker-Kulberg, R.L., Hwang, L., Szidon, A., and Morgan, D.O. (1998). The Polo-related kinase Cdc5 activates and is destroyed by the mitotic cyclin destruction machinery in *S. cerevisiae*. *Curr. Biol.* *8*, 497-507.

Cheng, L., Collyer, T., and Hardy, C.F. (1999). Cell cycle regulation of DNA replication initiator factor Dbf4p. *Mol Cell Biol* *19*, 4270-4278.

- Colman-Lerner, A., Chin, T.E., and Brent, R. (2001). Yeast Cbk1 and Mob2 activate daughter-specific genetic programs to induce asymmetric cell fates. *Cell* *107*, 739-750.
- Dawson, I.A., Roth, S., and Artavanis-Tsakonas, S. (1995). The *Drosophila* cell cycle gene *fizzy* is required for normal degradation of cyclins A and B during mitosis and has homology to the *CDC20* gene of *Saccharomyces cerevisiae*. *J. Cell Biol.* *129*, 725-737.
- Ditchfield, C., Johnson, V.L., Tighe, A., Ellston, R., Haworth, C., Johnson, T., Mortlock, A., Keen, N., and Taylor, S.S. (2003). Aurora B couples chromosome alignment with anaphase by targeting BubR1, Mad2, and Cenp-E to kinetochores. *J Cell Biol* *161*, 267-280.
- Dobbelaere, J., and Barral, Y. (2004). Spatial coordination of cytokinetic events by compartmentalization of the cell cortex. *Science* *305*, 393-396.
- Eggert, U.S., Mitchison, T.J., and Field, C.M. (2006). Animal cytokinesis: from parts list to mechanisms. *Annu Rev Biochem* *75*, 543-566.
- Epp, J.A., and Chant, J. (1997). An IQGAP-related protein controls actin-ring formation and cytokinesis in yeast. *Curr Biol* *7*, 921-929.
- Fang, G., Yu, H., and Kirschner, M.W. (1998). The checkpoint protein MAD2 and the mitotic regulator CDC20 form a ternary complex with the anaphase-promoting complex to control anaphase initiation. *Genes Dev.* *12*, 1871-1883.

Ferreira, M.F., Santocanale, C., Drury, L.S., and Diffley, J.F. (2000). Dbf4p, an essential S phase-promoting factor, is targeted for degradation by the anaphase-promoting complex. *Mol Cell Biol* 20, 242-248.

Finger, F.P., and Novick, P. (1998). Spatial regulation of exocytosis: lessons from yeast. *J Cell Biol* 142, 609-612.

Ghaemmaghami, S., Huh, W.K., Bower, K., Howson, R.W., Belle, A., Dephoure, N., O'Shea, E.K., and Weissman, J.S. (2003). Global analysis of protein expression in yeast. *Nature* 425, 737-741.

Glotzer, M. (2005). The molecular requirements for cytokinesis. *Science* 307, 1735-1739.

Glotzer, M., Murray, A.W., and Kirschner, M.W. (1991). Cyclin is degraded by the ubiquitin pathway. *Nature* 349, 132-138.

Gordon, D.M., and Roof, D.M. (2001). Degradation of the kinesin Kip1p at anaphase onset is mediated by the anaphase-promoting complex and Cdc20p. *Proc Natl Acad Sci U S A* 98, 12515-12520.

Guthrie, C., and Fink, G.R. (eds.) (1991). *Guide to yeast genetics and molecular biology*. Academic Press: San Diego.

Haarer, B.K., and Pringle, J.R. (1987). Immunofluorescence localization of the *Saccharomyces cerevisiae* CDC12 gene product to the vicinity of the 10-nm filaments in the mother-bud neck. *Mol Cell Biol* 7, 3678-3687.

Harrington, E.A., Bebbington, D., Moore, J., Rasmussen, R.K., Ajose-Adeogun, A.O., Nakayama, T., Graham, J.A., Demur, C., Hercend, T., Diu-Hercend, A., Su, M., Golec, J.M., and Miller, K.M. (2004). VX-680, a potent and selective small-molecule inhibitor of the Aurora kinases, suppresses tumor growth in vivo. *Nat Med* *10*, 262-267.

Hart, M.J., Callow, M.G., Souza, B., and Polakis, P. (1996). IQGAP1, a calmodulin-binding protein with a rasGAP-related domain, is a potential effector for cdc42Hs. *Embo J* *15*, 2997-3005.

Hauf, S., Cole, R.W., LaTerra, S., Zimmer, C., Schnapp, G., Walter, R., Heckel, A., van Meel, J., Rieder, C.L., and Peters, J.M. (2003). The small molecule Hesperadin reveals a role for Aurora B in correcting kinetochore-microtubule attachment and in maintaining the spindle assembly checkpoint. *J Cell Biol* *161*, 281-294.

Hendrickson, C., Meyn, M.A., 3rd, Morabito, L., and Holloway, S.L. (2001). The KEN box regulates Clb2 proteolysis in G1 and at the metaphase-to-anaphase transition. *Curr Biol* *11*, 1781-1787.

Hildebrandt, E.R., and Hoyt, M.A. (2001). Cell cycle-dependent degradation of the *Saccharomyces cerevisiae* spindle motor Cin8p requires APC(Cdh1) and a bipartite destruction sequence. *Mol Biol Cell* *12*, 3402-3416.

Huh, W.K., Falvo, J.V., Gerke, L.C., Carroll, A.S., Howson, R.W., Weissman, J.S., and O'Shea, E.K. (2003). Global analysis of protein localization in budding yeast. *Nature* *425*, 686-691.

- Iwase, M., Luo, J., Bi, E., and Toh, E.A. (2007). Shs1 plays separable roles in septin organization and cytokinesis in *Saccharomyces cerevisiae*. *Genetics*.
- Iwase, M., Luo, J., Nagaraj, S., Longtine, M., Kim, H.B., Haarer, B.K., Caruso, C., Tong, Z., Pringle, J.R., and Bi, E. (2006). Role of a Cdc42p effector pathway in recruitment of the yeast septins to the presumptive bud site. *Mol Biol Cell* *17*, 1110-1125.
- Jaspersen, S.L., Charles, J.F., and Morgan, D.O. (1999). Inhibitory phosphorylation of the APC regulator Hct1 is controlled by the kinase Cdc28 and the phosphatase Cdc14. *Curr. Biol.* *9*, 227-236.
- Jaspersen, S.L., and Morgan, D.O. (2000). Cdc14 activates cdc15 to promote mitotic exit in budding yeast. *Curr Biol* *10*, 615-618.
- Juang, Y.-L., Huang, J., Peters, J.-M., McLaughlin, M.E., Tai, C.-Y., and Pellman, D. (1997). APC-mediated proteolysis of Ase1 and the morphogenesis of the mitotic spindle. *Science* *275*, 1311-1314.
- Kamei, T., Tanaka, K., Hihara, T., Umikawa, M., Imamura, H., Kikyo, M., Ozaki, K., and Takai, Y. (1998). Interaction of Bnr1p with a novel Src homology 3 domain-containing Hof1p. Implication in cytokinesis in *Saccharomyces cerevisiae*. *J Biol Chem* *273*, 28341-28345.
- Kellogg, D.R., and Murray, A.W. (1995). NAP1 acts with Clb1 to perform mitotic functions and to suppress polar bud growth in budding yeast. *J. Cell. Biol.* *130*, 675-685.

- King, R.W., Peters, J.-M., Tugendreich, S., Rolfe, M., Hieter, P., and Kirschner, M.W. (1995). A 20S complex containing CDC27 and CDC16 catalyzes the mitosis-specific conjugation of ubiquitin to cyclin B. *Cell* *81*, 279-288.
- Kitayama, C., Sugimoto, A., and Yamamoto, M. (1997). Type II myosin heavy chain encoded by the *myo2* gene composes the contractile ring during cytokinesis in *Schizosaccharomyces pombe*. *J Cell Biol* *137*, 1309-1319.
- Kuranda, M.J., and Robbins, P.W. (1991). Chitinase is required for cell separation during growth of *Saccharomyces cerevisiae*. *J Biol Chem* *266*, 19758-19767.
- Lahav-Baratz, S., Sudakin, V., Ruderman, J.V., and Hershko, A. (1995). Reversible phosphorylation controls the activity of cyclosome-associated cyclin-ubiquitin ligase. *Proc. Nat. Acad. Sci. USA* *92*, 9303-9307.
- Lim, H.H., Goh, P., and Surana, U. (1998). Cdc20 is essential for the cyclosome-mediated proteolysis of both Pds1 and Clb2 during M phase in budding yeast. *Curr. Biol.* *8*, 231-234.
- Lippincott, J., and Li, R. (1998). Sequential assembly of myosin II, an IQGAP-like protein and filamentous actin to a ring structure involved in budding yeast cytokinesis. *J. Cell Biol.* *140*, 355-366.
- Lister, I.M., Tolliday, N.J., and Li, R. (2006). Characterization of the minimum domain required for targeting budding yeast myosin II to the site of cell division. *BMC Biol* *4*, 19.

- Lord, M., Laves, E., and Pollard, T.D. (2005). Cytokinesis depends on the motor domains of myosin-II in fission yeast but not in budding yeast. *Mol Biol Cell* *16*, 5346-5355.
- Luca, F.C., Mody, M., Kurischko, C., Roof, D.M., Giddings, T.H., and Winey, M. (2001). *Saccharomyces cerevisiae* Mob1p is required for cytokinesis and mitotic exit. *Mol Cell Biol* *21*, 6972-6983.
- Luo, J., Vallen, E.A., Dravis, C., Tcheperegine, S.E., Drees, B., and Bi, E. (2004). Identification and functional analysis of the essential and regulatory light chains of the only type II myosin Myo1p in *Saccharomyces cerevisiae*. *J Cell Biol* *165*, 843-855.
- Matsumura, F. (2005). Regulation of myosin II during cytokinesis in higher eukaryotes. *Trends Cell Biol* *15*, 371-377.
- McCallum, S.J., Wu, W.J., and Cerione, R.A. (1996). Identification of a putative effector for Cdc42Hs with high sequence similarity to the RasGAP-related protein IQGAP1 and a Cdc42Hs binding partner with similarity to IQGAP2. *J Biol Chem* *271*, 21732-21737.
- Menssen, R., Neutzner, A., and Seufert, W. (2001). Asymmetric spindle pole localization of yeast Cdc15 kinase links mitotic exit and cytokinesis. *Curr Biol* *11*, 345-350.
- Morgan, D.O. (1997). Cyclin-dependent kinases: engines, clocks, and microprocessors. *Annu. Rev. Cell Dev. Biol.* *13*, 261-291.
- Morgan, D.O. (2007). *The Cell Cycle: Principles of Control*. New Science Press: London.

Moussavi, R.S., Kelley, C.A., and Adelstein, R.S. (1993). Phosphorylation of vertebrate nonmuscle and smooth muscle myosin heavy chains and light chains. *Mol Cell Biochem* 127-128, 219-227.

Negron, J.A., Gonzalez, S., and Rodriguez-Medina, J.R. (1996). In vivo phosphorylation of type II myosin in *Saccharomyces cerevisiae*. *Biochem Biophys Res Commun* 221, 515-520.

Norden, C., Mendoza, M., Dobbelaere, J., Kotwaliwale, C.V., Biggins, S., and Barral, Y. (2006). The NoCut pathway links completion of cytokinesis to spindle midzone function to prevent chromosome breakage. *Cell* 125, 85-98.

Oshiro, G., Owens, J.C., Shellman, Y., Sclafani, R.A., and Li, J.J. (1999). Cell cycle control of Cdc7p kinase activity through regulation of Dbf4p stability. *Mol Cell Biol* 19, 4888-4896.

Osman, M.A., and Cerione, R.A. (1998). Iqg1p, a yeast homologue of the mammalian IQGAPs, mediates cdc42p effects on the actin cytoskeleton. *J Cell Biol* 142, 443-455.

Osman, M.A., Konopka, J.B., and Cerione, R.A. (2002). Iqg1p links spatial and secretion landmarks to polarity and cytokinesis. *J Cell Biol* 159, 601-611.

Peters, J.M. (2006). The anaphase promoting complex/cyclosome: a machine designed to destroy. *Nat Rev Mol Cell Biol* 7, 644-656.

Pfleger, C.M., and Kirschner, M.W. (2000). The KEN box: an APC recognition signal distinct from the D box targeted by Cdh1. *Genes Dev* 14, 655-665.

- Rape, M., Reddy, S.K., and Kirschner, M.W. (2006). The processivity of multiubiquitination by the APC determines the order of substrate degradation. *Cell* *124*, 89-103.
- Rigaut, G., Shevchenko, A., Rutz, B., Wilm, M., Mann, M., and Seraphin, B. (1999). A generic protein purification method for protein complex characterization and proteome exploration. *Nat. Biotechnol.* *17*, 1030-1032.
- Robinson, D.N., and Spudich, J.A. (2000). Towards a molecular understanding of cytokinesis. *Trends Cell Biol* *10*, 228-237.
- Rodriguez, J.R., and Paterson, B.M. (1990). Yeast myosin heavy chain mutant: maintenance of the cell type specific budding pattern and the normal deposition of chitin and cell wall components requires an intact myosin heavy chain gene. *Cell Motil Cytoskeleton* *17*, 301-308.
- Roh, D.H., Bowers, B., Schmidt, M., and Cabib, E. (2002). The septation apparatus, an autonomous system in budding yeast. *Mol Biol Cell* *13*, 2747-2759.
- Schmidt, M., Bowers, B., Varma, A., Roh, D.H., and Cabib, E. (2002). In budding yeast, contraction of the actomyosin ring and formation of the primary septum at cytokinesis depend on each other. *J Cell Sci* *115*, 293-302.
- Scholey, J.M., Taylor, K.A., and Kendrick-Jones, J. (1980). Regulation of non-muscle myosin assembly by calmodulin-dependent light chain kinase. *Nature* *287*, 233-235.

Schwab, M., Lutum, A.S., and Seufert, W. (1997). Yeast Hct1 is a regulator of Clb2 cyclin proteolysis. *Cell* *90*, 683-693.

Schwab, M., Neutzner, M., Mocker, D., and Seufert, W. (2001). Yeast Hct1 recognizes the mitotic cyclin Clb2 and other substrates of the ubiquitin ligase APC. *Embo J* *20*, 5165-5175.

Shah, R., Jensen, S., Frenz, L.M., Johnson, A.L., and Johnston, L.H. (2001). The Spo12 protein of *Saccharomyces cerevisiae*: a regulator of mitotic exit whose cell cycle-dependent degradation is mediated by the anaphase-promoting complex. *Genetics* *159*, 965-980.

Shannon, K.B., and Li, R. (1999). The multiple roles of Cyk1p in the assembly and function of the actomyosin ring in budding yeast. *Mol. Biol. Cell* *10*, 283-296.

Shannon, K.B., and Li, R. (2000). A myosin light chain mediates the localization of the budding yeast IQGAP-like protein during contractile ring formation. *Curr Biol* *10*, 727-730.

Shirayama, M., Matsui, Y., and Toh-e, A. (1994). The yeast *TEMI* gene, which encodes a GTP-binding protein, is involved in termination of M phase. *Mol. Cell. Biol.* *14*, 7476-7482.

Shirayama, M., Zachariae, W., Ciosk, R., and Nasmyth, K. (1998). The Polo-like kinase Cdc5p and the WD-repeat protein Cdc20p/fizzy are regulators and substrates of the anaphase promoting complex in *Saccharomyces cerevisiae*. *EMBO J.* *17*, 1336-1349.

Shuster, C.B., and Burgess, D.R. (2002). Transitions regulating the timing of cytokinesis in embryonic cells. *Curr Biol* 12, 854-858.

Sikorski, R.S., and Hieter, P. (1989). A system of shuttle vectors and yeast host strains designed for efficient manipulation of DNA in *Saccharomyces cerevisiae*. *Genetics* 122, 19-27.

Spellman, P.T., Sherlock, G., Zhang, M.Q., Iyer, V.R., Anders, K., Eisen, M.B., Brown, P.O., Botstein, D., and Futcher, B. (1998). Comprehensive identification of cell cycle-regulated genes of the yeast *Saccharomyces cerevisiae* by microarray hybridization. *Mol. Biol. Cell* 9, 3273-3297.

Straight, A.F., Cheung, A., Limouze, J., Chen, I., Westwood, N.J., Sellers, J.R., and Mitchison, T.J. (2003). Dissecting temporal and spatial control of cytokinesis with a myosin II Inhibitor. *Science* 299, 1743-1747.

Sudakin, V., Ganoth, D., Dahan, A., Heller, H., Hershko, J., Luca, F.C., Ruderman, J.V., and Hershko, A. (1995). The cyclosome, a large complex containing cyclin-selective ubiquitin-ligase activity, targets cyclins for destruction at the end of mitosis. *Mol. Biol. Cell* 6, 185-198.

Sullivan, M., and Morgan, D.O. (2007). A novel destruction sequence targets the meiotic regulator Spo13 for anaphase-promoting complex-dependent degradation in anaphase I. *J. Biol. Chem.* 282, 19710-19715.

Thornton, B.R., and Toczyski, D.P. (2003). Securin and B-cyclin/CDK are the only essential targets of the APC. *Nat Cell Biol* 5, 1090-1094.

- Thornton, B.R., and Toczyski, D.P. (2006). Precise destruction: an emerging picture of the APC. *Genes Dev* 20, 3069-3078.
- Tolliday, N., Bouquin, N., and Li, R. (2001). Assembly and regulation of the cytokinetic apparatus in budding yeast. *Curr Opin Microbiol* 4, 690-695.
- Tolliday, N., Pitcher, M., and Li, R. (2003). Direct evidence for a critical role of myosin II in budding yeast cytokinesis and the evolvability of new cytokinetic mechanisms in the absence of myosin II. *Mol Biol Cell* 14, 798-809.
- Tolliday, N., VerPlank, L., and Li, R. (2002). Rho1 directs formin-mediated actin ring assembly during budding yeast cytokinesis. *Curr Biol* 12, 1864-1870.
- Ubersax, J.A., Woodbury, E.L., Quang, P.N., Paraz, M., Blethrow, J.D., Shah, K., Shokat, K.M., and Morgan, D.O. (2003). Targets of the cyclin-dependent kinase Cdk1. *Nature* 425, 859-864.
- Vallen, E.A., Caviston, J., and Bi, E. (2000). Roles of Hof1p, Bni1p, Bnr1p, and myo1p in cytokinesis in *Saccharomyces cerevisiae*. *Mol Biol Cell* 11, 593-611.
- Versele, M., and Thorner, J. (2005). Some assembly required: yeast septins provide the instruction manual. *Trends Cell Biol* 15, 414-424.
- Visintin, R., Prinz, S., and Amon, A. (1997). CDC20 and CDH1: a family of substrate-specific activators of APC-dependent proteolysis. *Science* 278, 460-463.
- Vrabioiu, A.M., and Mitchison, T.J. (2006). Structural insights into yeast septin organization from polarized fluorescence microscopy. *Nature* 443, 466-469.

- Wagner, W., Bielli, P., Wacha, S., and Ragnini-Wilson, A. (2002). Mlc1p promotes septum closure during cytokinesis via the IQ motifs of the vesicle motor Myo2p. *Embo J* *21*, 6397-6408.
- Watts, F.Z., Shiels, G., and Orr, E. (1987). The yeast MYO1 gene encoding a myosin-like protein required for cell division. *Embo J* *6*, 3499-3505.
- Wheatley, S.P., Hinchcliffe, E.H., Glotzer, M., Hyman, A.A., Sluder, G., and Wang, Y. (1997). CDK1 inactivation regulates anaphase spindle dynamics and cytokinesis in vivo. *J. Cell Biol.* *138*, 385-393.
- Wolfe, B.A., and Gould, K.L. (2005). Split decisions: coordinating cytokinesis in yeast. *Trends Cell Biol* *15*, 10-18.
- Woodbury, E.L., and Morgan, D.O. (2007). Cdk and APC activities limit the spindle-stabilizing function of Fin1 to anaphase. *Nat Cell Biol* *9*, 106-112.
- Wäsch, R., and Cross, F. (2002). APC-dependent proteolysis of the mitotic cyclin Clb2 is essential for mitotic exit. *Nature* *418*, 556-562.
- Yoshida, S., Kono, K., Lowery, D.M., Bartolini, S., Yaffe, M.B., Ohya, Y., and Pellman, D. (2006). Polo-like kinase Cdc5 controls the local activation of Rho1 to promote cytokinesis. *Science* *313*, 108-111.
- Zachariae, W., Shevchenko, A., Andrews, P.D., Ciosk, R., Galova, M., Strak, M.J.R., Mann, M., and Nasmyth, K. (1998). Mass spectrometric analysis of the anaphase-

promoting complex from yeast: identification of a subunit related to cullins. *Science* 279, 1216-1219.

Zachariae, W., Shin, T.H., Galova, M., Obermaier, B., and Nasmyth, K. (1996). Identification of subunits of the anaphase-promoting complex of *Saccharomyces cerevisiae*. *Science* 274, 1201-1204.

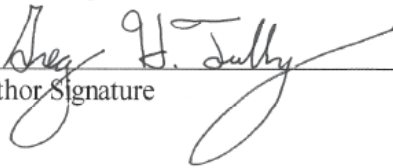
Zhao, W.M., and Fang, G. (2005). Anillin is a substrate of anaphase-promoting complex/cyclosome (APC/C) that controls spatial contractility of myosin during late cytokinesis. *J Biol Chem* 280, 33516-33524.

Publishing Agreement

It is the policy of the University to encourage the distribution of all theses and dissertations. Copies of all UCSF theses and dissertations will be routed to the library via the Graduate Division. The library will make all theses and dissertations accessible to the public and will preserve these to the best of their abilities, in perpetuity.

Please sign the following statement:

I hereby grant permission to the Graduate Division of the University of California, San Francisco to release copies of my thesis or dissertation to the Campus Library to provide access and preservation, in whole or in part, in perpetuity.



Author Signature

09-11-2007
Date